2 The Egyptian Nubian Shield Within the Frame of the Arabian–Nubian Shield

Mohamed Abd El-Wahed and Zakaria Hamimi

Abstract

Gondwana Supercontinent in eastern and southern Africa formed by collision and amalgamation of two crustal plates, provisionally named East Gondwana and West Gondwana and the Mozambique Ocean intake between 841 and 632 Ma. East Gondwana consists of the Arabian–Nubian Shield (ANS) and the older crystalline basement in Madagascar, India, Antarctica and Australia, while West Gondwana consists of much of Africa and South America. Collision and amalgamation of East and West Gondwana formed the East African Orogeny. The supercontinent of Gondwana ranged from Neoproterozoic (~550 Ma ago) to Carboniferous (~320 Ma ago). Gondwana became the largest continental crust during the Paleozoic Era (~100 million km^2). During the Carboniferous, Gondwana amalgamated with Euramerica resulting in the formation of the supercontinent, Pangaea. Three orogeneses were recognized during the 1990s: the East African Orogeny (650–800 Ma), Kuunga Orogeny (including the Malagasy Orogeny in southern Madagascar) (550 Ma)—the collision between East Gondwana and East Africa in two steps—and the Brasiliano Orogeny (660–530 Ma)—the collision between South American and African Cratons. Formation of arcs in the ANS occurred over a ~300-million-year period including supercontinent Rodinia break-up and the assembly of supercontinent Gondwana. The ANS represents one of the best documented examples of Late Proterozoic to Early Paleozoic (950–450 Ma) crustal growth through processes of lateral arc–arc terrane accretion. The tectonic development of the ANS spans three phases spanning over 600 Ma: accumulation of arc terrains inside the Hijaz Magmatic Arc, accompanied by accretion of the Hijaz Magmatic Arc against the Nile Craton and reworking of the accreted arc after accretion. The Egyptian Nubian Shield (ENS) covers ~100,000 km^2, crops out along the Red Sea Hills in the Eastern Desert and southern Sinai, as well as limited areas in the south Western Desert (Oweinat area, 2673 ± 21 Ma). The ENE covers the northeastern part of the East African Orogeny and stretches over approximately 800 km parallel with the Red Sea coast between latitudes 22° 00′ 00″ and 28° 40′ 00″ N. The rocks are covered by Nubia sandstone, Miocene and later sediments in their western and eastern margins. The Eastern Desert of Egypt is divided into three domains, namely, the northern Eastern Desert (NED), central Eastern Desert (CED) and southern Eastern Desert (SED); these domains were developed in different tectonic settings and show a characteristic younging from (SED) to (NED). Geologically, gneisses, migmatites and schists dominate the SED as the oldest units, and are followed by ophiolites, volcanic arc lithologies and granitoid plutons. The amount of ophiolites increases and forms with the arc metavolcanics the main types in the CED. The ophiolites and the metavolcanics are occasionally unconformably and tectonically overlained by Dokhan volcanics and molasse sediments. The older gneisses and migmatites form prominent domal structures (e.g. Meatiq, Sibai, Hafafit, El-Shalul). Syn-tectonic and late tectonic granitoids are also present. The NED is characterized by younger rocks, such as Gattarian granites, Dokhan volcanics and Hammamat molasse sediments, whereas older rock types rarely occur. The bulk of the crust of the SED was created prior to 650 Ma, while the major pulses of the CED occurred in the interval (685–575 Ma). In the NED and Sinai, the crust was principally formed in the period (625–575 Ma).

M. Abd El-Wahed (✉)
Geology Department, Faculty of Science, Tanta University, Tanta, 31527, Egypt
e-mail: mohamed.abdelwahad@science.tanta.edu.eg

Z. Hamimi
Department of Geology, Faulty of Science, Benha University, Benha, 13518, Egypt

Z. Hamimi et al. (eds.), *The Geology of the Egyptian Nubian Shield*, Regional Geology Reviews,
https://doi.org/10.1007/978-3-030-49771-2_2

2.1 Formation and Amalgamation of Gondwana Supercontinent

Gondwana is the name for the southern half of an ancient supercontinent known as Pangaea or Pangea that existed some 300 Ma, along with a northern supercontinent known as Laurasia (Meert et al. 2011). The continent broke up about 180 Ma and eventually split into landmasses we recognize today: South America, Africa, Madagascar, Sri Lanka, India, the Arabian Peninsula, Antarctica and Australia (Fig. 2.1). Gondwana was the largest unit of continental crust on Earth for more than two hundred million years. The name "Gondwana" or "Gondwanaland" is derived from a tribe in India (Gonds) and "wana" meaning "land of". This name was first used in 1879 by Medlicott and Blanford from the Indian Geological Survey. Wegener (1915) enlarged the concept of Gondwana and postulated his ideas regarding continental drift, and the existence of a previously united Gondwana. Wegener once believed that all of the continents were together in a "Urkontinent" before splitting apart and moving to their present places. Most of Wegener's findings on fossils and rocks are right, he was in certain ways highly incorrect. For instance, Wegener figured that the continents should have plowed like icebreakers into the ocean crust. Plate tectonics is now the widely accepted theory that Earth's crust is fractured into rigid, moving plates.

Several events, collectively known as the Pan-African orogeny, led to the amalgamation of most of the continental fragments of a much older supercontinent, Rodinia. Rodinia is a supercontinent that was united 1.3–0.9 billion years ago during Grenville Orogeny and broke up 750–633 million years ago (McMenamin and McMenamin 1990; Li et al. 2008; Meert 2012). It was surrounded by an ocean called Mirovia. Valentine and Moores (1970) were perhaps the first to identify a Precambrian supercontinent called Pangaea that was renamed as "Rodinia" by McMenamin and McMenamin (1990). The fragments of the break-up of Columbia collided and were assembled by global-scale 2.0–1.8 Ga collisional events and formed Rodinia at c. 1.23 Ga (Zhao et al. 2002, 2004). Condie (2002) reported that Rodinia was created between 1300 and 900 Ma and that the continental disintegration happened between 950 and 600 Ma (Fig. 2.2). The break-up of Rodinia started around 950 Ma ago and persisted until ca. 600 Ma (Condie 2002; Rogers and Santosh 2004).

The Mozambique Belt is one of the 800–650 Ma orogenic belts and was initially described as the suture dividing

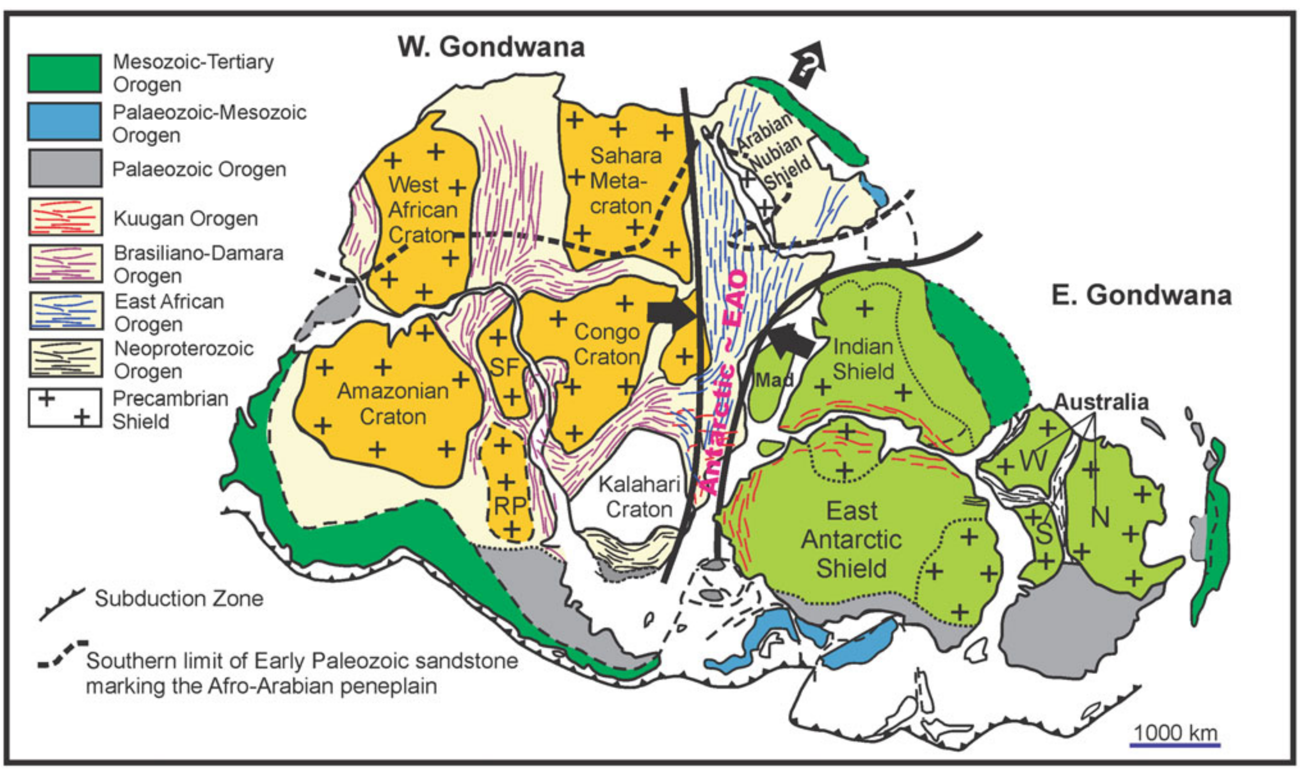

Fig. 2.1 The Gondwanaland supercontinent. The cratons comprising West Gondwana and those comprising East Gondwana (modified after Gray et al. 2008). Neoproterozoic orogenic belts crisscross the supercontinent. Those associated with the final amalgamation of the supercontinent are the East African Orogen (750–620 Ma; blue), the Brasiliano-Damara Orogen (630–520 Ma; dark red) and the Kuunga Orogen (570–530 Ma; red)

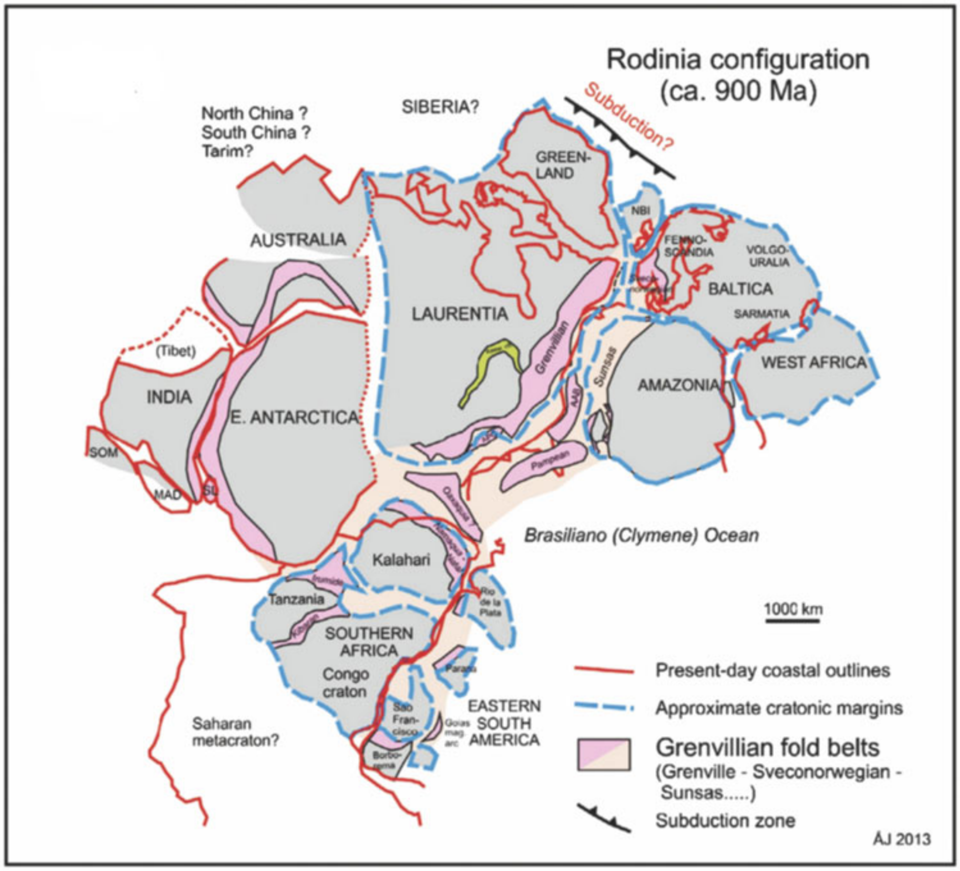

Fig. 2.2 A proposed reconstruction of the supercontinent Rodinia, about 990 million years (after Johansson 2014). Possible subduction zone outboard of Greenland margin follows the idea of the Valhalla orogenof Cawood et al. (2010). Separation and rotation of northern Australia relative to southern and western Australia according to Li and Evans (2011)

East from West Gondwana. The Mozambique Ocean separated the Congo–Tanzania–Bangweul Block of central Africa from Neoproterozoic India (India, the Antongil Block in far eastern Madagascar, the Seychelles, and the Napier and Rayner Complexes in East Antarctica). The Azania continent was an island in the Mozambique Ocean and include much of central Madagascar, the Horn of Africa and parts of Yemen and Arabia (Collins and Pisarevsky 2005). The final formation of Gondwana occurred about 500 million years ago (Figs. 2.3, 2.4 and 2.5). Gondwana is superficially divided into western half (South America and Africa) and an eastern half (Madagascar, Antarctica, Sri Lanka, India and Australia) and Ediacaran–Cambrian age by coalescence of East Gondwana with West Gondwana with closing of the Mozambique ocean and development of the Mozambique Belt (Stern 1994a, b; Meert et al. 2011; Johansson 2014).

Gondwana amalgamated with Euramerica during the Carboniferous to create a broader supercontinent called Pangaea. During the Mesozoic era, Gondwana (and Pangaea) were gradually fragmented. During Silurian, Gondwana supercontinent (Australia, Antarctica, India, Arabia, Africa, and South America, Florida, southern Europe, and the Cimmerian terranes, namely, Turkey, Iran, Afghanistan, Tibet and the Malay Peninsula) was centred over the South Pole. Rheic Ocean is an east–west ocean separating the southern European sector of Gondwana from northern Europe (Baltica) and was basically a southwestern extension of the Paleotethys Sea. During the Caledonian orogeny (410 Ma ago), a minor supercontinent named Euramerica was created due to collision between the Avalonia cratons, Baltica and Laurentian. The Caledonian orogeny was a mountain-building era recorded in the northern parts of Ireland and Britain, the Scandinavian Mountains, Svalbard, eastern Greenland and parts of north-central Europe (Torsvik and Cocks 2013). In the Permian, the supercontinent of Euramerica became part of the major Pangaea supercontinent. Euramerica became part of Laurasia in the Jurassic when Pangaea split into two separate continents, Gondwana and Laurasia. Some 180 Ma, in the Jurassic Period, the western half of Gondwana (Africa and South America) separated from the eastern half (Madagascar, India, Australia and Antarctica) (Figs. 2.6 and 2.7). In the Cretaceous, Africa broke away from South America, leading to opening of the South Atlantic Ocean at about 140 Ma. In the same period, the central part of the Indian Ocean opened, and India parted from Madagascar, and Australia slowly rifted away from Antarctica. Also, Laurasia divided into the North America

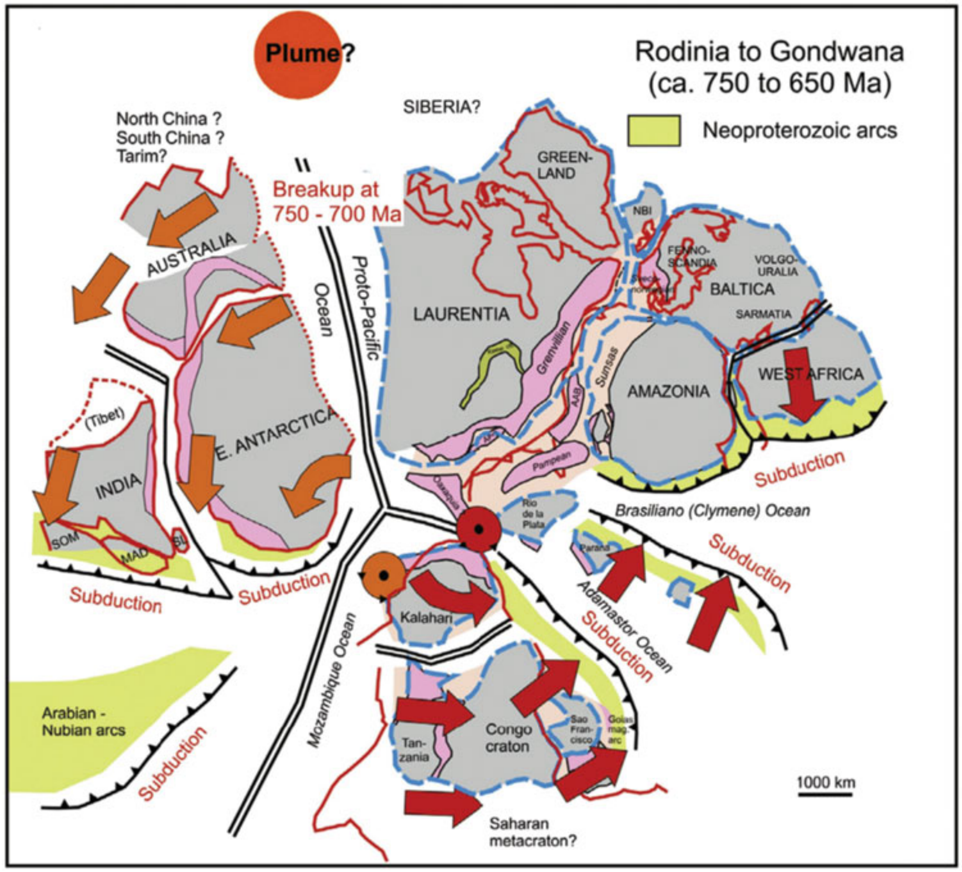

Fig. 2.3 Separation and rotation of the eastern South American and southern and central African cratons, as well as East Antarctica, Australia and India, relative to a fixed Laurentia, at 750–650 Ma (after Johansson 2014). Formation of large amounts of juvenile Neoproterozoic crust in island arcs, particularly in the Arabian–Nubian sector

and Eurasia continents. Baltica was part of Eurasia, and the Laurentian craton was part of North America while Avalonia became split between the two. The remains of Gondwana constitute two-thirds of the continental region of today (Torsvik and Cocks 2013). India collided with Eurasia creating the Himalayan Mountains 50 million years ago, when the northward-moving Australian plate has only started its collision on the southern edge of south-east Asia, a collision still ongoing today.

There are basically two geodynamic scenarios to explain the formation of the Gondwana Supercontinent in eastern and southern Africa during the Pan-African orogenic cycle (Westerhof et al. 2008). The first scenario involved collision and amalgamation of East Gondwana and West Gondwana (~640 to ~530 Ma) (Shackleton 1994; Kröner et al. 2001; Jacobs et al. 2006; Westerhof et al. 2008) and the Mozambique Ocean consumed between 841 and 632 Ma (Cutten and Johnson 2006). In this model, East Gondwana comprised juvenile crust (ANS, and older crystalline basement in Australia, Antarctica, India and Madagascar), and West Gondwana was composed of most of South America and Africa (Figs. 2.4, 2.5 and 2.7). Collision and amalgamation of East and West Gondwana produced the East Africa Orogen (EAO) (Stern 1994a, b) that it is an N–S directed fold belt (6000 km). This orogenic cycle dated ~650–490 Ma (Cahen and Snelling 1966). Kröner (2006) reported peak granulite facies metamorphism in East Africa and Madagascar between 640 and 550 Ma. The second scenario assumes collision and amalgamation of East Gondwana (ANS and older crystalline basement of the Dharwar Craton of southern India, Madagascar and the eastern granulites of Kenya and Tanzania), West Gondwana (Central Africa craton) and South Gondwana (Antarctica and the Kalahari craton) (Grantham et al. 2003) (Fig. 2.1). South Gondwana has been integral since the Grenvillian Orogeny at ~1.0 Ga. In this scenario, the EAO suture directed by the N–S implies Kuunga Orogen suture directed to the E–W, comprising from W to E, the Damara–Lufilian–Zambezi (DLZ) Belt (Fig. 2.8), the Lúrio Thrust Belt (LTB) and, further eastwards, thrust belts of Sri Lanka (Westerhof et al. 2008). In this scenario, pan-African remobilization of Mesoproterozoic and older crust south of the Kuunga Suture is confined to metamorphic overprinting throughout linear N–S-directed shear zones (Manica Shear Zone, Fig. 2.1) along the eastern margin of the Zimbabwe Craton (Manhiça et al. 2001; GTK Consortium 2006; Westerhof et al. 2008).

Collision and amalgamation of the Central Africa Craton (West Gondwana) and Kalahari Craton (South Gondwana)

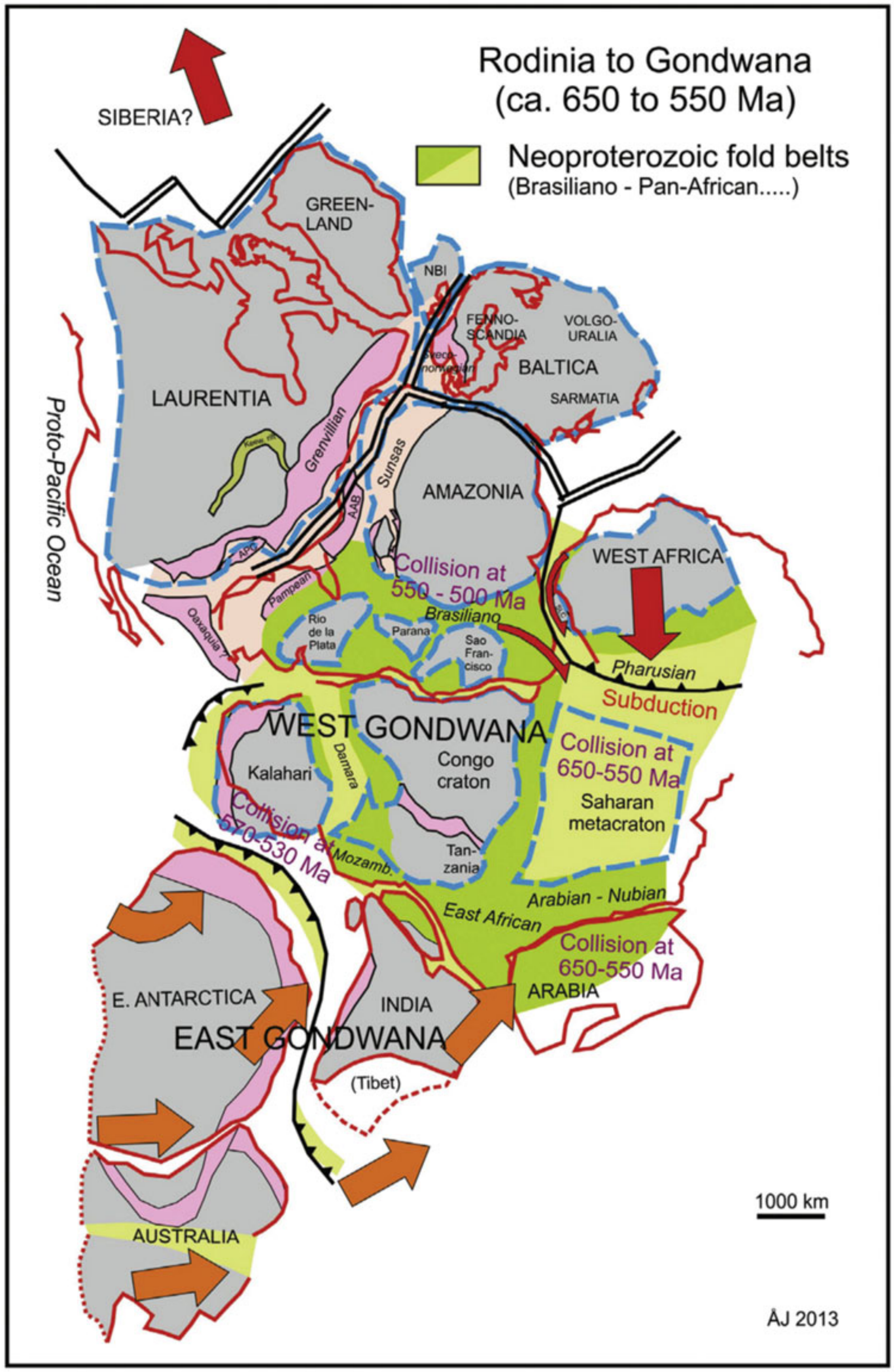

Fig. 2.4 Collision between the various Gondwana cratons along the Brasiliano and Pan-African orogens at 650–550 Ma; juvenile crust formation followed by arc collision and northwards extrusion in the Arabian–Nubian sector and extensive reworking of the Saharan metacraton (after Johansson 2014). Initial break-up between Laurentia, Amazonia and Baltica at 600 Ma

and Closure of the Zambezi–Adamastor Oceanic Basin (Johnson et al. 2005) resulted in the Damara–Lufilian–Zambezi Belt (Fig. 2.8), a major Neoproterozoic suture (Burke et al. 1977; Oliver et al. 1998; John et al. 2003; Johnson and Oliver 2000, 2004). The Lufilian and Zambezi segments of the Damara–Lufilian–Zambezi Belt can be described as a thin- and thick-skinned, double-verging orogen with thrust transport to the SSE (Müller et al. 2001;

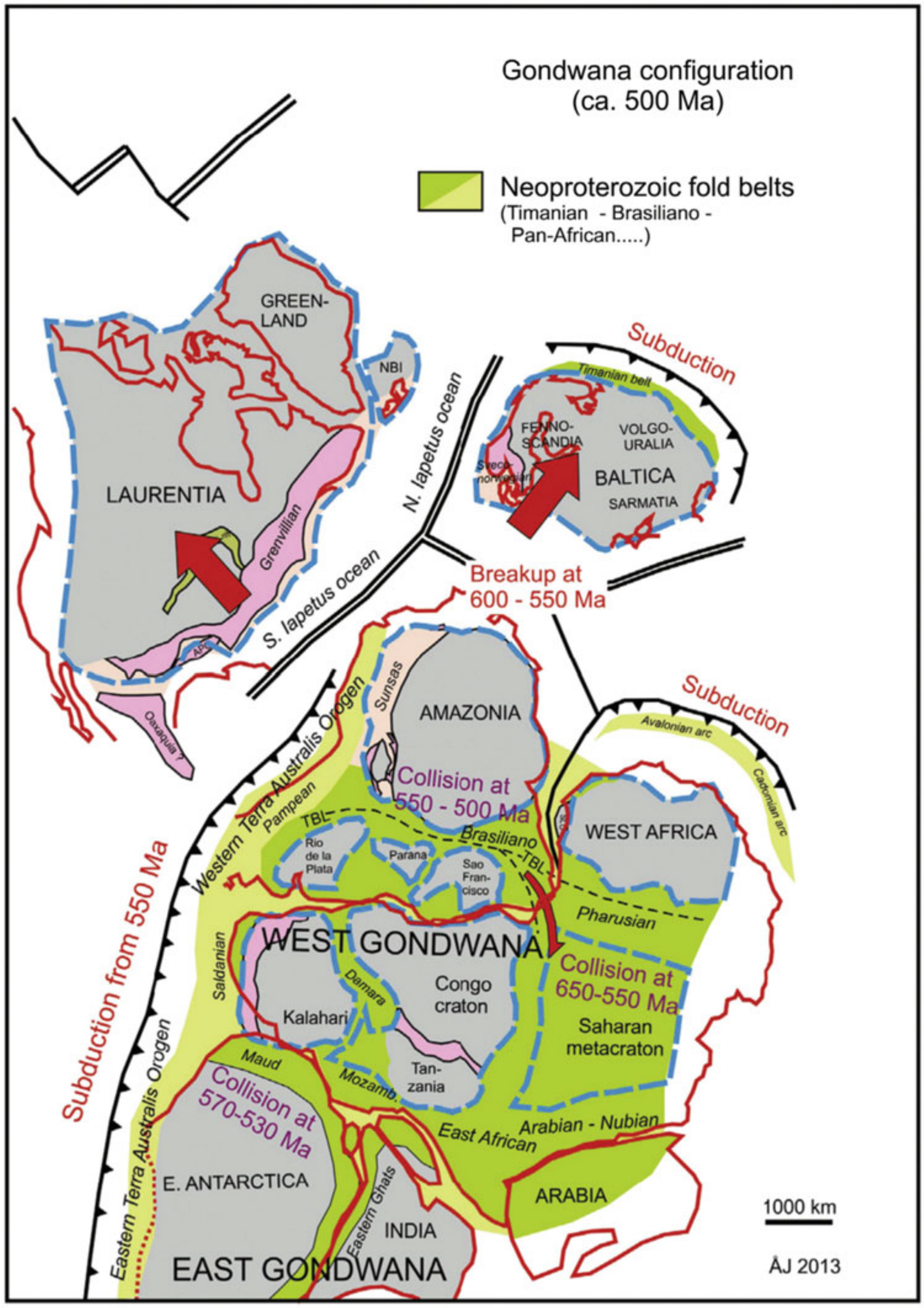

Fig. 2.5 Final assembly of Gondwana at around 550–500 Ma (after Johansson 2014). Separation of Baltica, Laurentia and Amazonia from each other

Kuribara et al. 2018) and NNE–NE (Hanson et al. 1994; Johnson and Oliver 2004), suggesting oblique convergence between West and South Gondwana (Westerhof et al. 2008).

2.2 Orogens that Shaped the Greater Gondwana

The assembly of continental blocks forming West Gondwana began within the 900–700 Ma time frame, and reached completion at 550–530 Ma, based on paleomagnetic, geologic and isotopic data (Meert and Van Der Voo 1997; Rogers and Santosh 2004; Teixeira et al. 2007). Three orogenies were recognized during the 1990s: (i) The East African Orogeny (650–800 Ma), (ii) Kuunga Orogeny (including the Malagasy Orogeny in southern Madagascar) (550 Ma) and (iii) The Brasiliano Orogeny (660–530 Ma). The East African and Kuunga are the resultant of the collision between East Gondwana and East Africa, whereas the Brasiliano Orogeny is the result of the collision between South American and African Cratons (Meert and Van Der Voo 1997).

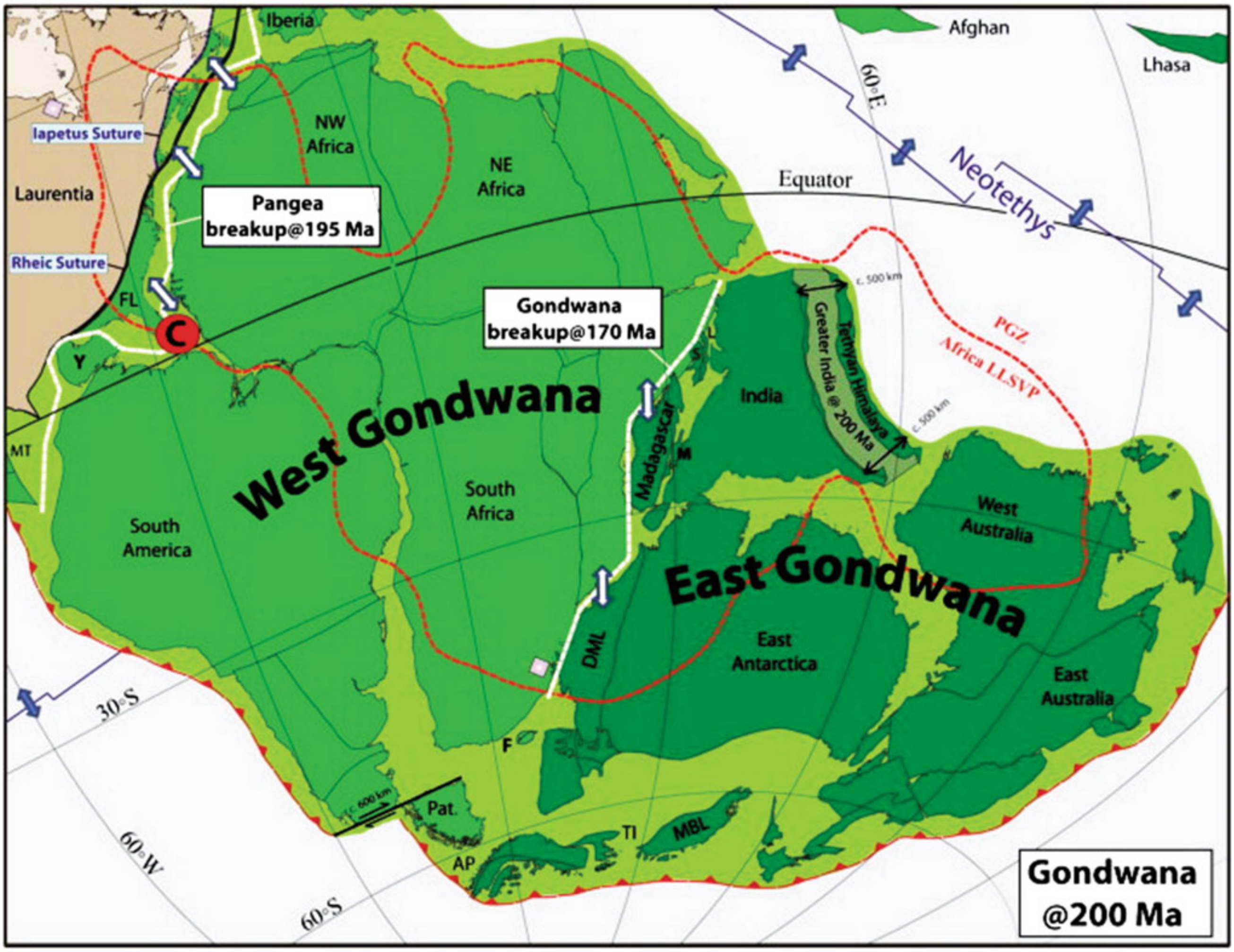

Fig. 2.6 Gondwana and other adjacent sectors within the still largely united Pangea at 200 Ma, Triassic–Jurassic boundary time. Palaeolongitudes at 30° intervals were calculated from the position of Pangea over the Africa large low-shear velocity province (LLSVP), (after Torsvik and Cocks 2013). The black dotted lines indicate the closed Iapetus and Rheic sutures, and the white dotted lines the future zones of the break-up of Pangea to form the Atlantic Ocean at 195 Ma and the Indian Ocean at 175 Ma. The 'Greater India' area is subjectively added as a northern extension of India at this time (following van Hinsbergen et al. 2012). The island arcs which undoubtedly surrounded parts of the supercontinent are omitted: AP, The Antarctic Peninsula; C, centre of the Central Atlantic Magmatic Province LIP (for its vast extent, see Fig. 2.6); DML, Dronning Maud Land, Antarctica; F, Falkland Isles, Fl, Florida; MBL, Marie Byrd Land, Antarctica; MT, the Mexican terranes of Mixteca-Oaxaquia and Sierra Madre; Pat., Patagonia; TI, Thurston Island, Antarctica; Y, Yucatan. Dotted red lines are the plume generation zones (PGZ). Solid red lines are subduction zones, with teeth on their downward sides. Blue lines are ocean spreading centres

2.2.1 The West- African–Brasiliano Orogeny

Kennedy (1964) identified a major period of deformation and metamorphism in Africa that occurred at approximately 500 Ma. Orogeny at this time was soon recognized to be widespread throughout Africa and was referred to as "Pan-African". Geologists in South America also found numerous orogenic belts of the same age and named them Brasiliano. The descendants of Rodinia have evolved during the whole Neoproterozoic and the Cambrian, and they interacted during that time (ca. 410 Ma as a whole) and generated the so-called Brasiliano/Pan-African Mobile Belts (Figs. 2.9 and 2.10) (Brito-Neves et al. 1999). Brasiliano Orogeny refers to a sequence of Neoproterozoic orogenies found mostly in Brazil, and elsewhere in South America. The Brasilia Belt is a complex orogenic system (thin and thick skin), 1100 km long, displaying structural vergence towards the São Francisco Craton, with P and T

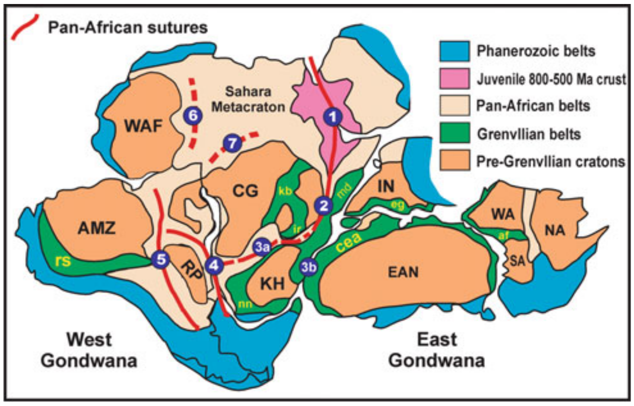

Fig. 2.7 Pan-African (c.500 Ma) and Grenville-age (c. 1000 Ma) belts in Gondwana after Harley et al. (2013) and Hoffman (1991). A major Pan-African suture was inferred to pass from juvenile Neoproterozoic arc rocks and ophiolite of the Arabian–Nubian shield (1) into the Mozambique Belt (2), and then pass either into the Damara–Zambezi Orogen (3a: Hoffman 1991) or Antarctica (3b: Shackleton 1996). Two principal sutures were identified within West Gondwana: one along the Gariep and Kaoko belts of SW Africa and the Dom Feliciano and Brasilia belts of South America (4; site of the Adamastor Ocean: Hartnady et al. 1985), and one along the Pampean, Paraguay and Araguaia belts of South America (5; site of the Clymene Ocean: Trindade et al. 2006). Extrapolation of these belts into northern Africa is hindered by a poor understanding of the Saharan Metacraton (Abdelsalam et al. 2002) but potential extensions include the Tuareg Shield (6: Black et al. 1994) and the Oubanguides Belt (7: Pin and Poidevin 1987). Pre-Grenvillian cratons: AMZ, Amazon; CG, Congo; EAN, East Antarctic; IN, Indian; KH, Kalahari; NA, North Australian; RP, Río de la Plata; SA, South Australian; WA, West Australian; WAF, West African. Grenville-age orogenic belts: af, Albany– Fraser; cea, Circum East Antarctic; e.g., Eastern Ghats; ir, Irumide; kb, Kibaran; md, Madagascar; nn, Namaqua– Natal; rs, Rondônia–Sunsas (Figure and comment are modified after Harley et al. 2013)

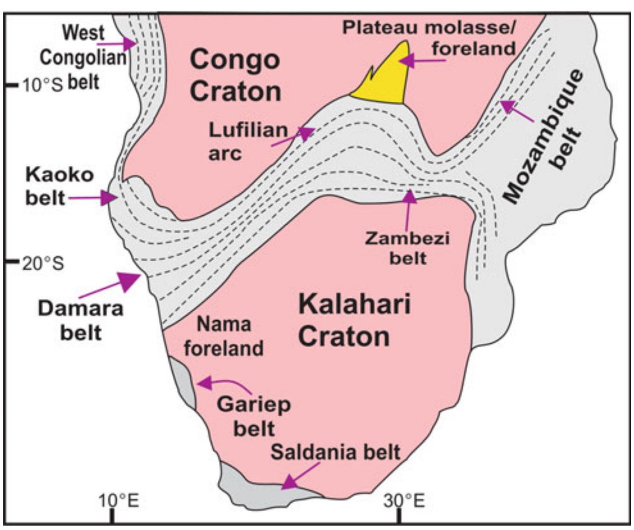

Fig. 2.8 Position of the Lufilian arc among the Pan-African belts of central and southern Africa (modified after Van Hinsbergen et al. 2012)

metamorphic conditions increasing progressively towards the west (Brito-Neves et al. 1999). The Brasiliano Orogeny is a common term for Pan-African/Brasilian Orogeny that extended not only in South America but across most of Gondwana (Rogers and Santosh 2004; Kröner and Stern 2004). The orogeny resulted in the closing of several oceans including the Puncoviscana, the Peri-Franciscano, the Goianides and the Adamastor (Tohver et al. 2010; Frimmel and Hartwig 2010). The West African–Brasilian Orogeny had been tectonically active until the end of the Cambrian period (∼490 Ma; Schmitt et al. 2004; Meert and Lieberman 2008). Prior to Gondwana break-up, the Congo Craton originally linked with the Sao Francisco Craton forming a larger continental mass wrapped by Brasiliano orogenic belts (Trompette 1994, 2000). In southern Africa, the Congo and Kalahari Cratons are separated by a transcontinental Pan-African orogeny comprising the Damara Belt, the Lufilian Arc and the Zambezi Belt (Figs. 2.8 and 2.9) (Kuribara et al. 2018). Brasiliano Orogeny along the western margin of southern Africa comprises the West Congo, Kaoko, Gariep and Saldania Belts (Figs. 2.9 and 2.10) (Hanson 2003).

2.2.2 The Damara–Zambesi–Lufilian Orogeny

The Damara–Zambezi–Lufilian Orogeny developed essentially by closure of linked, narrow ocean basins (Hanson 2003). The Zambezi Belt (Figs. 2.8 and 2.9) lies between the

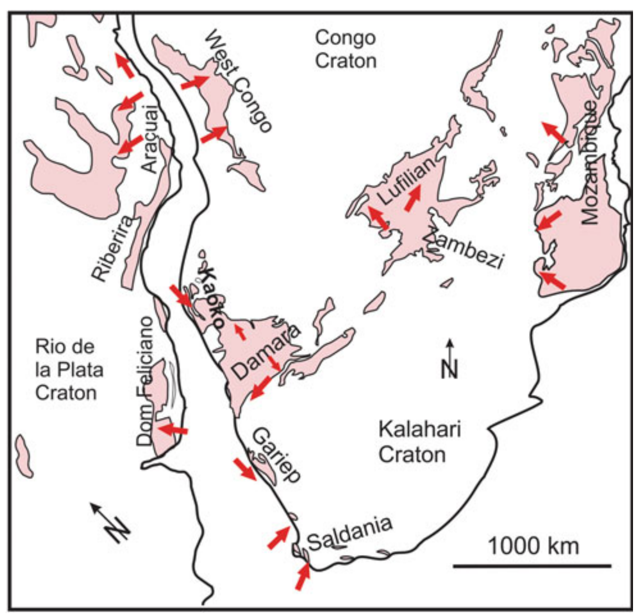

Fig. 2.9 Distribution of Neoproterozoic units in Pan-African/Brasiliano tectonic belts in southern Africa and south-eastern South America (shown in an Upper Cretaceous Gondwana break-up position); main orogenic kinematic transport directions are indicated by arrows (modified after Frimmel 2009)

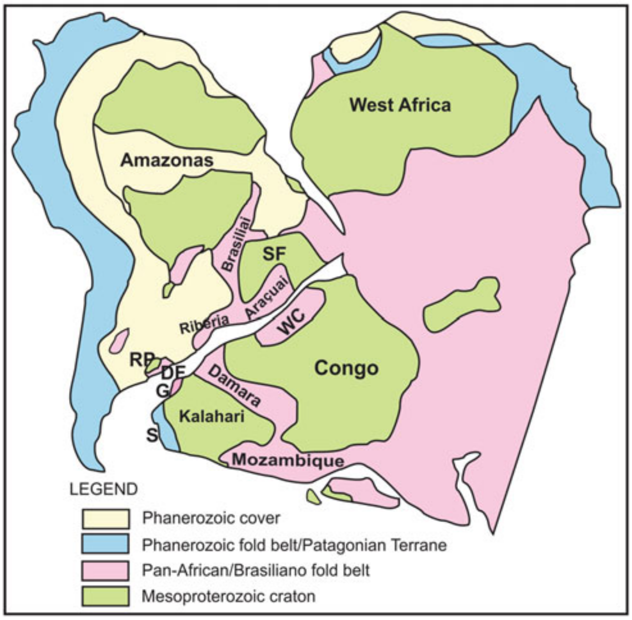

Fig. 2.10 Collage of Pan-African/Brasiliano tectonic belts around Archaean to Mesoproterozoic cratonic blocks in Africa and South America with focus on southern Africa; DF; Dom Feliciano Belt, G; Gariep Belt, LA; Luiz Alvez microplate, RP; Riodela Plata Craton, S; Saldania Belt (basement of Permo-Triassic Cape Fold Belt) modified from Unrug (1996) and Frimmel (2009)

Congo Craton and the Kalahari Craton and branches off the Mozambique Belt in northern Zimbabwe and southern Zambia (Johnson and Oliver 2002; Kröner and Stern 2004; Rogers and Santosh 2004; Kuribara et al. 2018). The Kalahari Craton is an old and stable part of the continental lithosphere that consists of the Kaapvaal, the Zimbabwe Craton, the Limpopo Belt and the Namaqua Belt, and occupies a large portion of South Africa (Johnson and Oliver 2002). The Congo Craton is an ancient Precambrian craton covered by the Palaeozoic to recent. Congo Basin together with Tanzania, West African, Zimbabwe and Kaapvaal cratons constitutes the recent continent of Africa (Johnson and Oliver 2002). These four cratons were formed between about 3.6 and 2.0 Ga and have been tectonically stable since that time (Johnson and Oliver 2002).

The Zambezi Belt was developed through two tectonothermal events, one between about 890 and 880 Ma and the other about 550 and 520 Ma. Both events affected the existing Archean to Mesoproterozoic rocks (Johnson and Oliver 2002; Kuribara et al. 2018). The second event was produced during the assembly of the Gondwana Supercontinent as a result of the Congo–Kalahari collision at the end of the Neoproterozoic (Johnson and Oliver 2002; Hargrove et al. 2003).

The Damara Orogeny occurred late in the creation of Gondwana, and the Damara Belt is exposed mainly in Namibia between the Kalahari and the Congo cratons (Jung and Mezger 2003; Gray et al. 2008). Damara Belt (Figs. 2.8, 2.9 and 2.10) is produced by the closing of the Damara and Adamastor oceans and continues northwards into the Kaoko Belt and southwards into the Saldania and Gariep Belts (Kröner and Stern 2004). The Damara Orogeny involved the suturing of the Congo–São Francisco and Río de la Plata Cratons at 580–550 Ma (together with India forming northern Gondwana) before the amalgamation of the Kalahari and Mawson Cratons in the Kuunga–Damara Orogeny at 530 Ma (southern Gondwana) (Jung and Mezger 2003; Gray et al. 2008). The Adamastor Ocean closed southwards from the Araçuaí Belt (São Francisco Craton, now in South America) to the Kaoko Belt (Congo Craton, now in Africa) 580–550 Ma and 545–530 Ma Kalahari Craton in southern Africa (Gray et al. 2008). The Kaoko Belt is developed by closing the Adamastor Ocean and comprises a shear zone in southern Angola known as the 733–550 Ma-old Puros lineament (Kröner and Stern 2004). It branches north-west from the Damara Belt into Angola and contains strongly deformed rocks (2030–1450 Ma-old). No island arcs or ophiolite are known from the Kaoko Belt (Kröner and Stern 2004). The peak of deformation and metamorphism in Damara Orogeny occurred at 530–500 Ma, while thrusting against the Kalahari Craton occurred at 480 Ma (Jung and Mezger 2003; Gray et al. 2008). All African cratons were assembled by c. 550 Ma, and the final amalgamation of north and South Gondwana were intra-cratonic during the last stages of the Damara–Kuunga Orogeny (Gray et al. 2008). The Damara Orogeny produced the Naukluft Mountains in central Namibia from 550 Ma to 495 Ma (Gray et al. 2008).

The Lufilian Arc (Fig. 2.8) is about 800 km long that extends across eastern Angola, the Katanga Province of the southern Congo and the north-west of Zambia (Ray et al. 2010; Laznicka 2010; Ray et al. 2010). It represents the continuation of the Damara Belt in Namibia northern Botswana (Kröner and Stern 2004). Its global economic importance comes from its enrichment in copper and cobalt deposits.

2.2.3 The East African Orogeny

The EAO (~6000 km N–S) represents the largest continuous Neoproterozoic–Cambrian orogeny on Earth (Fritz et al. 2013). It is subdivided into the ANS in the north, composed largely of juvenile Neoproterozoic crust (Stern 1994a, b, 2002; Johnson et al. 2011; Fritz et al. 2013) and the Mozambique Belt (MB) in the south (Figs. 2.1 and 2.11) comprising mostly pre-Neoproterozoic crust with a Neoproterozoic–early Cambrian tectonothermal overprint (Fritz et al. 2005; Collins 2006; De Waele et al. 2006; Bingen et al. 2009; Fritz et al. 2013).

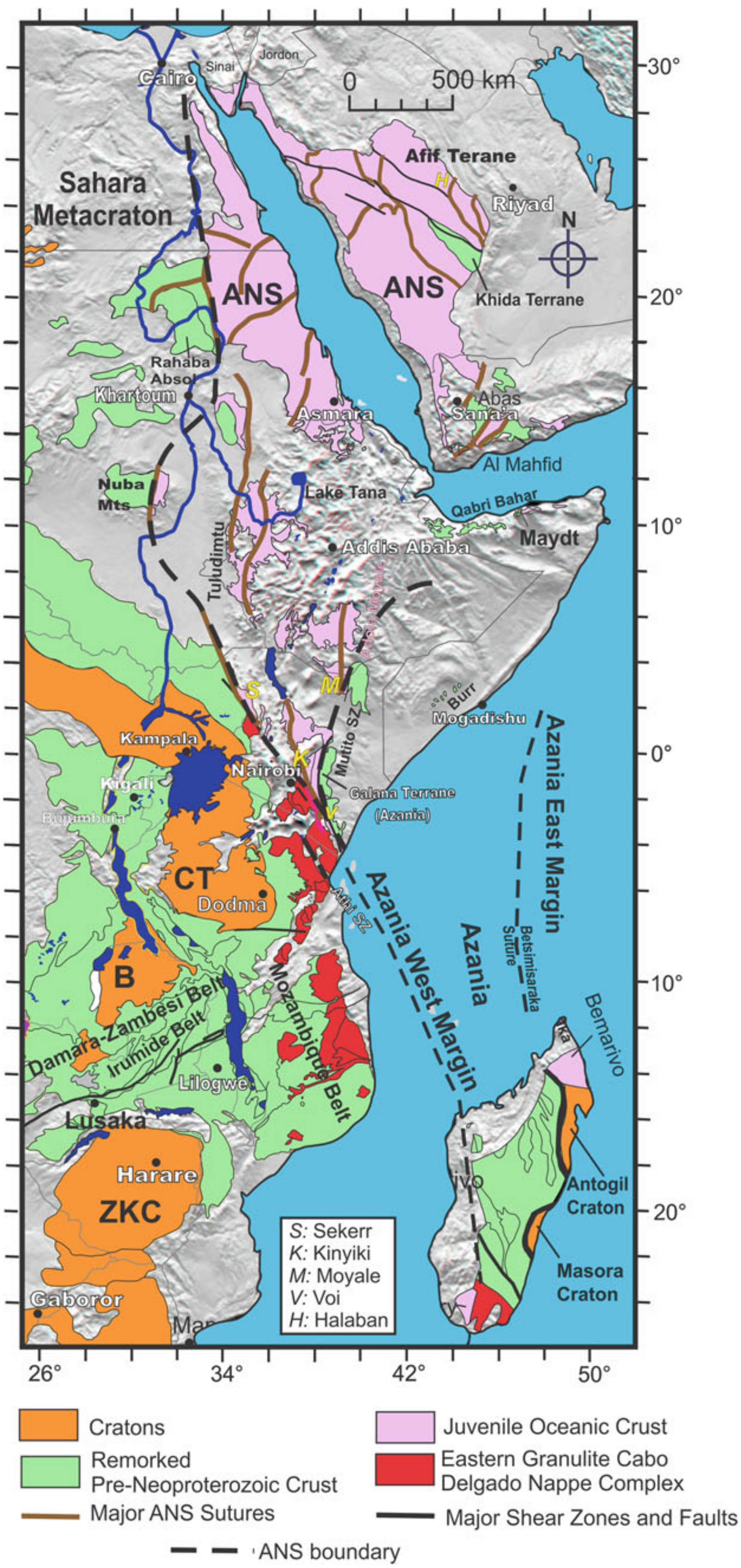

Fig. 2.11 Distribution of crustal domains in the East African Orogen. ANS, Arabian–Nubian shield; CTB, Congo–Tanzania–Bangweulu Cratons; ZKC, Zimbabwe–Kalahari Cratons (modified after Johnson et al. 2011; Fritz et al. 2013)

In the early 1980s, the concept of Gondwana assembly in the Neoproterozoic via East and West Gondwana (Australia–India–Antarctica and Africa–South America) at the Pan-African Mozambique Belt (MB) was first proposed (McWilliams 1981; Stern 1994a, b). The main stage in the Late Precambrian Gondwana assembly and the continental collision between East and West Gondwana along the line of the Mozambique Belt was named the EAO (Stern 1994a, b). The Mozambique Belt is a suture in the earth's crust between East and West Gondwana that extends from East Antarctica through East Africa (Tanzania, Kenya, Uganda, Rwanda, Burundi and South Sudan) up to the Arabian–Nubian Shield (Cutten 2002). Some of the components in the Mozambique Belt produced when the Mozambique Ocean opened and the other formed when the ocean later closed.

Bogdanova et al. (2009) concluded that Rodinia broke up in four stages between 825 and 550 Ma:

(i) The break-up was superplume initiated (Large low-shear-velocity provinces, LLSVPs) around 825–800 Ma whose influences—including crustal arching, copious bimodal magmatism and thick rift-type sedimentary sequences—have been recorded in the Arabian–Nubian Craton, Tarim, India, South China, South Australia and Kalahari.
(ii) Rifting proceeded in these same cratons (800–750 Ma) extending to Laurentia and maybe Siberia. India, Madagascar and the Congo–Säo Francisco Craton were split from Rodinia at this time or were never actual components of the supercontinent.
(iii) As the central areas of Rodinia reached the Equator around 750–700 Ma, a new pulse of magmatism and rifting continued the disassembly in western Kalahari, West Australia, South China, Tarim and most margins of Laurentia.
(iv) 650–550 Ma several events coincided: the opening of the Lapetus Ocean; the closing of the Braziliano, Adamastor, and Mozambique Oceans; and the Pan-African Orogeny. The result was the formation of Gondwana.

The late Mesoproterozoic–early Neoproterozoic events of the southern segment of the East African Orogeny include separation of the Congo and the contiguous East Sahara Cratons from Rodinia ($\sim$1200 Ma), evolution of the sedimentary basin in Kenya ($\sim$820 Ma), development of a passive margin east of the Tanganyika shield of the Congo craton, and migmatization, ophiolite emplacement and metamorphism in the Kenyan segment of the East African orogen (Shackleton 1986; Mosley 1993; Unrug 1997). In the northern EAO, bimodal rift-related magmatism has been dated at 870–840 Ma in the Nubian shield and at 880 Ma in the Arabian shield (Stern 1994a, b; Unrug 1997). The rifting events in the late Mesoproterozoic–early Neoproterozoic include opening of large Arabian–Nubian and Pharusian Oceans east and west of the Congo–East Sahara–Nile craton cluster. At about 1000 Ma, passive margins developed along the eastern borders of the Rio de la Plata, Amazonian and West African cratons (Trompette 1994). The Adamastor Ocean opened between the Congo, Saõ Francisco, Rio de la Plata and Kalahari cratons (Powell 1993).

Two partly incomparable scenarios have been proposed for Gondwana assembly (Meert 2003). In the first model, the EAO developed from an accretionary orogeny involving the amalgamation of arcs and evolved into a collisional orogeny when the Neoproterozoic Azania Continent collided with the Congo–Tanzania–Bangweulu Block at c. 640 Ma (Collins and Windley 2002). In the other model, the East Gondwana assembly c. 750–530 Ma was produced via two main orogenies: the younger Kuunga Orogeny (c. 570–530 Ma) and the older is the EAO ($\sim$750–620 Ma) (Meert 2003).

The EAO extends for more than 6000 km in Gondwana. The preserved relics of the EAO include exhumed high-PT metamorphic belts of the Mozambique Belt (Southern India, Madagascar, East Africa) to greenschist or lower grade facies belts in the ANS (NE Africa and Arabia) (Cox et al. 2012). The EAO have been resulted from the collision of amalgamated arc terranes of the ANS with the Azania and Afif terranes to the east and the Sahara and Congo–Tanzania Cratons to the west (Fritz et al. 2013) (Figs. 2.11 and 2.12). Azania is a continental block between the Indian Shield and Congo–Tanzania–Bangweulu Craton, named after the classical name for the East African coast (Collins and Pisarevsky 2005). Also, Azania is defined as microcontinent of Archean and Paleoproterozoic crust (2900–2450 Ma) extend over Somalia, Madagascar and Arabia (Afif terrane) (Fritz et al. 2013) (Fig. 2.11). A Neoarchean continental block named Al-Mahfid Block of Yemen links between Azania and Afif (Windley et al. 1996; Whitehouse et al. 2001). As a result of the Mozambique Ocean rollback, the Azania Microcontinent detached from the Congo–Tanzania–Bangweulu Craton and the subducted oceanic crust beneath central Madagascar from a subduction zone marked by the eastern Betsimisaraka Malagasy Suture (Collins and Windley 2002; Collins et al. 2000; 2007 and 2012). Separation of Azania Microcontinent from the Congo–Tanzania–Bangweulu Block ($\sim$800–750 Ma) produced a back-arc basin that formed behind the continental arc created on Azania (Collins and Pisarevsky 2005). Both the eastern and western margins of Azania are marked by Neoproterozoic volcanosedimentary sequences and rocks formed in an oceanic environment (Collins and Pisarevsky 2005). The Azanian western margin of Kenya, Ethiopia, Eritrea, and Sudan, Egypt and Saudi Arabia is marked by ophiolites of Neoproterozoic age and juvenile volcanics (Abdelsalam and Stern 1996; Rogers and Santosh 2004). The ocean between Azania and East Africa was consumed in the Tonian along an intra-oceanic arc (Collins et al. 2012). The ocean closed at ∼630 Ma by collision between the Azanian and Congo-Tanzanian continents (Collins and Windley 2002; Collins 2006). This collision produced highly grade metamorphosed and deformed rocks in eastern Africa (Hauzenberger et al. 2004, 2007) and southwestern Madagascar (Jöns and Schenk 2011). At the same moment, or not long after the East African Orogeny, a sequence of Cadomian terranes such as Avalonia and Armorica were rifted off the northern Gondwana margin early in the Paleozoic and accreted to Laurentia (Keppie et al. 2003; Fritz et al. 2012, 2013). The rifting of these terranes, likely due to the withdrawal of the Cadomian arc, may have enabled the ANS to be expelled to the north (Jacobs and Thomas 2004; Meert and Lieberman 2008; Fritz et al. 2012, 2013).

2.2.4 Kuunga Orogeny

The EAO resulted from the amalgamation of arc terranes in the northern ANS and continental collision between East African pieces and parts of the Azania terrane in the south (Collins and Pisarevsky 2005). The change from arc suturing to continental collision settings is seen in southern Kenya where southernmost arcs of the ANS merge with thickened continental margin suites of the Eastern Granulite Belt. The younger ca. 570–530 Ma Kuunga Orogeny heads from the Damara–Zambesi–Irumide Belts (De Waele et al. 2006) over

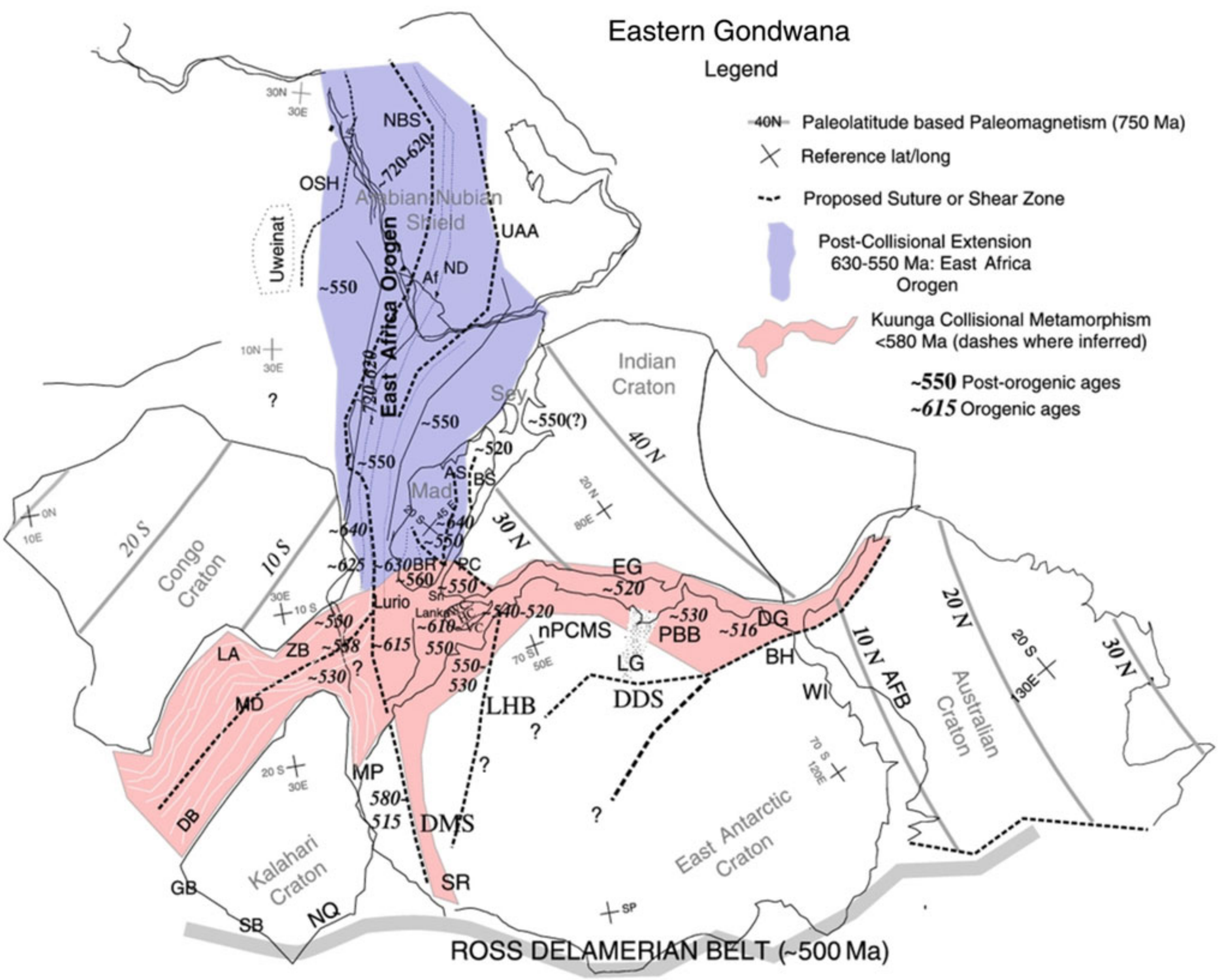

Fig. 2.12 Kuunga-570 to 530 Ma collisional metamorphism of the Kuunga orogeny in red, 620–550 Ma post-collisional extension of the East African Orogeny in blue (after Meert 2003)

Tanzania–Mozambique to southern India and clashes with the EAO in southern-central Tanzania (Fig. 2.12). Two transitional orogen settings may be defined, (1) that between island arcs and inverted passive continental margin within the EAO and (2) that between N–S trending East African and W–E trending Kuunga Orogenies. SE-Kenya's Neoproterozoic arc suites are revealed as a thin stripe between west Azania and the eastern granulite belt. This suture is a long, NNW extended belt that roughly aligns with the prominent southern ANS shear zones that intersect at the ANS's southern tip (Athi and Aswa Shear Zones) (Collins and Pisarevsky 2005; Fritz et al. 2009, 2012, 2013).

The Kuunga Orogeny (Fig. 2.12) is an orogeny that occurred during the Ediacaran and Cambrian in South-East Africa. It is slightly younger than the East African orogeny and produced by collisions between India and Australia–East Antarctica and Azania and India (Meert 2003; Collins 2003; Jacobs and Thomas 2004; Boger and Miller 2004; Collins and Pisarevsky 2005; Kelsey et al. 2008; Cox et al. 2012). It documents the collision between north and south Gondwana, or what is today Dronning Maud Land in Antarctica and northern Mozambique in Africa (Meert 2003; Grantham et al. 2013). India collided with Australia–East Antarctica and India collided with Azania in the Kuunga orogeny before the formation of Gondwana (Collins and Pisarevsky 2005; Kelsey et al. 2008; Cox et al. 2012). The proposed location of the Azania–India collision named the Malagasy Orogeny by Collins and Pisarevsky (2005) for the Ediacaran to Cambrian orogeny that resulted as India collided with Azania and the Congo–Tanzania–Bangweulu Blocks. The Kuunga Orogeny is prevalent in the southern East African orogeny in southern India (Fig. 2.12), Madagascar and central Arabia (Stern 1994a, b; Fritz et al. 2013). In East Africa, an E–W trending belt with Kuunga ages spreads from Zambia–Malawi across Mozambique and further into southern India and Sri Lanka (Collins et al. 2007; Plavsa et al. 2012; Fritz et al. 2013). Overprinting of Kuunga structures with the 620 Ma East African fabrics has led to complex patterns of interference in the Eastern Granulites.

2.3 The Arabian–Nubian Shield (ANS)

The ANS is southward narrowing belt that forms the suture shared between East and West Gondwana at the northern end of the EAO (Stern and Kröner 1993; Stern 2002; Stern et al. 2010; Ali et al. 2009a, b, 2012a, b; Johnson et al. 2011; Merdith et al. 2017). It stretches over 3500 km to the north and 1500 km to the east and west (Fig. 2.13), underlying an area of $\sim 2.7 \times 10^6$ km^2 in the northern half of the EAO (Stern 1994a, b; Johnson 2014). It is representative of the continental crust that underlies NE Africa, SW Asia and Arabia where the eastern half of the shield is a segment of the Arabian Plate, while the western part pertains to the African Plate (Johnson and Woldehaimanot 2003; Rogers and Santosh 2004).

The East Gondwana assembly was driven mainly by the Mozambique subduction recorded in the formation of two main orogens, Eastern Orogen and Kuunga (Meert 2003; Collins and Pisarevsky 2005; Merdith et al. 2017). West Gondwana is represented by Archaean and Palaeoproterozoic continental crust belonging to the Saharan Metacraton, which was strongly reworked by Neoproterozoic thermal and deformational events and is discontinuously exposed west of the Nile (Fritz et al. 2013). The Saharan Metacraton is a large area of continental crust in the north-central part of Africa. Other names have been used to describe the general area that reflects different views of its nature and extent. These include "Nile Craton", " Ghost Sahara Congo Craton" and "Eastern Saharan Craton" (Stern 2002). Abdelsalam et al. (2011) defined a metacraton as "a craton that has been remobilized during an orogenic event but is still recognizable dominantly through its rheological, geochronological and isotopic characteristics". Liégeois et al. (2013) summarized the main distinctive characteristics of the metacraton as follows: (1) absence of pre-collisional events; (2) absence of lithospheric thickening, high-pressure metamorphism being generated by subduction, leading to high gradient in strain and metamorphic intensity; (3) preservation of pre-collision allochthonous ocean terranes; (4) abundant post-collisional magmatism associated with shear zones but not with lithospheric thickening; (5) presence of high-temperature–low-pressure metamorphism linked to post-collisional magmatism; (6) intracontinental orogenic belts not related to either subduction or oceanic basin closure.

2.3.1 Geology of the Arabian–Nubian Shield

The ANS consists of Precambrian metamorphic rocks cropping out along the coastline of the Red Sea, and exposed in areas of the Arabian and Sahara Deserts (Fig. 2.14), and in the highlands of Yemen, the Asir Province of Arabia and Ethiopian Highlands of the south (Figs. 2.11, 2.13 and 2.14). The ANS includes areas of western Arabia and northeastern Africa (Somalia, Yemen, Ethiopia, Eritrea, Sudan, Saudi Arabia, Egypt, Jordan and Palestine) (Johnson and Woldehaimanot 2003; Johnson et al. 2011; Fritz et al. 2012, 2013; Johnson 2014). Formation of arcs in the ANS occurred over a $\sim$300-million-year period including supercontinent Rodinia break-up and the assembly of supercontinent Gondwana. The arc assemblages include metavolcanics and volcanoclastic metasediments as well as large amounts of diorite, tonalite, trondhjemite and granodiorite. Geochemically, the arcs have calc-alkaline to tholeiitic and locally MORB chemistry (Johnson 2014). The oceanic crust in the

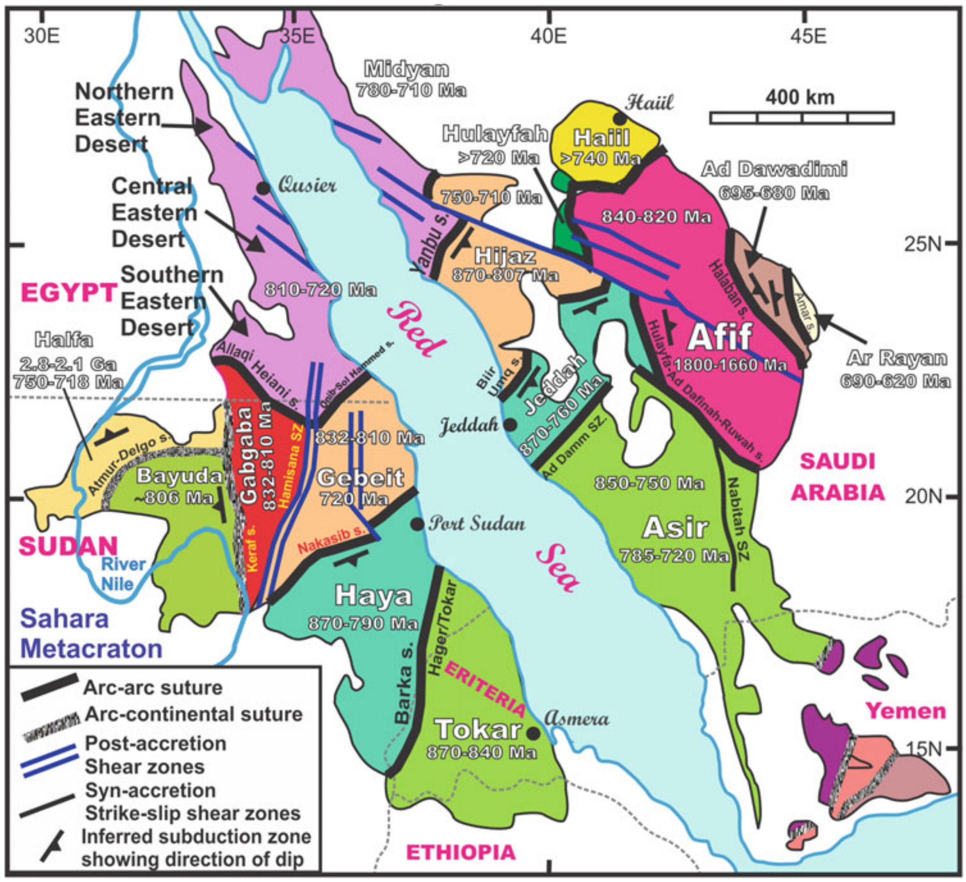

Fig. 2.13 Tectonic map of the Arabian–Nubian shield showing the locations and extents of terranes, sutures and post-accretionary structures Modified after Johnson and Woldehaimanot (2003), Hargrove et al. (2006) and Abdelsalam (2010)

ANS is represented by ophiolite complexes, ranging from 845 to 675 Ma (Stern et al. 2004; Johnson 2014) (Fig. 2.14). The arc assemblages range from ~870 to 615 Ma (Stern et al. 2004). Based on differences in age of formation, structural style and, locally, isotopic characteristics, the arc assemblages are divided into tectonostratigraphic terranes (Johnson et al. 2011; Stern et al. 2004; Johnson 2014) (Figs. 2.11 and 2.13). Boundaries between the terranes are ophiolite-decorated shear zones or sutures and transcurrent shear zones (Johnson 2014) (Fig. 2.13). Most protoliths are early to middle Cryogenian, but Tonian rocks are locally preserved in the central and southern ANS (Johnson 2014). Arc amalgamation and suturing occurred between ~780 and 600 Ma. The accretion between the ANS and the Saharan Metacraton reflects a terminal collision between the ANS and West Gondwana blocks at approximately 650–580 Ma (Johnson et al. 2011; Fritz et al. 2012, 2013; Johnson 2014). Metamorphic grades in the ANS range from granulite facies in the south, decreasing to greenschist facies to the north and occurred during transpressional east–west shortening, north–south extension, strike–slip shearing and tectonic escape (Johnson 2014).

In the south, the west margin of the ANS is defined by juxtaposition of ophiolite and ophiolitic mélanges and juvenile Neoproterozoic arc magmatic terranes with the MB, the Sahara Metacraton and the Archean Congo–Tanzania Craton (Fritz et al. 2012, 2013) (Figs. 2.11, 2.13 and 2.15). The Congo Craton is an ancient Precambrian craton that with the Kaapvaal, Zimbabwe, Tanzania and West African Cratons form the modern continent of Africa (Rogers and Santosh 2004; Ernst et al. 2013). These cratons were formed between about 3.6 and 2.0 Ga and have been tectonically stable since that time (Rogers and Santosh 2004; Ernst et al. 2013). The Congo Craton occupies a significant portion of Central South Africa, from the Kasai region of the Democratic Republic of Congo to Sudan and Angola. It forms parts of the countries of Gabon, Cameroon and the Central African Republic. A small portion extends into Zambia as well, where it is called the Bangweulu Block (Ernst et al. 2013).

Most of the ANS western margin is not defined in the north, as it is covered by Mesozoic to Cenozoic sedimentary rocks (Fritz et al. 2013). In Sudan and Kenya, the western margin crops out in the Keraf Arc-Continent Suture (Abdelsalam et al. 1998), the Kabus ophiolite (Shellnutt et al. 2017, 2018), the Sekerr ophiolite of northwestern Kenya (Mosley 1993; Shellnutt et al. 2017) and the Kinyiki ophiolite (Fig. 2.13) of southern Kenya (Frisch and Pohl

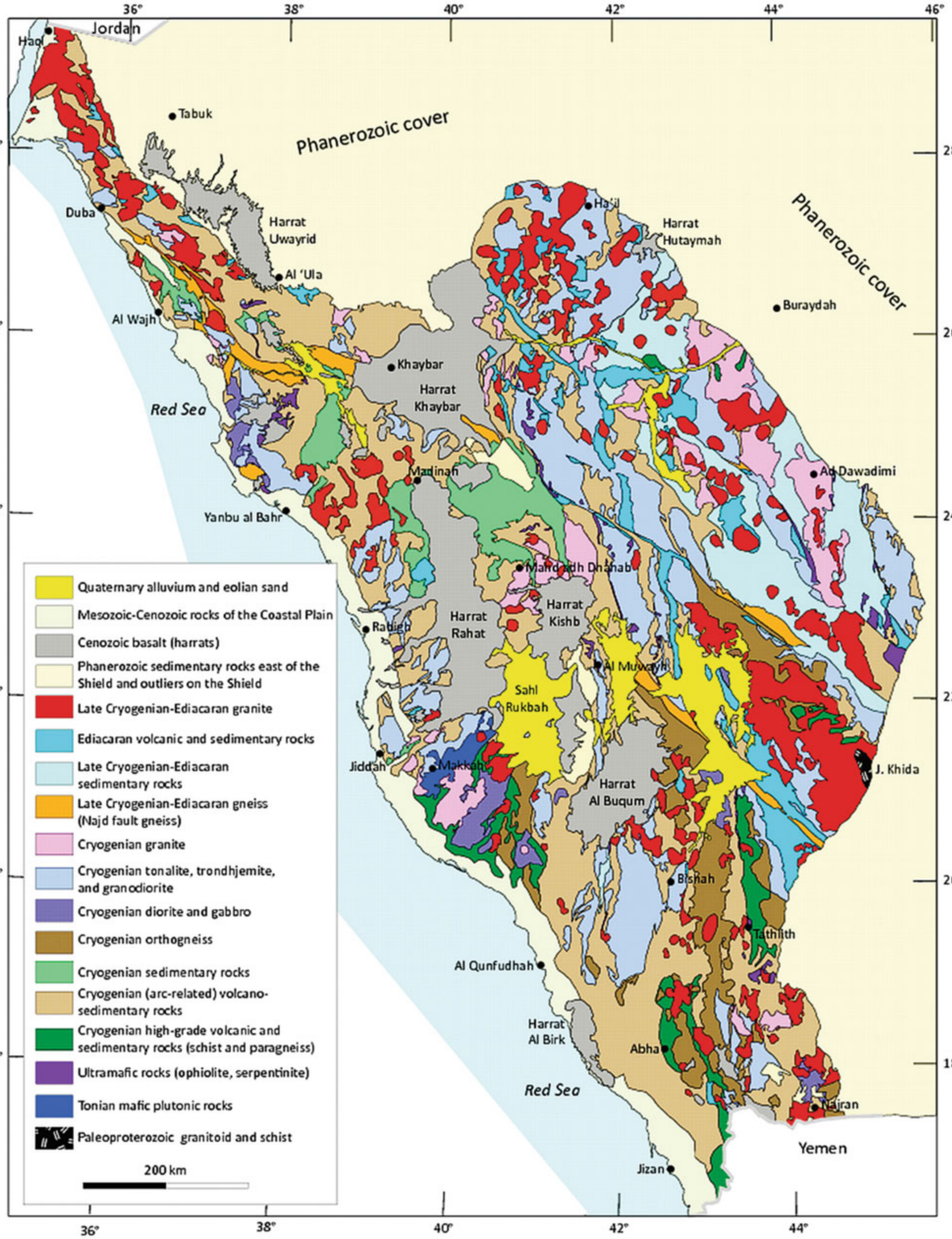

Fig. 2.14 Simplified geological map of the Arabian shield (after Johnson 2006)

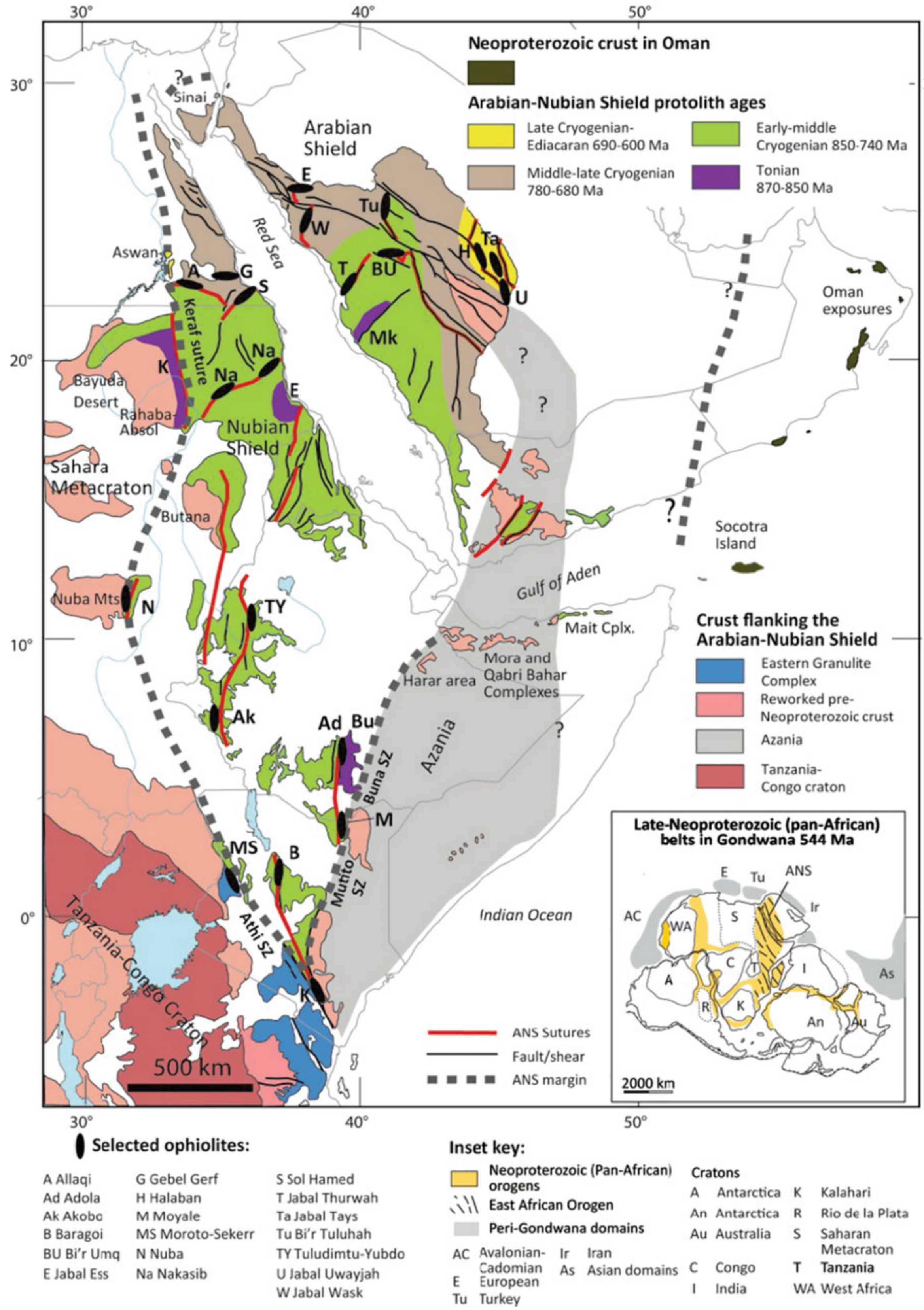

Fig. 2.15 The Arabian–Nubian Shield in relation to older crust on its margins (after Fritz et al. 2013 and Johnson 2014). Ophiolites schematically shown after (Berhe 1990): A Allaqi; Ad Adola; Ak Akobo; B Baragoi; BU Bi'r Umq; E Jabal Ess; G Gebel Gerf; H Halaban; K Kinyiki; M Moyale; MS Moroto-Sekerr; N Nuba; Na Nakasib; S Sol Hamed; T Jabal Thurwah; Ta Jabal Tays; Tu Bi'r Tuluhah; TY Tuludimtu-Yubdo; U Jabal Uwayjah; W Jabal Wask (after Johnson 2014)

1986). The Keraf Suture is an N-trending suture about 500 km long and ~50 km wide. It formed during Gondwana amalgamation and lies between the ANS in the east and the older Nile Craton to the west (Abdelsalam et al. 1998). The southern part of the suture is dominated by N- and NNW-striking, sinistral strike–slip shear zones, whereas the northern part is deformed by N-trending upright folds (Abdelsalam et al. 1998). The southern tip of the ANS is represented by old amphibolites and gneisses (955–845 Ma) close to Galana–Athi shear zone (Fig. 2.15) which is considered as part of Azania craton (Bauernhofer et al. 2008) (Figs. 2.11 and 2.13).

The eastern margin of the ANS in Kenya, Ethiopia and Somalia is marked by the Mutito-Bruna Shear Zone (Mosley 1993). Mutito-Bruna Shear Zone (Figs. 2.11 and 2.15) occurs in contact with Azania and represents intense ductile shearing producing closely spaced steep, upright, N–S or NNW–SSE ductile zones, often with a constrictional, linear tectonite fabric generally with a sinistral shear sense (Mosley 1993). The Mutito shear zone (Figs. 2.11 and 2.15) separates the Barsaloi-Adola Moyale ophiolitic belts from the poorly exposed older suites of the Burr Complex in southern Somalia (Mosley 1993). The boundary between shared by Azania and the ANS in Yemen is probably defined by arc-continent sutures along the Abas and Al-Mahfid terranes (Figs. 2.11 and 2.13). The boundaries between the ANS and the Afif Terrane and Khida Subterrane in eastern Saudi Arabia are arc–arc sutures (Johnson et al. 2011); therefore, they considered as crustal blocks within the ANS (Fig. 2.13).

The ANS initiated by at c. 870 Ma by rifting of Rodinia, closure of the Mozambique Ocean and accumulation of volcanic arcs during a few hundred million years before ~600 Ma (Rogers and Santosh 2004; Johnson et al. 2011; Fritz et al. 2013) on thin juvenile crust of the Mozambique Ocean. This region of juvenile crust extends to the northern margin of the Ethiopian flood basalts and also appears in scattered outcrops just south of the basalts (Rogers and Santosh 2004; Fritz et al. 2013). The ANS incorporates Middle Cryogenian–Ediacaran (790–560 Ma) terrestrial and shallow-marine sedimentary and volcanic successions (Fig. 2.16) which lie unconformably on Cryogenian juvenile crust. The older units were deposited in the central ANS after 780–760 Ma shearing and suturing. In the northern ANS, ~700 Ma suturing is consistent with Middle Cryogenic Basins. In the eastern ANS, Late Cryogenian basins were superimposed and accompanied by Nabitah Orogeny at 680–640 Ma (Johnson et al. 2011, 2013). Ediacaran successions are found in pull-apart and transpressive basins formed during final consolidation of the ANS (Johnson et al. 2011, 2013).

Ediacaran post-amalgamation basins are widespread in the ANS (Fig. 2.17). The fill of these basins includes Dokhan volcanics and sedimentary rocks belonging to Hammamat and Thalbah Groups, and the Saramuj Conglomerates (Johnson et al. 2011, 2013). Deposition of oceanic volcanic arcs was followed by intrusion of post-tectonic granites and stabilization of the terrane between 600 and 500 Ma, terminated at c. 550 Ma by the transformation of the northerly sections of the EAO into a passive margin on the southern shore of palaeo-Tethys (Fritz et al. 2013). The Kuunga shortening phase occurs under central Arabia's Phanerozoic and is absent from the exposed ANS (Johnson et al. 2011; Cox et al. 2012).

2.3.2 Ophiolites of the Arabian–Nubian Shield

The ANS formed from ~870 to 550 Ma is one of the largest tracts of juvenile Neoproterozoic crust (Johnson 2014). The main diagnostic features of the ANS ophiolites are (i) greenschist facies metamorphism, (ii) dismembered, altered and consist mainly of tectonized harzburgites, pillowed basalts and gabbros as well as plagiogranite (Fig. 2.15), (iii) several ophiolites have sheeted dike complexes (such as Ghadir, Onib and Ess), (iv) shearing along NW-trending strike–slip faults and shear zones pertaining to the Najd Fault System especially ophiolites in the northern ANS (Sultan et al. 1988; Stern et al. 2004) and (v) form nappe complexes along terrane sutures, especially In the northern ANS.

Mid-Neoproterozoic ophiolites (690–890 Ma) are well represented in the ANS and extend 3000 km N–S and >1000 km E–W from the farthest north (Jebel Ess) almost to the equator, and from Rahib in the west to Jabal Uwayjah (45°E) in the east (Stern et al. 2004), encompassing an area of around two million square kilometres (Fig. 2.1, Stern et al. 2004). The ophiolite belts represent sutures marking the location of island arcs extending to those in Saudi Arabia on a pre-Red Sea drift reconstruction and further south to Mozambique (Fig. 2.15). North of the Bi'r Umq-Nakasib suture, the ophiolite belts strike nearly E–W (Stern et al. 2004). Bi'r Umq-Nakasib suture extends SW from Thurwah and Bi'r Umq Ophiolites in Arabia and extends over the Red Sea through Oshib and Meritri Ophiolites in Sudan.

Reconstruction of relative ages across the ANS demonstrates that the ophiolite belts young to the east (Berhe 1990). Geological and geochemical studies suggest rifting at c. 1200 Ma, and subsequent convergence led to the development of intra-oceanic arcs and associated marginal basins in the north and narrow basins further south in Kenya and Tanzania (Berhe 1990). Many of the ANS mafic–ultramafic complexes evolved in a seafloor spreading environment, while others are the substrate of island arcs (Quick 1990, 1991; Stern et al. 2004), while others may be layered

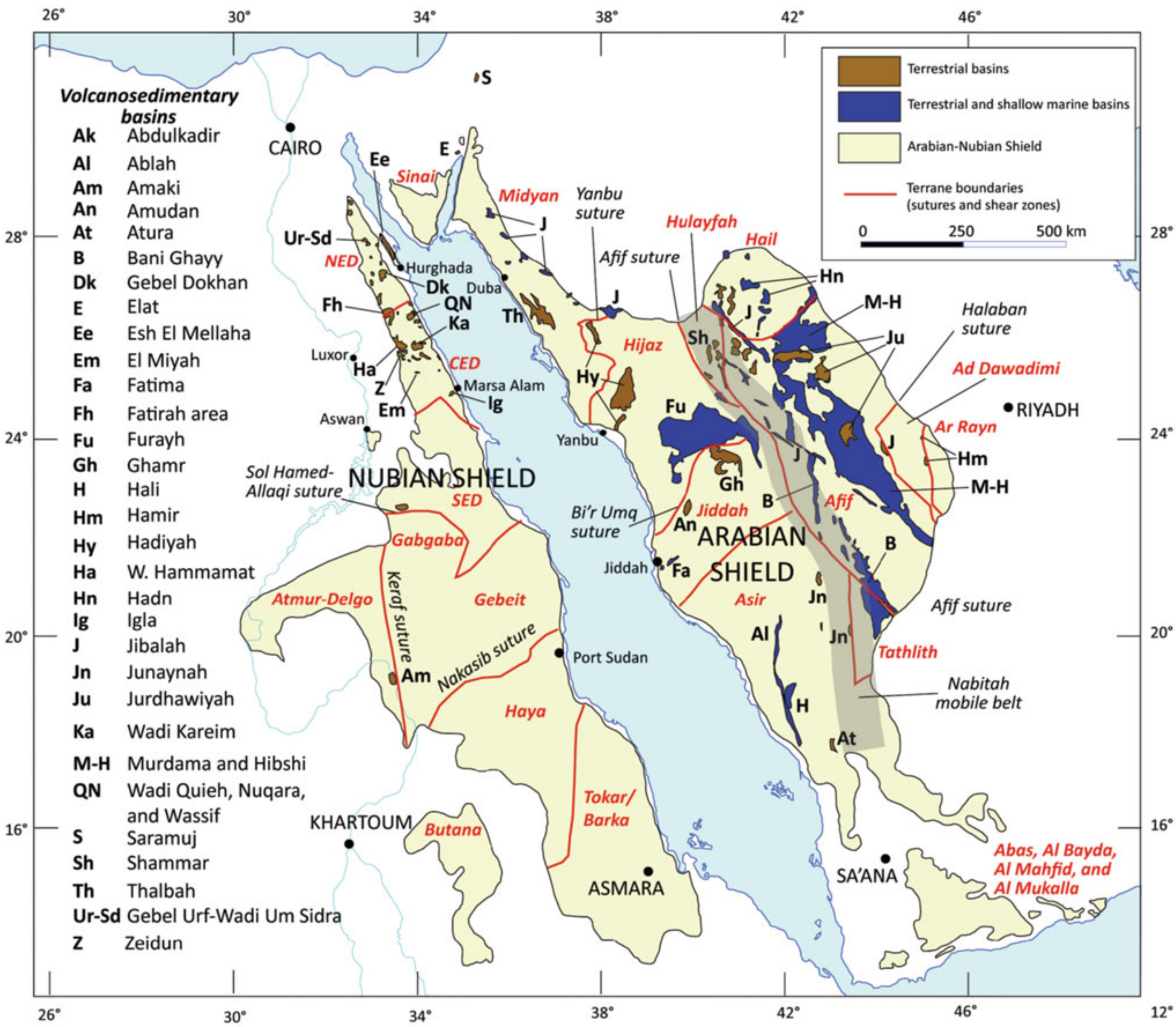

Fig. 2.16 Volcanosedimentary basins in the Arabian–Nubian Shield unconformable on basement composed of older arc rocks and amalgamated terranes (terrane names in red italics) (after Johnson et al. 2011, 2013)

intrusions (Stern et al. 2004). The Yubdo complex in Western Ethiopia consists of harzburgite, cumulate sequence of ultramafic, gabbroic rocks and metabasalts (Berhe 1990). The Baragoi complex in Kenya is composed of tectonized harzburgite, dunite with chromite pods, ultramafics and gabbroic rocks. Available evidence for the Adola Moyale Belt, in Southern Ethiopia and NE Kenya, point to MORB and island-arc geochemistry, of a back-arc environment (Berhe 1990). The Ingessana Complex in Sudan has an island-arc tholeiitic tectonic affinity that indicates development in a supra-subduction setting. The data from Sol Hamed Complex in Egypt suggest a back-arc basin (Berhe 1990).

ANS ophiolitic lavas often describe a subalkaline suite of low K and high Ti contents. They reveal both tholeiitic and calc-alkaline affinities and include a significant subordinate proportion of boninites Arabian shield (Stern et al. 2004). ANS ophiolites are frequently associated with a 1- to 3-km-thick sequence of ultramafic cumulates (dunite- and pyroxene-rich lithologies) transitioning into higher layered gabbroic rocks (Stern et al. 2004). A supra-subduction zone setting for the Egyptian Eastern Desert ophiolites is commonly accepted (e.g. El Bahariya and Arai 2003; Azer and Khalil 2005; Azer and Stern 2007; Farahat et al. 2011; Ahmed et al. 2012; Abdel-Karim et al. 2016; El Bahariya 2018). Furthermore, a back-arc setting is generally favoured

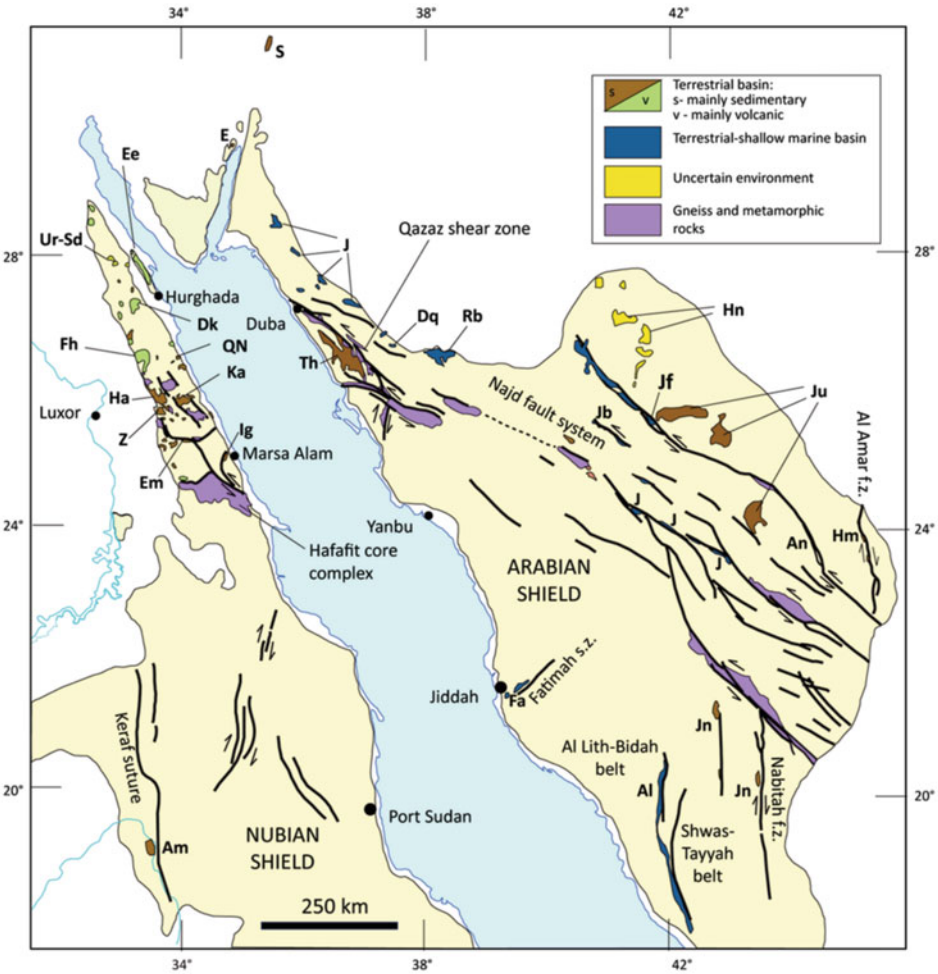

Fig. 2.17 Ediacaran sedimentary and volcanic basins in the Arabian–Nubian Shield, showing their common juxtaposition to shear zones, gneiss belts and core complexes (gneiss domes) (after Johnson et al. 2011, 2013). Identified successions and basins: Al—Ablah; Am—Amaki; An—Antaq; E—Elat Conglomerate; Ee—Esh El Mellaha; Em—El-Miyah; Dk—Gebel Dokhan; Dq—Dhaiqa; Fa—Fatima; Fh—Fatirah area; Ha—Wadi Hammamat; Hm—Hamir; Hn—Hadn; Ig—Wadi Igla; J—unnamed Jibalah group basins; Jb—Jibalah; Jf—Jifn; Jn—Junaynah; Ju—Jurdahiway; Ka—Wadi Kareim; QN—Wadi Quieh, Nuqara, and Wassif; Rb—Rubtayn; S—Saramuj Conglomerate; Th—Thalbah; Ur-Sd—Gebel Urf-Wadi Um Sidra; Z—Zeidun

(El-Sayed et al. 1999; Ahmed et al. 2001; El Bahariya and Arai 2003; Farahat et al. 2004; El Gaby 2005; Abdel-Karim et al. 2008; El Bahariya 2018). Also, a fore-arc environment was proposed on the basis of whole-rock chemistry and mineral analyses of serpentinites (Stern 2004; Azer and Stern 2007; Azer et al. 2013).

Neoproterozoic ophiolites and ophiolitic mélange (El Bahariya 2012) are widespread in the southern and central sectors of the ENS. The components of ophiolites are dismembered and altered and include harzburgite, cumulate ultramafics, sheeted dikes, pillowed basalt, layered gabbro and plagiogranite (Stern et al. 2004). A complete ophiolite section was detected in a few places in the ENS (e.g. Gerf, Fawkhir, Ghadir) including serpentinized ultramafics, layered and isotropic gabbros, sheeted dykes and mafic lavas including pillow basalts. Mostly, the Egyptian ophiolites occur as tectonized masses, sheets, lenses and mélanges of these ophiolitic components (El Sharkawy and El Bayoumi 1979; Azer et al. 2013). The ophiolites in the Central Eastern Desert show characteristics of both MORB-type and SSZ-type ophiolites and classified from oldest to youngest by El Bahariya (2018) based on mode of occurrences and geological characteristics into (1) MORB intact ophiolites (e.g. Muweilih, Ghadir), (2) dismembered ophiolites and (3) arc-associated ophiolites (e.g. El Sid, Esel). Dismembered ophiolites occur either as (i) ophiolite blocks in mélanges (e.g. Kareim El Abiad tectonic mélange, Garf tectonic mélange, Muweilih olistostrome, Esel olistostrome, Um Esh olistostromal mélange and Mubarak olistostromal mélange) or as (ii) ophiolites along structural contacts (Abu Meriewa occurrence, Sodmien occurrence, Um Saneyat occurrence and Um Khariga occurrence (El Bahariya 2018).

2.3.3 How Juvenile Is the Arabian–Nubian Shield?

As mentioned before, the ANS is the northern half of a great collision zone called the EAO. This collision zone was created at the end of the Neoproterozoic time, when East and West Gondwana combined to create the Gondwana supercontinent. Across what is now Southern Africa, the most intense part of the collision occurred, where older crust in Tanzania, Mozambique and Madagascar was remobilized to form the Mozambique Belt (MB). This great collision was responsible for the Pan-African Orogeny near the end of Neoproterozoic time (Kröner and Stern 2004). The crust of the MB is quite different from that of the Arabian–Nubian Shield, which is predominantly "juvenile" crust, that is, crust that formed from partial melting of Earth's mantle, although much older Archean and Paleoproterozoic crustal materials, is exposed west of the Nile in Egypt, in the SE part of the shield in Arabia, in eastern Ethiopia and in Yemen (Kröner and Stern 2004).

The Arabian shield retains a sustained magmatic record of amalgamated juvenile terranes that contain a wide variety of early Neoproterozoic to Cambrian granitoids intruding into volcanosedimentary basin assemblages. Robinson et al. (2014) provided U–Pb zircon dating of 19 examples of granitoids that intruded eight terranes of the Arabian shield and defined four separate magmatic events: anorogenic (~ 525 Ma), post-tectonic (~ 620 Ma), syncollisional (~ 710 Ma) and island arc (~ 845 Ma).

With the development of island-arc magmatism associated with the closing of the Mozambique Ocean, syncollisional magmatism in the ANS at 715 Ma reflects the first level of terrane amalgamation in the Mozambique Ocean due to the convergence associated with East Africa and East Gondwana subduction. The accretion/arc collision in the western ANS (west of Afif) was terminated at ~ 630 Ma due to collision of Azania with the Congo–Tanzania–Bangweulu Block (Collins and Windley 2002; Collins and Pisarevsky 2005). The emergence of post-tectonic magmatism intruding the Nabitah Belt and the creation of western ANS back-arcs reinforce this understanding. East of Afif, the appearance of ~ 611–607 Ma post-tectonic magmatism cross-cutting the Halaban Suture, possibly corresponds with the collision of the Afif-Abas Block and eastern Arabia (Collins and Pisarevsky 2005). The final phases of the Gondwana assembly are reported from ~ 5570–530 Ma in the northern EAO and split into two orogenic periods, the Kuunga and Malagasy, respectively (Collins et al. 2014 and references therein). It is proposed that India's interaction with the Congo–Tanzania–Bangweulu Block (Malagasy Orogeny) has produced the ca. 525 Ma A-type magmatism (Hijaz Terrane). It is well known that the major transform fault systems such as the NFS are spread throughout the northern Arabian shield and shape a sequence of reactivated events that cause magmatism (Stern 1985; Johnson et al. 2011) such as ~ 525 Ma Mardabah Complex.

However, no crust older than ~ 890 Ma (Deschamps et al. 2004; Hargrove et al. 2006) is exposed in the core of the juvenile ANS, and crust of Mesoproterozoic age is not exposed anywhere in the ANS. Hargrove et al. (2006) concluded that the ANS is less juvenile than presently appreciated and may contain a significant amount of continental crust and estimates of crust-formation rates that cite the ANS as a model for juvenile crust should consider this possibility.

2.3.4 Accretion and Thickening in the Arabian–Nubian Shield

The relics of the EAO (≈6000 km long in Gondwana) include high-grade metamorphic complexes in the Mozambique Belt, and greenschist or lower grade belts of volcanics, plutons and sedimentary rocks in the Arabian–Nubian shield (Cox et al. 2012). The metamorphism connected to the closing of the Mozambique Ocean in southern India and eastern Madagascar was linked to an Ediacaran collision between the Congo–Tanzania–Bangweulu Block and India in the Neoproterozoic time (Clark et al. 2009; Collins et al. 2003, 2007; Cox et al. 2012) that had previously accreted a continent known as Azania during the Cryogenian (Collins 2006; Collins and Windley 2002) to form the Malagasy Orogen (Collins and Pisarevsky 2005).

The ANS took about 300 million years to develop. The oldest rocks related to the ANS crust's formative cycle created by the coalescence of island-arc and back-arc basins and even oceanic plateaus. The oldest rocks in this series are around 870 Ma and are located in E Sudan and southeast Saudi Arabia (Whitehouse et al. 2001; Collins and Windley 2002; Hargrove et al. 2006). The oldest units are commonly ophiolites, which demonstrate that the creation of continental ANS crust began with the forming of oceanic crust by the expansion of the seafloor, accompanied by subduction and island-arc development (Johnson et al. 2011). The early magmatic stages in the ANS involve the presence of dense oceanic tholeiite sequences in intra-oceanic settings accompanied by bimodal volcanism of island-arc chemistry 950–650 Ma. Such processes culminated in huge amounts of mafic crust and lithospheric mantle within the ANS and crustal overprinting (Bentor 1985; Stein and Goldstein 1996; Stein 2003) for producing, these upwelling plumes possibly provide the lithophile element-enriched sources for younger calc-alkaline (640–590 Ma) and alkaline (590–550 Ma) magmatism (Robinson et al. 2014).

Over the time 780–620 Ma, various island arcs collided and these tectonic terranes sutured and developed a progressively large and dense nucleus of continental juvenile crust. This thickening resulted in the formation of several suture zones, marked by obduction of ophiolites and intense deformation (Johnson et al. 2011; Cox et al. 2012). Crustal thickening was also accompanied by melting and magmatic fractionation of mafic magmas that ponded deep in the crust.

These melts rose upwards to be emplaced as granitic plutons. Magmatism during this episode is characterized by tholeiites and calc-alkaline suites (Robinson et al. 2014).

The juvenile ANS crust was trapped between great tracts of converging continental crust. A protracted episode of continental collision started at about 610 Ma ago and continued for about 50 million years. Collision was more intense in the south, but it also strongly affected the ANS (Kröner and Stern 2004). The arc terranes and sutures in the southern ANS were deformed by N–S-oriented upright folds and shear zones forming elongated systems such as the Hamisana Shear Zone in North Sudan and South Egypt (Johnson and Woldehaimanot 2003). The ANS was influenced more far north and east by the development of the broad NW-SE pattern of the Najd Fault System (NFS). The composition of igneous rocks became distinctively more evolved as the collision continued and the crust continued to thicken. Deep erosion, possibly by a continental ice sheet, happened during this time. All tectonic and magmatic activities ended by the time the Cambrian sandstones were deposited, about 530 million years ago (Stein 2003; Robinson et al. 2014). A variety of characteristics have been traced to late stage extension tectonics, including a large NE–SW trending dyke swarm, NE–SW trend normal faults and NW-SE trend sedimentary basins filled with post-orogenic molasse deposits (Blasband et al. 2000; Johnson and Woldehaimanot 2003; Kröner and Stern 2004).

2.3.5 Tectonic Models of the Arabian–Nubian Shield

The ANS contains a vast expanse of Neoproterozoic juvenile oceanic arc crust surrounded by older cratonic crust to the west and east (Stoeser and Frost 2006). Fritz et al. (2013) and Hamimi et al. (2019) recognized five main phases produced the ANS: (1) rifting of the African craton ($\sim$1200–950 Ma); (2) ensimatic island-arc development ($\sim$950–715 Ma); (3) formation of the Arabian–Nubian Neocraton by microplate accretion and continental collision (715–640 Ma); (4) collision-related intra-cratonic magmatism and tectonism ($\sim$640–550 Ma); and (5) epicontinental subsidence (<550 Ma), commonly found in fault-bound basins (Nettle et al. 2013).

The Arabian shield in Western Saudi Arabia was developed in Neoproterozoic through three main stages: (1) Island-arc creation and accretion, primarily during the time $\sim$870–620 Ma; (2) Continental orogenesis after collision with East Gondwana's north-western margin, $\sim$660–620 Ma; and (3) post-collisional extension, magmatism and sedimentation $\sim$620–540 Ma (Greenwood et al. 1976; Al-Shanti and Mitchell 1976; Schmidt et al. 1979; Stoeser and Camp 1985; Kröner 1985; Genna et al. 2002; Johnson and Woldehaimanot 2003; Stoeser and Frost 2006). The collision was occurred in the south, whereas subduction of oceanic crust continued in the north until approximately 620 Ma (Doebrich et al. 2007); therefore, there is overlap in ages for arc formation and collision.

During collisional orogenesis, the Najd Fault System (NFS) (a major left-lateral fault system) developed throughout the northern part of the Arabian shield. The Najd was described as the product of tectonic escape, similar to those arising from the collision between India and Asia (Schmidt et al. 1979; Burke and Sengor 1986). Three of the most prominent of the Najd Fault Zones, Ruwah, Ar Rika and Halaban-Zarghat (Al-Saleh et al. 1998) are shown in Figs. 2.17 and 2.18. Moore (1979) described this system as a major transcurrent (strike–slip) fault system, of Proterozoic age in the Arabian shield. The NFS was identified originally as a huge late Proterozoic and early Phanerozoic NW-trending brittle–ductile shear zone with 300 km width and length over 1100 km extending over the north part of the ANS (Stern 1985; Johnson et al. 2011). The displacement along the strike of the NFS was reported by Brown (1972) and Hamimi et al. (2019) as 240 km cumulative displacement but field displacements can be demonstrated as only tens of kilometres for faults (Johnson et al. 2011). The NFS and other NW-trending strike–slip faults in the ANS are known to be post-accretionary structures and were deduced from the squeezing of the Arabian–Nubian shield between East and West Gondwana (Berhe 1990; Stern 1994a, b; Abdelsalam 1994; Abdelsalam and Stern 1996; Abdelsalam et al. 2003; Hamimi et al. 2019). The formation of NFS is a result of simple shear that allowed the Nubian and southern Arabian shield to move several hundred kilometres sinistrally with respect to northern Arabia (Moore 1979; Hamimi et al. 2019).

Stoeser and Frost (2006) recognized two stages for terrane accretion of the Arabian shield: (1) Accretion of terrane emerging from the closure of ocean basins (e.g. Stoeser and Camp 1985; Johnson and Woldehaimanot 2003) and (2) Lateral transpressional accretion as suggested for the North American Western Margin (Samson and Patchett 1991). Furthermore, although most theories include mainly the accretion of oceanic island arcs, some have indicated that the accretion of oceanic plateaus has also played an important role in the evolution of the ANS (e.g. Stein and Goldstein 1996).

The terrane concept has been applied to the ANS since the mid-1980s, developing out of earlier plate-tectonic/subduction zone and accreted island-arc concepts, and leads to the interpretation that the exposed and immediately adjacent concealed Proterozoic rocks of western Arabia and northeastern Africa are a collage of crustal blocks, or terranes that, with varying degrees of confidence,

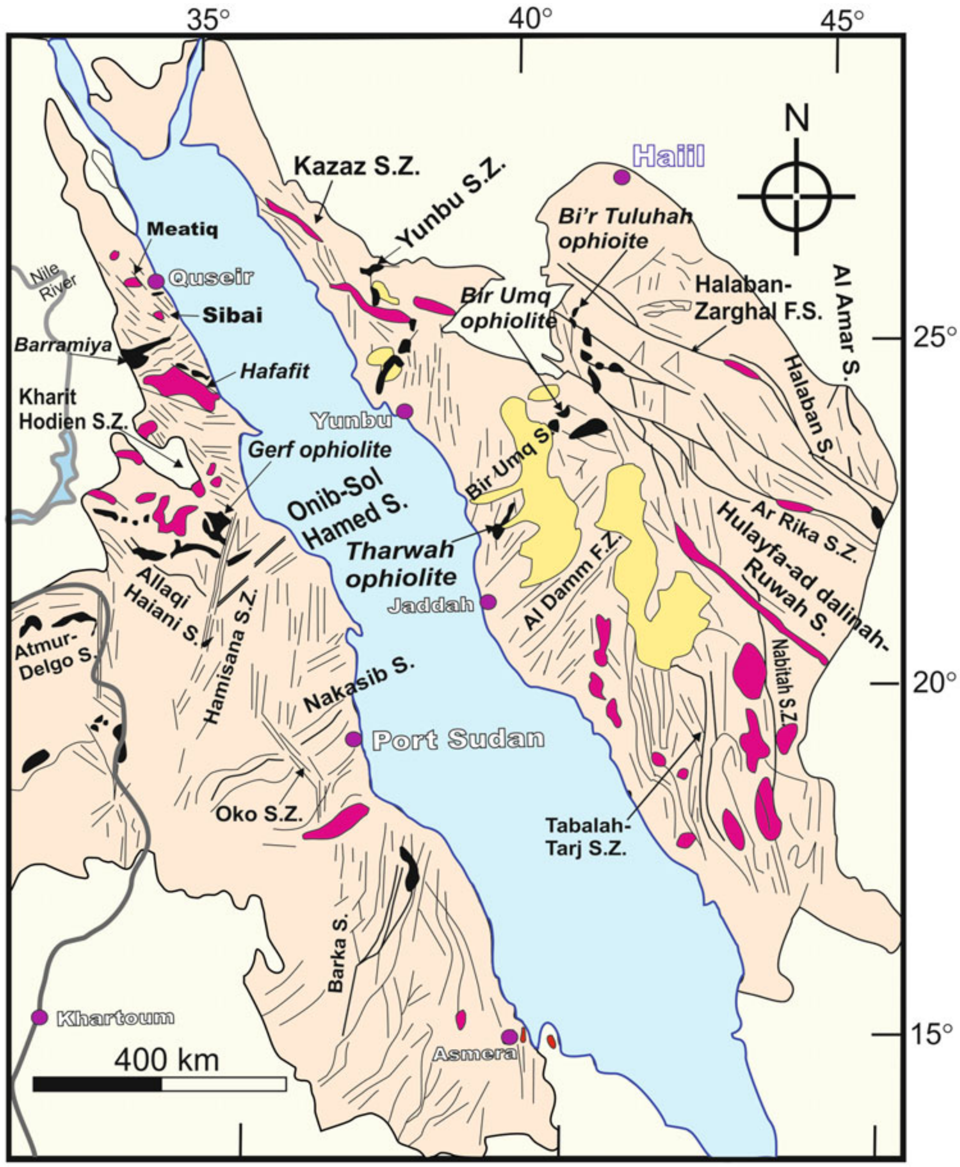

Fig. 2.18 Major sutures and shear zones in the Arabian–Nubian Shield (modified after Johnson 2006)

can be correlated across the Red Sea, thereby linking the now separated Arabian and Nubian shields. Given the reconnaissance nature of geologic mapping in the Arabian shield, details about the origins, ages, structure and convergence of the terranes remain to be established, and the terrane-collage model is, strictly speaking, a working hypothesis.

2.4 The Egyptian Nubian Shield

Although Precambrian rocks underlie the entire Egypt and Sudan, they are best known where exposed in the Nubian Shield, in the Egyptian Eastern Desert and Northern Sudan. In the shield, the Precambrian rocks are mostly Neoproterozoic. The tectonic development of the ANS spans three phases spanning over 600 Ma: accumulation of arc terrains within the Hijaz Magmatic Arc, accompanied by accretion of the Hijaz Magmatic Arc towards the Nile Craton and reworking of the accreted arc after accretion (Fritz et al. 1996; Abdelsalam and Stern 1996; Augland et al. 2012). The Egyptian Nubian Shield (ENS) covers $\sim 100{,}000$ km^2, crops out along the Red Sea Hills in the Eastern Desert and southern Sinai, as well as limited areas in the south Western Desert (Oweinat area) (El Gaby et al. 1990; Hassan and Hashad 1990). The basement complex of the ENS comprises four main tectonostratigraphic units (Hamimi et al. 2019) from bottom upward as follows: (1) high-grade gneisses and migmatites, (2) arc-type volcanic/volcanosedimentary units, along with dismembered ophiolites, (3) the Ediacaran Hammamat and Dokhan supracrustal sequences, and (4) granitoids. During the Cambrian until the Cretaceous, the

Nubian Shield's rocks were almost constantly hidden by Phanerozoic sedimentary rocks, until the uplift and deforestation correlated with the division of Arabia and Africa culminated in the Nubian shield becoming revealed as it is today. Juvenile Neoproterozoic rocks predominate in the Nubian shield and extend distances of 1000 km from northern Sudan to northern Egypt.

Four major lithological components describe the ENS (Fig. 2.19): predominantly juvenile arc, supracrustal series, ophiolites and gneiss domains enclosing core complexes and intrusions of granitoids (Fritz et al. 1996, 2002; Abd El-Naby et al. 2000, Shalaby et al. 2005; Abd El-Wahed 2008, 2014; Ali et al. 2015; Hamimi et al. 2019; Abd El-Wahed et al. 2019a, b; Hamimi et al. 2019; Zoheir et al. 2019b; Hamimi and Abd El-Wahed 2020; Fowler and Hamimi 2020; Abd El-Wahed and Hamimi 2020). These units were tectonically mixed by thrusting associated with accretion and sinistral strike–slip shearing along the Najd and other NW-striking shear zones, particularly in the central part of Eastern Desert of Egypt (Abd El-Wahed 2010; Hamimi et al. 2019). Sheared granitoid gneisses occur locally in antiformal "domal" locations in the Eastern Desert of Egypt, typically surrounded by low-grade supracustal assemblages, such as the Meatiq (Sturchio et al. 1983; Fritz et al. 1996; Andresen et al. 2009, 2010; Hamdy et al. 2017; Mohammad et al. 2019), Hafafit (Greiling et al. 1994, Abd El-Naby et al. 2008, Lundmark et al. 2012; Ali et al. 2015; Makroum 2017; Hamimi et al. 2019), El-Shalul (Hamimi et al. 1994, Osman 1996, Ali et al. 2012a) and in the region along Wadi Beitan (Abdel Khalek et al. 1992; Ali et al. 2015). The gneiss domes of the Egyptian Eastern Desert were previously interpreted to represent a pre-Neoproterozoic (pre-Pan-African) basement (e.g. El-Ramly and Akaad 1960; El-Ramly 1972; El-Gaby et al. 1984, 1988, 1990; Hamimi et al. 1994). However, other authors argued that the Eastern Desert gneissic rocks are of juvenile origins and formed in intra-oceanic or continental arc settings within, or on the margin of, the Mozambique Ocean, or along one or more magmatic arcs along the western margin of this ocean prior to amalgamation of East and West Gondwana at ~630 Ma (El-Ramly et al. 1984, 1993; Greiling et al. 1984, 1988; Stern 1994a, b; Abd El-Wahed 2008, 2014; Andresen et al. 2009, 2010; Abd El-Wahed and Kamh 2010; Augland et al. 2012, Lundmark et al. 2012; Ali et al. 2009a, b; 2010a, b, 2012a, b, 2015; Abd El-Wahed et al. 2016, 2019a, b; Zoheir et al. 2019b: Hamimi et al. 2019; Hamimi and Abd El-Wahed 2020; Fowler and Hamimi 2020; Abd El-Wahed and Hamimi 2020).

The Egyptian Eastern Desert was subdivided by Stern and Hedge (1985) into Northern, Central and South-Eastern Desert regions (NED, CED and SED); all reveal different aspects of the region's protracted and intense Neoproterozoic episode of deformation and igneous activity.

2.4.1 The South-Eastern Desert (SED)

The details of the Neoproterozoic of the SED are still poorly known. The SED differs from the CED in several styles (Stern 2018): (i) it is much less studied; (ii) it lacks interesting sediments such as BIF and diamictite; (iii) it has some volcanogenic massive sulphides, whereas the CED does not (Abd El-Rahman et al. 2012); (iv) there are no major sedimentary or volcanic Ediacaran successions as described in the NED and CED, such as the Hammamat Group and Dokhan Volcanics; and (v) it contains equal amounts of serpentinites to those of CED except for Abu Dahr ophiolites (Gahlan et al. 2015) and those defining the Allaqi–Heiani Suture in the southern SED (Zimmer et al. 1995; Gahlan and Arai 2009; Ali et al. 2010a; Azer et al. 2013). The SED usually tends to be more deeply exposed than the CED and is less influenced by Najd shearing (Stern 2018). Gneisses in the ENS represent the infrastructure rocks that exposed in tectonic windows beneath the suprastructure rocks. Gneisses and related rocks in the SED are sheared and ductility-deformed at shallow depths such as the gneisses of El-Hudi, Haimur-Abu Swayel, Abu Fas, Beitan, Khuda, Sikait and Hamisana.

The SED is characterized by the presence of Allaqi–Heiani Suture (AHS) and the Hamisana shear zone (HSZ). The AHS is a part of the megascopic Allaqi–Heiani–Oneib–Sol Hamed–Yanbu Suture (AHOSHYS) (Abdelsalam and Stern 1996, Abdelsalam et al. 2003; Zoheir et al. 2019a) that extends ~E–W for at least 600 km, from the western edge of the shield in Egypt to the eastern edge of basement exposures in NW Arabia (Ali et al. 2010a). The AHS tracks eastward from Wadi Allaqi's entry into Lake Nasser along the Egyptian–Sudan border to Gabal Gerf along the Red Sea (Ali et al. 2010a). Here, the suture is thought to be displaced southwards along the N–S HSZ and continues NE along the Onib segment to the Red Sea, across which it can be traced into northwestern Saudi Arabia (Ali et al. 2010a). The Allaqi–Heiani belt is an arc–arc suture accreted and formed between ~730 and 709 Ma (Ali et al. 2010a, b). It separates the Midyan–South-Eastern Desert terrane in the North from the ~830–720 Ma Hijaz–Gebeit terrane to the South (Shackleton 1994; Abdelsalam and Stern 1996; Abdelsalam et al. 2003; Hamimi et al. 2019; Zoheir et al. 2019a). In the central and western portions of the Allaqi–Heiani suture, ophiolites form imbricate thrust-bound sheets and slices of serpentinite, amphibolite, metagabbro and metabasalt, embedded in a strongly tectonized carbonate talc matrix, creating an elongated WNW–ESE or E–W belt (Abdelsalam and Stern 1996; Abdelsalam et al. 2003; Zoheir and Klemm 2007).

The HSZ is an ophiolite-decorated post-accretionary structure (Stern et al. 1990) and not a suture as suggested by Berhe (1990). The AHOSHYS is broad and consists of four major lithologic associations: (i) ophiolites, (ii) island-arc metavolcanic and metasedimentary successions,

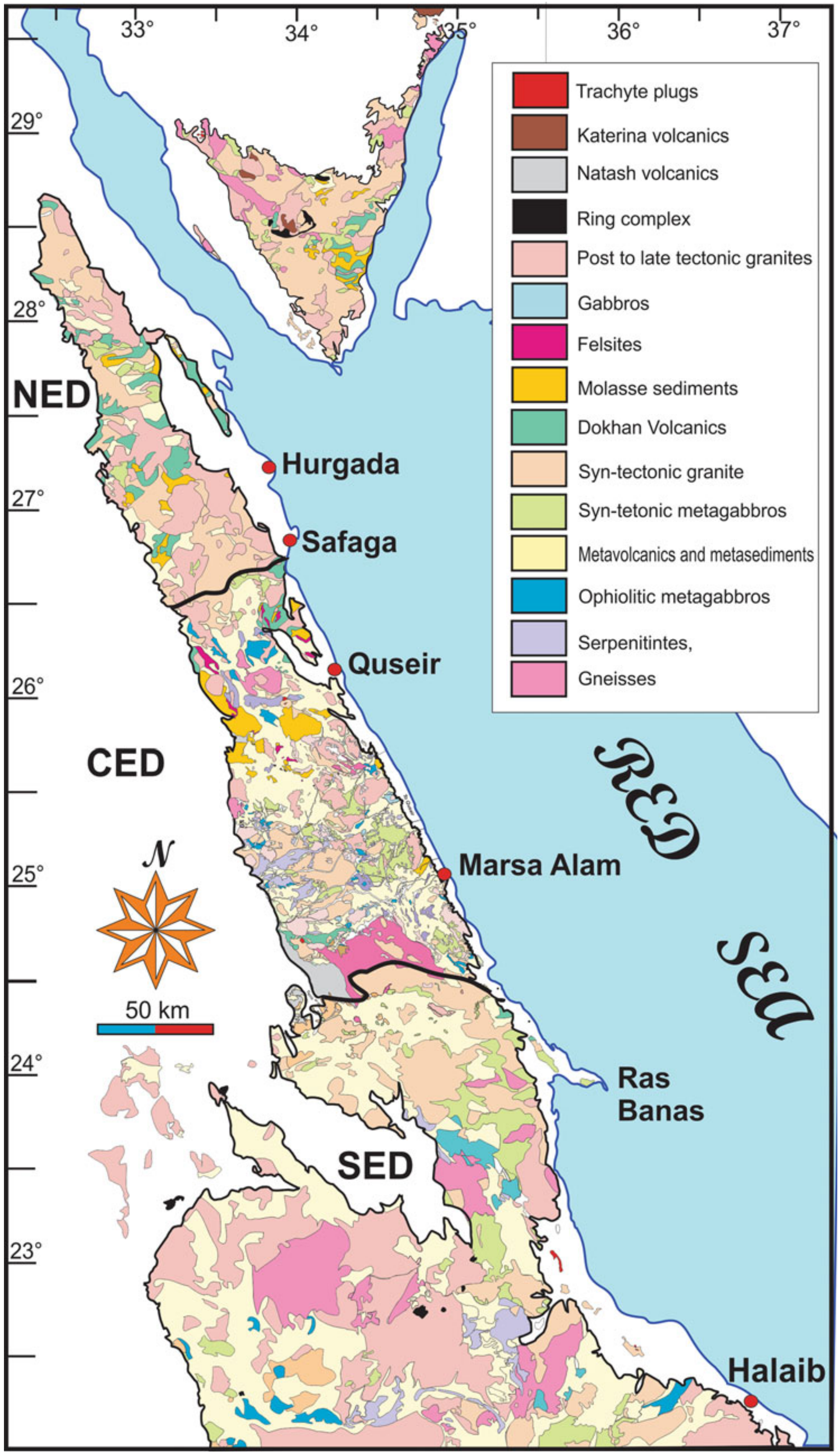

Fig. 2.19 Geological map of the Egyptian Nubian Shield Compiled from the Geological Map of Egypt (El-Ramly 1972) and the CONCO geological maps (Klitzch et al. 1987)

(iii) gabbroic to granitic intrusions and (iv) gneiss (Stern et al. 1990, Abdelsalam et al. 2003, Zoheir and Klemm 2007; Gahlan and Arai 2009; Ali et al. 2010a). The Allaqi segment of the AHOSHYS separates the SE segment of the Eastern Desert Terrane in the north from the Gabgaba Terrane to the south (Abdelsalam and Stern 1996; Ali et al. 2010a).

2.4.2 The Central Eastern Desert (CED)

The CED is in several respects the best known of the three subdivisions of the Eastern Desert, as its supracustal sequences are especially fascinating and insightful. The CED was characterized by two prominent tectonostratigraphic units; (i) The lower unit is commonly referred to as the structural basement (Infrastructure) (El-Gaby et al. 1990) or as "lower tier" (e.g. Bennett and Mosley 1987; Greiling et al. 1994) and comprises high-grade metamorphic gneisses, migmatites, schists and amphibolites; and (ii) the second unit is commonly referred to as structural cover (Suprastructure) or the Pan-African nappes and is described as the upper unit including low-grade metamorphosed ophiolite slices (serpentinites, pillow lavas, metagabbros), arc metavolcanics and arc metasediments (e.g. El-Gaby et al. 1990; Gahlan et al. 2012). Abdel-Karim and Ahmed (2010) summarized what is known about 38 different occurrences of ophiolitics in CED and SED. Greenschist facies arc volcanics and volcanoclastic metasedimentary rocks are important supracrustal constituents of the CED above the ophiolites (Figs. 2.20 and 2.21). Collectively, the infrastructure and supracrustal rocks were intruded by syn-tectonic calc-alkaline granites and metagabbros–diorite complex and covered by Phanerozoic sediments (Abd El-Wahed et al. 2010).

The ensimatic (oceanic) assemblage in the CED represents the oldest units, with $\sim$750 Ma U-Pb zircon ages (Kröner et al. 1992; Andresen et al. 2009; Ali et al. 2009b; Stern 2018). It is perforated with Cryogenian I-type granitoids and Ediacaran A-type granites (Ali et al. 2012b) and dislocated by a number of magmatic–metamorphic core complexes (Stern 2018).

The later stages of the CED's crustal growth are distinguished by eruption of Dokhan volcanics that is consistent with the deposition of molasse-type Hammamat molasse sediments formed in terrestrial alluvial fan/braided stream environment (Grothaus et al. 1979; Abd El-Wahed 2010; Bezenjania et al. 2014). In response to the differential relief between more elevated regions of the NED and topographically lower areas of the CED which followed Najd fault deformation of the CED and volcanic rifting in the NED,

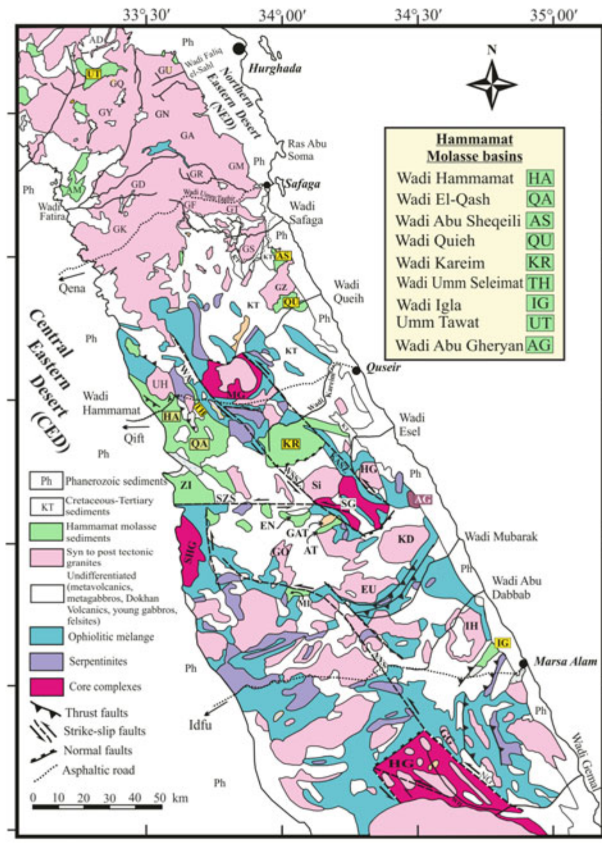

Fig. 2.20 Simplified geological map of the Central and part of the Northern Eastern Desert of Egypt showing distribution of Hammamat molasse basins (after Abd El-Wahed 2010; Compiled from the Geological Map of Egypt (El-Ramly 1972) and the geological map of Quseir (Klitzch et al. 1987). Major structures are after Fritz et al. (1996), Bregar et al. (2002), Shalaby et al. (2005) and Abd El-Wahed (2008). HG, Hafafit gneiss; WH, Wadi Hafafit; NG, Wadi Nugrus; GG, Gebel (G.) Nugrus; IG, Wadi Igla molasse basin; IH, Igl Al-Ahmar monzogranite, GX, G. Umm Nagat; NNS, Um Nar-Nugrus shear zone; EU, Gebel El-Umra older granite; MI, El-Miyah molasse basin; KD, Kadabora monzogranite pluton; SHG, El-Shalul gneisses; AT, Atawi molasse basin; GAT; Gebel Atawi Alkali feldspar granite; EN, Andiya molasse basin; AG, Abu Gheryan molasse basin; Si, Gebel Sibai alkali feldspar granite; SG, Sibai gneisses; WSSZ, Wadi Sitra shear zone; KASZ, Kab Ahmed Shear zone, HG; Homrat Ghaunam alkali feldspar granite; ZI, Wadi Zeidun molasse basin; SZS, Wadi Zeidoun-Wadi El-Shush strike–slip fault; QA, Wadi El-Qash molasse basin; KR, Kareim molasse basin; TH, Um Esh-Um Seleimat molasse basin; HA, Hammamat molasse basin; UH, Um Had granite pluton; WA, Wadi Atalla; MG, Meatiq gneisses; QU, Wadi Quieh molasse basin; AS, Abu Sheqeili molasse basin; GZ, G. Umm Zarabit; GK, G. Kafari; GS, G. Gasus; GD, G. el-Dob; GF, G. Abu Furad; GT, G. Umm Taghir; GR, G. Ras Barud; GM, G. el-Magal; GA, G. Umm Anab; GY, G. Samyuk; GN, G. Shayib el Banat; GQ, G. Qattar; GU, G. Umm Araka; UT, Umm Tawat molasse basin and AD, Gebel Dokhan

Hammamat basins developed (Stern 2018). In addition, the crustal rocks were intruded by late to post-tectonic granites.

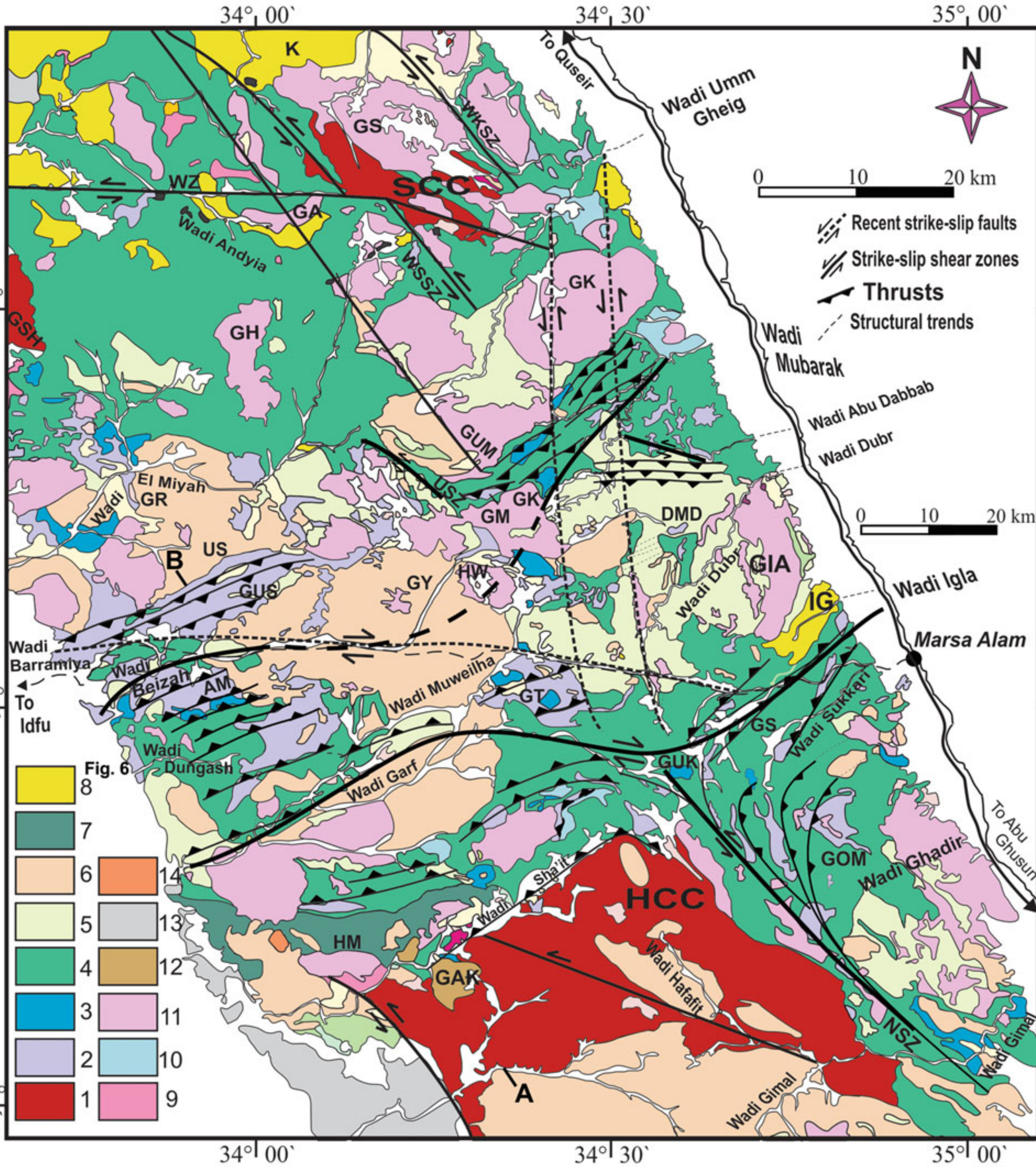

Fig. 2.21 Geological map of the southern part of the Central Eastern Desert of Egypt (modified after Conoco 1987). 1; core complexes 2; serpenitintes, 3; ophiolitic metagabbros, 4; metavolcanics and metasediments, 5; syn-tetonic intrusive metagabbros, 6; syn-tectonic granite, 7; Dokhan volcanics, 8; molasse sediments, 9; felsites, 10; gabbros, 11; post to late tectonic granites; 12; ring complex, 13; Natash volcanics and 14; trachyte plugs. GAK; Gebel Abu Khruq, HCC; Hafafit core complex, GOM; Wadi Ghadir ophiolitic mèlange, HM; Hamash gold mine, NSZ; Wadi Nugrus shear zone, GS; Gebel Sukkari and Sukkari gold mine, GUK; Gebel Um Khariga, IG; Igla molasse basin, DMD; Dubr metagabbro–diorite complex, GIA; Gebel Igl Al- Ahmar, HW, Gebel Homrat Waggad, GY, Gebel El-Yatima, GUS; Gebel Umm Salim, US, Gebel Umm Saltit, GK; Gebel Abu Karanish, GM, Gebel Al Miyyat, USZ; Um Nar shear zone, GUM; Gebel El-Umra, GK; Gebel Kadabora, GA; GH; Gebel El-Hidilawi, GU; Gebel Umm Atawi, GSH; Gebel El-Shalul, GR; Gebel El Rukham; SCC; Sibai core complex, GS; Gebel Sibai, WZ; Wadi Zeidon, WSSZ; Wadi Sitra shear zone, WKSZ; Wadi Kab Ahmed shear zone, K; Kareim molasse basin. The major structures are after Akaad et al. (1993), Fritz et al. (1996) Helmy et al. (2004), Shalaby et al. (2005), Abd El-Wahed (2008) and Abd El-Wahed and Kamh (2010)

The CED is mostly distinguished by the domination of NW-striking tectonic structure (Fig. 2.21) marking the NW–SE sinistral shear zone of the NFS (Abd El-Wahed and Kamh 2010; Abd El-Wahed 2014; Abdeen et al. 2014; Abd El-Wahed et al. 2016, 2019a, b; Hamimi et al. 2019; Hamimi and Abd El-Wahed 2020; Fowler and Hamimi 2020; Abd El-Wahed and Hamimi 2020). Nappe transport directions reported from the CED show a variance from top to the NE (e.g. El Bayoumi and Greiling 1984), top-to-the-NW (Ries et al. 1983; Greiling 1987), top-to-the-SE (Kamal El Din et al. 1992) and top-to-the-SW (Abdeen et al. 2002; Abdelsalam et al. 2003). Oblique convergence transpression (Abd El-Wahed and Kamh 2013), whether dextral or sinistral, is a current mechanism adopted by many authors (Fritz et al. 1996, 2002, 2013; Loizenbauer et al. 2001; Makroum 2001; Bregar et al. 2002; Helmy et al. 2004; Shalaby et al. 2005; Abd El-Wahed 2008, 2010; 2014; Shalaby 2010; Abd El-Wahed and Kamh 2010; Zoheir and Lehmann 2011; Zoheir and Weihed 2014; Abd El-Wahed et al. 2016; Abd El-Wahed and Thabet 2017; Makroum 2017; Hamdy et al. 2017; Stern 2018) to explain and imply the deformation styles in the CED.

Simply and collectively, Abd El-Wahed and Kamh (2010) listed the deformation events of the CED as follows: (1) D_1 associated with NNW-ward thrusts; (2) D_2 related to NE- and SW-directed thrusts; (3) D_3 attributed to sinistral movement along the NW-striking shears of the NFS; (4) D_4 associated with dextral movement along NE-trending shear zones; and (e) D_5 later events. The NNW-directed thrusts were created as a result of oblique convergence during island-arc accretion (690–650 Ma) in Sibai gneisses (Bregar et al. 2002; Fowler et al. 2007; Augland et al. 2012) and 630 and 609 Ma in Meatiq and Hafafit gneiss-cored domes (Andresen et al. 2009). The tectonic system changed from the compressional arc accretion setting to the sinistral transpressional regime between 650 and 540 Ma. In the CED, exhumation of the core complexes (e.g. Meatiq, Sibai, El-Shalul and Hafafit) is related to the sinistral slip along the NFS, which bound them from the SW and NE (Fritz et al. 1996). Not only core complexes of CED but also the Hammamat sediments are tectonically affected by the NFS (Abd El-Wahed 2010).

The NFS and the other NW-trending strike–slip shear zones of the ANS were initially post-accretionary structures and were deduced from the stretching of the ANS between East and West Gondwana (Berhe 1990; Stern 1994a, b; Abdelsalam and Stern 1996; Abdelsalam et al. 2003). The NFS comprises brittle and ductile shears in a region up to 300 km in width and about 1,100 km long, including the north part of the Arabian shield.

Different scenarios were suggested to interpret one of the major landmarks of the CED, the gneissic domes or core complexes (Meatiq, Sibai, El-Shalul and Hafafit). Gneiss domes have been diversely interpreted as (1) antiformal stacks produced by thrusting (Greiling et al. 1994), (2) core complexes associated with NW-SE crustal extension (Fritz et al. 1996; Bregar et al. 2002; Abd El-Wahed 2008; Makroum 2017; Hamdy et al. 2017; Abd El-Wahed et al. 2019a, b; Abd El-Wahed and Hamimi 2020) and (3) interference patterns of sheath folds (Fowler and El Kalioubi 2002—for the Hafafit Complex). Recently, there are two tectonic models to explain the formation and exhumation of these core complexes in the CED: (1) Orogen-parallel extension model (Fritz et al. 1996) assigned evolution of the core complexes to sinistral shear activity on NFS-related shear zones and (2) extensional tectonics model as a result of simultaneous NW–SE folding and NW–SE extension (Fowler et al. 2007; Andresen et al. 2010).

Nugrus shear zone is one of the CED's main NW-trending shear zones that divides the CED from Egypt's SED and forms the border between the Wadi Ghadir region (East) and the Hafafit Core Complex (West). Nugrus shear zone starts with a thickness of 750 m retaining its width at least as far as Gabal Sikait, where its thickness decreased by 50 m (Harraz and El-Sharkawy 2001; Fowler and Osman 2009). Lundmark et al. (2012) dated to ≤ 595 Ma the sinistral shearing on the Nugrus Shear Zone.

Nugrus shear zone is interpreted as thrust showing top-to-W- or SW tectonic transport over the continental margin (El Bayoumi and Greiling 1984; El-Ramly et al. 1984; El-Gaby et al. 1988) or as roof thrust linked up NW-dipping thrust imbricates of gneissic rocks and allowing NW-ward displacement of low-grade CED metavolcanics over the gneisses (Greiling et al. 1994 and Greiling 1997). Many workers considered Nugrus shear zone as a Najd-related ductile strike–slip shear (Fritz et al.1996; Shalaby et al. 2005; Abd El-Wahed et al. 2016; Makroum 2017). Fowler and Osman (2009) described Nugrus shear zone as an example of E–W striking low-angle normal ductile shear with low-angle N-dip.

The NW-trending sinistral shear zone-related transpression is conjugated and overprinted by the dominant dextral transpression along NE–SW trending shear zones (Shalaby et al. 2005; Abd El-Wahed and Kamh 2010) (Fig. 2.21). Abd El-Wahed (2014) documented a huge NE-trending shear belt (up to 110 km in length) occupying the area between Wadi Barramiya and Wadi Sha'it (Fig. 2.21) to the west (up to 60 km in width) and extends through the whole width of the Central Eastern Desert to include the area between Wadi Mubarak and Wadi Ghadir on the Red Sea coast (up to 120 km in width) (Fig. 2.21). The 40–60-km-wide, ENE–WSW trending Mubarak–Barramiya Shear Belt (MBSB) deforms supracrustal successions and structures associated with the NW-trending shear fabric (Fig. 2.21). The MBSB is interpreted as a dextral transpressive shear zone ceased the extension of the NSZ and modelled in terms of a regional "flower structure" (Abd El-Wahed and Kamh 2010).

2.4.3 The Northern Eastern Desert (NED)

The NED (Fig. 2.20) is remarkably different from both the CED and the SED. The NED is characterized mainly by (i) a wide range of Ediacaran igneous rocks and associated Hammamat sediments (Wilde and Youssef 2000), (ii) absence of ophiolites and scarcity of gneisses, (iii) BIF and diamictite is unknown, (iv) absence of Najd deformation, (v) abundance of dike swarms that trend E–W to NE–SW, (vi) abundance of epizonal A-type granites indicating strong extension, and (vii) abundance of Dokhan Volcanics (Stern and Hedge 1985). The Dokhan volcanics occupy a limited area of the Egyptian basement and are best exposed north of latitude 26° N in the Eastern Desert (e.g. NED and northernmost CED) particularly at their type locality Gabal Dokhan. Dokhan Volcanics are unmetamorphosed rocks felsic to intermediate composition and have medium- to high-K calc-alkaline affinities. Dokhan Volcanics have been formed in subaerial environment and commonly associated and/or interbedded with Hammamat molasse sediments (Abd El-Wahed 2010; Eliwa et al. 2014b; El-Bialy 2020). Breitkreuz et al. (2010) reported the eruption of the Dokhan Volcanics during two major volcanic pulses: 630–623 and 618–592 Ma. The Hammamat molasses of the ENS were developed between 650 and 580 Ma in individual basins in variable tectonic settings (Fritz and Messner 1999; Shalaby et al. 2006; Abd El-Wahed 2010). Dessouky et al. (2019) indicated that the Hammamat molasse sediments have been deposited during three tectonic settings: (i) pre-collision stage comprise fore-arc, intra-arc and back-arc basins; (ii) syn-collision stage include fore-arc basins and low land basins; and (iii) late-collision stage embrace low land and intramontane basins.

The most exciting recent developments in the studies of the NED are the presence of small tracts of Cryogenian and Tonian igneous rocks (Stern 2018) including the 666 Ma Mons Claudianus granodiorite (Stern 2018), Tonian muscovite tonalite and I-type muscovite-bearing trondhjemite and granodiorite with complexity in the U-Pb zircon ages at ~740 Ma (Eliwa et al. (2014a), the presence of ~720 Ma ignimbrites unconformably overlying the ~740 Ma granitoids (Bühler et al. 2014), the presence of ~780 Ma dacite (Abd El-Rahman et al. 2017).

2.4.4 The Egyptian Nubian Shield in Sinai

The basement rocks in Sinai (Fig. 2.19) comprise four complexes: the Feiran–Solaf, Sa'al–Zaghra, Kid and Taba Metamorphic complexes. The metamorphic complexes are composed of orthogneisses and metasedimentary–metavolcanic sequences. They are surrounded by younger non-metamorphosed intrusions and volcanosedimentary sequences and metamorphosed at greenschist to amphibolite and rarely up to granulite facies conditions (Shimron 1984; Jarrar et al. 1993; El-Shafei and Kusky 2003; Abu El-Enen et al. 2003, 2004; Fowler and Hassan 2008; Abu-Alam and Stüwe 2009, 2010; Azer and Farahat 2011).

These metamorphic complexes were considered to be pre-Pan-African by El-Gaby et al. (1990) and Abu Anbar et al. (2004). Nonetheless, other studies have recorded geochronological evidence that point to the Pan-African period (Bielski 1982; Stern and Manton 1987; Eliwa et al. 2008). A younger tectono-magmatic period in Sinai is distinguished by large intrusions of calc-alkaline magma during ca. 635–590 Ma (Ali et al. 2009a, b; Be'eri-Shlevin et al. 2009). Post-collisional calc-alkaline granitoids were placed from c. 635 to 590 Ma, while the alkaline granite suite was developed over a span of c. Ma 608–580 (Be'eri-Shlevin et al. 2009). Despite close association in space and time, calc-alkaline and alkaline granitoids are clearly distinguished in some major and trace element characteristics. This was demonstrated for 27 key plutons and plutonic complexes (Be'eri-Shlevin et al. 2009; Azer et al. 2010; Eyal et al. 2010; Azer and Farahat 2011). The alkaline activity was dominated by bimodal alkaline volcanism and shallow intrusions of granitoids, which are mostly A-types, along with dike swarms (Beyth et al. 1994; Kessel et al. 1998; Samuel et al. 2007; Eyal et al. 2010). The volcanosedimentary successions of southern Sinai (Kid, Ferani, Rutig, Sa'al–Zaghra, Iqna Shar'a, Khashabi and Meknas) have been associated with the Dokhan–Hammamat successions (Shimron 1980; Bentor 1985; El-Gaby et al. 1991; Basta 1997; Azzaz et al. 2000; Moussa 2003; Azer 2007; El-Bialy 2010; Azer and Farahat 2011).

The Katherina Volcanics at Gabal Ma'ain (580–590 Ma) in the Sinai consists of porphyritic rhyolite lavas (450 m thick) with minor pyroclastics intruded by alkaline granitoids (578 ± 8 Ma) (El-Bialy and Hassen 2012). The Tarr Albitites complex comprises intrusive and volcanic eruptions of albitite surrounded by an emplacement breccia containing veins and dykes of carbonates (Azer et al. 2008). Zircons separated from the albitites yield a U–Pb age of 605 ± 15 Ma, and this is also the age of the intrusive carbonates (Azer et al. 2008). Geochemical signatures of Tarr Albitites indicate that they represent pristine igneous rocks and are not metasomatic products (Azer et al. 2008)

2.5 Summary and Concluding Remarks

1. Rodinia was created at c. 1.23 Ga by accretion and aggregation of fragments formed by the break-up of an older supercontinent, Columbia, created by global events of 2.0–1.8 Ga. Between 1300 and 900 Ma, Rodinia was established and the continental break-up occurred between 950 and 600 Ma. The first components of Gondwana begin to collide around the same time period, leading towards the creation of a global supercontinent.

2. There are basically two geodynamic scenarios to explain the formation of the Gondwana Supercontinent in eastern and southern Africa during the Pan-African Orogenic Cycle:
   i. collision and amalgamation of East Gondwana and West Gondwana ($\sim$640 to $\sim$530 Ma) and closing of the Mozambique Ocean between 841 and 632 Ma as well as deformation during the East African Orogeny.
   ii. collision and amalgamation of East Gondwana (ANS and older crystalline basement of the Dharwar Craton of southern India; Madagascar and the eastern granulites of Kenya and Tanzania), West Gondwana (Central Africa craton) and South Gondwana (Antarctica and the Kalahari craton).
3. The Brasiliano Orogeny is the term used for the larger Pan-African/Brasiliano Orogeny that extended not only in South America but across most of Gondwana. The Damara–Zambezi–Lufilian Orogeny developed essentially by closure of linked, narrow ocean basins. The Zambezi Belt lies between the Congo Craton and the Kalahari Craton and branches off the MB in northern Zimbabwe and southern Zambia. The Damara Orogeny occurred late in the creation of Gondwana and the Damara Belt is exposed mainly in Namibia between the Kalahari and the Congo Cratons. The Lufilian Arc is about 800 km (500 mi) long extends across eastern Angola, the Katanga Province of the southern Congo and the northwest of Zambia. The Kaoko Belt branches north-west from the Damara Belt into Angola.
4. The relics belonging to the East African Orogeny include high-grade metamorphic rocks within the Mozambique belt to greenschist facies rocks in NE Africa and the ANS. The late Mesoproterozoic–early Neoproterozoic events of the southern segment of the East African Orogeny include separation of the Congo and the contiguous East Sahara Cratons from Rodinia ($\sim$1200 Ma).
5. The Kuunga Orogeny is an orogeny that occurred during the Ediacaran and Cambrian in SE Africa. It is slightly younger than the East African Orogeny and produced by collisions between India and Australia–East Antarctica and Azania and India.
6. The ANS is southward narrowing belt straddling the suture separating East and West Gondwana at the northern end of the EAO. It extends over 3500 km north–south and more than 1500 east–west at its widest, underlying an area of $\sim 2.7 \times 10^6$ km^2 in the north half of the East African Orogeny. The ANS combines areas of western Arabia and northeastern Africa (Palestine, Jordan, Saudi Arabia, Egypt, Sudan, Ethiopia, Eritrea, Somalia and Yemen).
7. Mid-Neoproterozoic ophiolites are common in the ANS, and range from 690 to 890 Ma and extend 3000 km N–S and > 1000 km E–W. A supra-subduction zone setting for the Egyptian Eastern Desert ophiolites is broadly popular but also a back-arc setting has also been inferred.
8. Two stages for terrane accretion of the Arabian shield: (1) terrane accretion and (2) lateral transpressional accretion.
9. The ANS took about 300 million years to form. The earliest rocks identified with the ANS crust's formative process produced by the coalescence of island-arc and back-arc basins, and probably ocean plateaus. The oldest rocks of this series are around 870 Ma and are exposed in the eastern Sudan and South Arabia.
10. The ENS covers $\sim$100,000 km^2, crops out along the Red Sea Hills in the Eastern Desert and southern Sinai, as well as limited areas in the south Western Desert (Oweinat area). The basement complex of the ENS comprises four main tectonostratigraphic units from bottom upward as follows: (1) high-grade gneisses and migmatites, (2) arc-type volcanic/volcanosedimentary units, along with dismembered ophiolites, (3) the Ediacaran Hammamat and Dokhan supracrustal sequences, and (4) granitoids.
11. The CED is dominated by ophiolitic rocks, arc volcanics and volcaniclastics as well as BIF and diamictite. The CED is mainly defined by the predominance of an NW-trending structural fabric that marks the NW–SE sinistral strike–slip shear zone related to Najd Fault System.
12. The SED differs from the CED in several styles: (i) it is much less studied, (ii) it lacks interesting sediments such as BIF and diamictite, (iii) it has some volcanogenic massive sulphides, whereas the CED does not, (iv) lacks Hammamat molasse sediments and Dokhan Volcanics found in the NED and CED, and (v) has a similar abundance of serpentinite as the CED.
13. The NED differs from the CED or the SED. It is characterized mainly by (i) abundance of Hammamat sediments and Dokhan Volcanics, (ii) absence of ophiolites and scarcity of gneisses, (iii) absence of BIF and diamictite, (iv) absence of Najd deformation, (v) abundance of bimodal dike swarms, (vi) abundance of epizonal A-type granites indicating strong extension, and (vii) abundance of Dokhan Volcanics.
14. The basement rocks in Sinai are divided into four metamorphic complexes: the Feiran–Solaf, Sa'al–Zaghra, Kid and Taba Metamorphic Complexes. The metamorphic complexes contain orthogneisses and metasedimentary-metavolcanic sequences.

References

Abd El-Naby A, Frisch W, Hegner E (2000) Evolution of the Pan-African Wadi Haimur metamorphic sole, Eastern Desert, Egypt. J Metamorph Geol 18:639–651

Abd El-Naby A, Frisch W, Siebel W (2008) Tectono-metamorphic evolution of the Wadi Hafafit culmination (central Eastern Desert, Egypt): implication for Neoproterozoic core complex exhumation in NE Africa. Geologica Acta 6:293–312

Abd El-Rahman Y, Polat A, Dilek Y, Kusky TM, El-Sharkawi M, Said A (2012) Cryogenian ophiolite tectonics and metallogeny of the central eastern desert of Egypt. Int Geol Rev 54:1870–1884

Abd El-Rahman Y, Seifert T, Gutzmer J, Said A, Hofmann M, Gärtner A, Linnemann U (2017) The South Um Mongul Cu-Mo-Au prospect in the Eastern Desert of Egypt: from a mid-Cryogenian continental arc to Ediacaran post-collisional appinite-high Ba-Sr monzogranite. Ore Geol Rev 80:250–266

Abd El-Wahed MA (2008) Thrusting and transpressional shearing in the Pan-African nappe southwest El-Sibai core complex, Central Eastern Desert, Egypt. J Afr Earth Sci 50:16–36

Abd El-Wahed MA (2010) The role of the Najd Fault System in the tectonic evolution of the Hammamat molasse sediments, Eastern Desert, Egypt. Arab J GeosciArab J Geosci 3:1–26

Abd El-Wahed MA (2014) Oppositely dipping thrusts and transpressional imbricate zone in the Central Eastern Desert of Egypt. J Afr Earth Sci 100(2014):42–59

Abd El-Wahed MA, Hamimi Z (2020) Neoproterozoic Tectonic Events of Egypt. Acta Geologica Sinica-English Edition (in press). https://doi.org/10.1111/1755-6724.14410

Abd El-Wahed MA, Kamh SZ (2010) Pan-African dextral transpressive duplex and flower structure in the Central Eastern Desert of Egypt. Gondwana Res 18:315–336

Abd El-Wahed MA, Kamh SZ (2013) Evolution of conjugate strike-slip duplexes and wrench-related folding in the central part of Al Jabal Al Akhdar, NE Libya. J Geol 12(2):173–195

Abd El-Wahed MA, Thabet IA (2017) Strain geometry, microstructure and metamorphism in the dextral transpressional Mubarak Shear Belt, Central Eastern Desert, Egypt. Geotectonics 51(4):438–462

Abd El-Wahed MA, Ashmawy MH, Tawfik HA (2010) Structural setting of Cretaceous pull-apart basins and Miocene extensional folds in Quseir-Umm Gheig region, northwestern Red Sea, Egypt. Lithosphere 2:13–32. https://doi.org/10.1130/L27.1

Abd El-Wahed MA, Harraz HZ, El-Behairy MH (2016) Transpressional imbricate thrust zones controlling gold mineralization in the Central Eastern Desert of Egypt. Ore Geol Rev 78:424–446

Abd El-Wahed MA, Kamh S, Ashmawy M, Shebl A (2019a) Transpressive structures in the Ghadir Shear Belt, Eastern Desert, Egypt: evidence for partitioning of oblique convergence in the Arabian-Nubian Shield during Gondwana Agglutination. Acta Geologica Sinica-English Edition 93(6), 1614–1646. https://doi.org/10.1111/1755-6724.13882

Abd El-Wahed MA, Lebda E, Ali A, Kamh S, Attia M (2019b) The structural geometry and metamorphic evolution of the Umm Gheig shear belt, Central Eastern Desert, Egypt: implications for exhumation of Sibai Core Complex during oblique transpression. Arab J Geosci 12:764. https://doi.org/10.1007/s12517-019-4760-y

Abdeen MM, Abdelsalam MG, Dowidar HM, Abdelghaffar AA (2002) Varying structural style along the Neo-Proterozoic Allaqi-Heiani suture, Southern Egypt. In: 19th colloquium of African geology. El Jadida, Morocco (Abstract)

Abdeen MM, Greiling RO, Sadek MF, Hamad SS (2014) Magnetic fabrics and Pan-African structural evolution in the Najd Fault corridor in the Eastern Desert of Egypt. J Afr Earth Sci 99:93–108

Abdel Khalek ML, Takla MA, Sehim A, Hamimi Z, El Manawi AW (1992) Geology and tectonic evolution of Wadi Beitan area, south Eastern Desert, Egypt. Geol Arab World Cairo Univ 1:369–393

Abdel-Karim A-AM, Ahmed Z (2010) Possible origin of the ophiolites of Eastern Desert, Egypt, from geochemical perspectives. Arab J Sci Eng 35(2010):115–143

Abdel-Karim AM, Azzaz SA, Moharem AF, El-Alfy H (2008) Petrological and geochemical studies on the ophiolite and island arc association of Wadi Hammaryia, Egypt. Arab J Sci Eng 33 (1C):117–138

Abdel-Karim A-AM, Ali S, Helmy HM, El-Shafei SA (2016) A fore-arc setting of the Gerf ophiolite, Eastern Desert, Egypt: Evidence from mineral chemistry and geochemistry of ultramafites. Lithos 263:52–65

Abdelsalam MG (1994) The Oko Shear Zone: post-accretionary deformation in the Arabian-Nubian Shield. J Geol Soc Lond 151:767–776

Abdelsalam MG (2010) Quantifying 3D post-accretionary tectonic strain in the Arabian-Nubian Shield: superimposition of the Oko Shear Zone on the Nakasib Suture, Red Sea Hills, Sudan. J Afr Earth Sci 56(4–5):167–178. https://doi.org/10.1016/j.jafrearsci.2009.07.003

Abdelsalam MG, Stern RJ (1996) Sutures and shear zones in the Arabian-Nubian Shield. J Afr Earth Sci 23:289–310

Abdelsalam MG, Stern RJ, Copeland P, Elfaki EE, Elhur B, Ibrahim FM (1998) The Neoproterozoic Keraf Suture in NE Sudan: sinistral transpression along the eastern margin of west gondwana. J Geol 106:133–147

Abdelsalam MG, Lie´geois JP, Stern RJ (2002) The Saharan Metacraton. J Afr Earth Sc 34:119–136

Abdelsalam MG, Abdeen MM, Dowaidar HM, Stern RJ, Abdelghaffar AA (2003) Structural evolution of the Neoproterozoic Western Allaqi-Heiani suture, southeastern Egypt. Precambrian Res 124:87–104

Abdelsalam MG, Gao SS, Liégeois J-P (2011) Upper mantle structure of the Saharan Metacraton. J Afr Earth Sci 60:328–336

Abu Anbar M, Pichardo GS, Bernal MSH, Contreras JM, Trevino TH (2004) SmNd and Sr-Sr isotopes of Feiran gneisses and amphibolites: evidences of PrePan-African continental crust in Sinai, Egypt. In: Proceedings of the 6th international conference on geochemistry, Alexandria University, Egypt, pp 727– 745

Abu El-Enen MM, Okrusch M, Will TM (2003) The metamorphic evolution of the Pan-African basement in the Sinai Peninsula Egypt. In: Proceedings of the 5th international conference on geology of the Middle East, Cairo, Egypt, pp 207– 217

Abu El-Enen MM, Will TM, Okrusch M (2004) P-T evolution of the Pan-African Taba metamorphic belt, Sinai, Egypt: constraints from metapelitic mineral assemblages. J Afr Earth Sci 38:59–78

Abu-Alam TS, Stüwe K (2009) Exhumation during oblique transpression: the Feiran-Solaf region, Egypt. J Metamorph Geol 27:439–459

Ahmed AH, Arai S, Attia AK (2001) Petrological characteristics of podiform chromitites and associated peridotites of the Pan African ophiolite complexes of Egypt. Miner Depos 36:72–84

Ahmed AH, Gharib ME, Arai S (2012) Characterization of the thermally metamorphosed mantle–crust transition zone of the Neoproterozoic ophiolite at Gebel Mudarjaj, south Eastern Desert, Egypt. Lithos 142–143:67–83

Ali BH, Wilde SA, Gabr MMA (2009a) Granitoid evolution in Sinai, Egypt, based on precise SHRIMP U-Pb zircon geochronology. Gondwana Res 15:38–48

Ali KA, Stern RJ, Manton WI, Kimura J-I, Khamis HA (2009b) Geochemistry, Nd isotopes, and U-Pb SHRIMP zircon dating of Neoproterozoic volcanic rocks from the central eastern desert of Egypt: new insights into the ~750 Ma crust forming event. Precambrian Res 171:1–22

Ali KA, Azer MK, Gahlan HA, Wilde SA, Samuel MD, Stern RJ (2010a) Age constraints on the formation and emplacement of neoproterozoic ophiolites along the Allaqi-Heiani suture, South Eastern Desert of Egypt. Gondwana Res 18:583–595

Ali KA, Stern RJ, Manton WI, Johnson PR, Mukherjee SK (2010b) Neoproterozoic Atud diamictite of the eastern desert of Egypt and northern Saudi Arabia: evidence of ~750 Ma glaciation in the Arabian-nubian shield? Int J Earth Sci 99:705–726

Ali KA, Andresen A, Stern RJ, Manton WI, Omar SA, Maurice AE (2012a) U-Pb zircon and Sr-Nd-Hf isotopic evidence for a juvenile origin of the c 634 Ma El-Shalul Granite, Central Eastern Desert, Egypt. Geol Mag 149:783–797

Ali KA, Moghazi A-KM, Maurice AE, Omar SA, Wang Q, Wilde SA, Moussa EM, Manton WI, Stern RJ (2012b) Composition, age, and origin of the _620 Ma Humr Akarim and Humrat Mukbid A-type granites: no evidence for pre-Neoproterozoic basement in the Eastern Desert, Egypt. Int J Earth Sci 101:1705–1722

Ali KA, Kröner A, Hegner E, Wong J, Li S-Q, Gahlan HA, Abu El Ela FF (2015) U-Pb zircon geochronology and Hf–Nd isotopic systematics of Wadi Beitan granitoid gneisses, South Eastern Desert, Egypt. Gondwana Res 27(2):811–824

Al-Saleh AM, Boyle AP, Mussett AE (1998) Metamorphism and 40Ar/39Ar dating of the Halaban ophiolite and associated units: evidence for two-stage orogenesis in the eastern Arabian shield. J Geol Soc Lond 155:165–175

Al-Shanti AMS, Mitchell AHG (1976) Late Precambrian subduction and collision in the Al Amar-Idsas region, Arabian Shield, Kingdom of Saudi Arabia. Tectonophysics 30:T27–T41

Andresen A, Abu El-Rus MA, Myhre PI, Boghdady GY, Corfu F (2009) U-Pb TIMS age constraints on the evolution of the neoproterozoic Meatiq gneiss dome, eastern desert of Egypt. Int J Earth Sci 98:481–497

Andresen A, Augland LE, Boghdady GY, Lundmark AM, El Nady OM, Hassan MA, El Rus MA (2010) Structural constraints on the evolution of the Meatiq gneiss dome (Egypt), east-African orogen. J Afr Earth Sci 57:413–422

Akaad MK, Abu El Ela AM, El Kamshoshy HI (1993) Geology of the region West of Mersa Alam Eastern Desert Egypt. Ann Egypt Geol Surv 19:1–18

Augland LE, Andresen A, Boghdady GY (2012) U-Pb ID-TIMS dating of igneous and metaigneous rocks from the El-Sibai area: time constraints on the tectonic evolution of the Central Eastern Desert, Egypt. Int J Earth Sci 101:25–37

Azer MK (2007) Tectonic significance of Late Precambrian calc-alkaline and alkaline magmatism in Saint Katherina area, South Sinai, Egypt. Geologica Acta 5:255–272

Azer MK, Farahat ES (2011) Late Neoproterozoic volcano-sedimentary successions of Wadi Rufaiyil, southern Sinai, Egypt: a case of transition from late- to post-collisional magmatism. J Asian Earth Sci 42(6):1187–1203

Azer MK, Khalil AES (2005) Petrological and mineralogical studies of Pan-African serpentinites at Bir AlEdeid area, central Eastern Desert, Egypt. J Afr Earth Sci 43:525–536

Azer MK, Stern RJ (2007) Neoproterozoic (835–720 Ma) Serpentinites in the Eastern Desert, Egypt: fragments of Forearc Mantle. J Geol 115:457–472

Azer MK, Stern RJ, Kimura J-I (2008) Origin of a late Neoproterozoic (605 ± 13 Ma) intrusive carbonate–albitite complex in Southern Sinai, Egypt. Int J Earth Sci 99(2):245–267

Azer MK, Stern RJ, Kimura J-I (2010) Origin of a Late Neoproterozoic (605 ± 13 Ma) intrusive carbonate-albitite complex in Southern Sinai, Egypt. Int J Earth Sci 99:245–267

Azer MK, Samuel MD, Ali KA, Gahlan HA, Stern RJ, Ren M, Moussa HE (2013) Neoproterozoic ophiolitic peridotites along the Allaqi-Heiani suture, south Eastern Desert, Egypt. Mineral Petrol 107(5):829–848

Azzaz SA, El Baroudy AF, Abd Allah SE (2000) Volcano-sedimentary association and Dokhan volcanics of the northwestern Sharm El-Sheikh, Sinai, Egypt. Egypt Mineral 12:217–245

Basta FF (1997) Petrology, geochemistry and Rb/Sr geochronology of Wadi Meknas Volcanics, South Eastern Sinai, Egypt. In: Proceedings of the 3rd international conference on geochemistry, Alexandria University, Egypt, pp 171–183

Bauernhofer AH, Hauzenberger CA, Wallbrecher E, Muhongo S, Hoinkes G, Mogessie A, Tenczer V (2008) Geochemistry of basement rocks from SE Kenya and NE Tanzania: indications for rifting and early Pan-African subduction. Int J Earth Sci 98 (8):1809–1834

Be'eri-Shlevin Y, Katzir Y, Whitehouse M (2009) Post-collisional tectonomagmatic evolution in the northern Arabian-Nubian Shield (ANS): time constraints from ion-probe U-Pb dating of zircon. J Geol Soc 166:71–85

Bennett JD, Mosley PN (1987) Tiered-tectonics and evolution, Eastern Desert and Sinai. In: Matheis G, Schandelmeier H (eds) Current research in African Earth sciences. Balkema, Rotterdam, pp 79–820

Bentor YK (1985) The crustal evolution of the Arabo-Nubian Massif with special reference to Sinai Peninsula. Precambrian Res 28:1–74

Berhe SM (1990) Ophiolites in Northeast and East Africa: implications for Proterozoic crustal growth. J Geol Soc Lond 147:41–57

Black R, Latouche L, Lie´geois J-P, Caby R , Bertrand JM (1994) Pan-African displaced terranes in the Tuareg Shied (central Sahara). Geology 22:641–644

Beyth M, Stern R, Altherr R, Kröner A (1994) The late Precambrian Timna igneous complex, Southern Israel: evidence for comagmatic-type sanukitoid monzodiorite and alkali granite magma. Lithos 31:103–124

Bezenjania RN, Pease V, Whitehouse MJ, Shalaby MH, Kadi KA, Kozdroj W (2014) Detrital zircon geochronology and provenance of the NeoproterozoicHammamat Group (Igla Basin), Egypt and the Thalbah Group, NW Saudi Arabia: implications for regional collision tectonics. Precambrian Res 245:225–243

Bielski M (1982) Stages in the evolution of the Arabian-Nubian Massif in Sinai. PhD thesis, Hebrew University, Gerusalam, 155 pp

Bingen B, Jacobs J, Viola G, Henderson IHC, Skara Ø, Boyd R, Thomas RJ, Solli A, Key RM, Daudi EXF (2009) Geochronology of the Precambrian crust in the Mozambiquebelt in NE Mozambique and implications for Gondwana assembly. Precambrian Res 170:231–255

Blasband B, White S, Brooijmans H, De Boorder H, Visser W (2000) Late Proterozoic extensional collapse in the Arabian-Nubian Shield. J Geol Soc Lond 157:615–628

Bogdanova SV, Pisarevsky SA, Li ZX (2009) Assembly and breakup of Rodinia (Some results of IGCP Project 440). Strat Geol Correl 17 (3):259–274

Boger SD, Miller JM (2004) Terminal suturing of Gondwana and the onset of the Ross-Delamerian Orogeny: the cause and effect of an Early Cambrian reconfiguration of plate motions. Earth Planet Sci Lett 219:35–48

Bregar M, Bauernhofer A, Pelz K, Kloetzli U, Fritz H, Neumayr P (2002) A late Neoproterozoic magmatic core complex in the Eastern

Desert of Egypt; emplacement of granitoids in a wrench-tectonic setting. Precambrian Res 118:59–82
Breitkreuz C, Eliwa HA, Khalaf IM, El Gameel K, Bühler B, Sergeev S, Larionov A, Murata M (2010) Neoproterozoic SHRIMP U-Pb zircon ages of silica-rich Dokhan Volcanics in the North Eastern Desert, Egypt. Precambrian Res 182:163–174
Brito-Neves BB, Campos-Neto MC, Fuck RA (1999) From Rodinia to Western Gondwana: an approach to the Brasiliano-Pan African cycle and orogenic collage. Episodes 22(1999):155–166
Brown GB (1972) Tectonic Map of the Arabian Peninsula. Saudi Arabian Directorate General of Mineral Resources Map AP-2, Scale 1:4,000,000
Bühler B, Breitkreuz C, Pfänder JA, Hofmann M, Becker S, Linnemann U, Eliwa HA (2014) New insights into the accretion of the Arabian-Nubian Shield: Depositional setting, composition and geochronology of a Mid-Cryogenian arc succession (North Eastern Desert, Egypt). Precambrian Res 243:149–167
Burke K, Sengor C (1986) Tectonic escape in the evolution of the continental crust. Am Geophys Union Geodyn Ser 14:41–53
Burke K, Dewey JF, Kidd WSF (1977) World distribution of sutures; the sites of former oceans. Tectonophysics 40:69–99
Cahen L, Snelling NJ (1966) The geochronology of equatorial Africa. North-Holland Publishing Cy, Amsterdam, p 195
Cawood PA, Kroner A, Collins WJ, Kusky TM, Mooney WD (2009) Windley BF (2010) Accretionary Orogens through Earth History. Geol Soc Lond Spec Publ 318:1–36.https://doi.org/10.1144/SP318.1
Clark C, Collins AS, Timms NE, Kinny PD, Chetty TRK, Santosh M (2009) SHRIMP U-Pb age constraints on magmatism and high-grade metamorphism in the Salem Block, southern India. Gondwana Res 16:27–36
Collins AS (2003) Structure and age of the northern Leeuwin Complex, Western Australia: constraints from field mapping and U-Pb isotopic analysis. Aust J Earth Sci 50:585–599
Collins AS (2006) Madagascar and the amalgamation of Central Gondwana. Gondwana Res 9:3–16
Collins AS, Pisarevsky SA (2005) Amalgamating eastern Gondwana: the evolution of the Circum-Indian Orogens. Earth Sci Rev 71:229–270
Collins AS, Windley BF (2002) The tectonic evolution of central and northern Madagascar and its place in the final assembly of Gondwana. J Geol 110:325–340
Collins AS, Razakamanana T, Windley BF (2000) Neoproterozoic extensional detachment in central Madagascar: implications for the collapse of the East African Orogen. Geol Mag 137:39–51
Collins AS, Fitzsimons ICW, Hulscher B, Razakamanana T (2003) Structure of the eastern margin of the East African Orogen in central Madagascar. Precambrian Res 123:111–133
Collins AS, Clark C, Sajeev K, Santosh M, Kelsey DE, Hand M (2007) Passage through India: the Mozambique Ocean suture, high-pressure granulites and the Palghat-Cauvery shear zone system. TerraNova 19:141–147
Collins AS, Kinny PD, Razakamanana T (2012) Depositional age, provenance and metamorphic age of metasedimentary rocks from Southern Madagascar. Gondwana Res 21:353–361
Collins AS, Clark C, Plavsa D (2014) Peninsular India in Gondwana: the tectonothermal evolution of the Southern Granulite Terrain and its Gondwanan counterparts. Gondwana Res 25(1):190–203
Condie KC (2002) Breakup of a Paleoproterozoic Supercontinent. Gondwana Res 5:41–43
Cononco (1987) Geological map of Egypt, Egyptian General Petroleum Corporation-Conoco Coral. Scale 1:500,000, Cairo
GTK Consortium (2006) Map Explanation; Volume 2: Sheets 1630–1634, 1732–1734, 1832–1834 and 1932–1934. Geology of Degree Sheets Mecumbura, Chioco, Tete, Tambara, Guro, Chemba, Manica, Catandica, Gorongosa, Rotanda, Chimoio and Beira, Mozambique. Direcção Nacional de Geologia (DNG), Maputo, 411 p + Ann
Cox GM, Lewis CJ, Collins AS, Halverson GP, Jourdan F, Foden J, Nettle D, Kattan F (2012) Ediacaran terrane accretion within the Arabian-Nubian Shield. Gondwana Res 21:341–352
Cutten HNC (2002) The Mozambique Belt, Eastern Africa—tectonic evolution of the Mozambique Ocean and Gondwana Amalgamation. Geol Soc Am: 12–28
Cutten HNC, Johnson SP (2006) Tectonic evolution of the Mozambique Belt, eastern Africa. Colloquium of African Geology (CAG21), 2006, Maputo, Mozambique. Abstract Volume, 33–34
De Waele B, Kampunzu B, Mapani BSE, Tembo F (2006) The Mesoproterozoic Irumide belt of Zambia. J Afr Earth Sci 46:36–70
Deschamps Y, Lescuyer JL, Guerrot C, Osman AA (2004) Lower Neoproterozoic age of the Ariab volcanogenic massive sulphide mineralization, Red Sea Hills, NE Sudan, 20th Colloquium of African Geology (Orléans, France) Abstracts, 2004, p 133
Doebrich JL, Al-Jehani AM, Siddiqui AA, Hayes TS, Wooden JL, Johnson PR (2007) Geology and metallogeny of the Ar Rayn terrane, eastern Arabian shield: evolution of a Neoproterozoic continental-margin arc during assembly of Gondwana within the East African orogen. Precambrian Res 158(1–2):17–50
Dessouky OK, Dardier AM, Abdel Ghani IM (2019) Egyptian Hammamat molasse basins and their relations to arc collision stages: Implications forradioactive elements mineralization potential. Geol J 54:1205–1222. https://doi.org/10.1002/gj.3220
El Bahariya G (2012) Classification and origin of the Neoproterozoic ophiolitic mélanges in the Central Eastern Desert of Egypt. Tectonophysics 568–569:357–370
El Bahariya G (2018) Classification of the Neoproterozoic ophiolites of the Central Eastern Desert, Egypt based on field geological characteristics and mode of occurrence. Arab J Geosci 11(12). https://doi.org/10.1007/s12517-018-3677-1
El Bahariya GA, Arai S (2003) Petrology and origin of Pan-African serpentinites with particular reference to chromian spinel compositions, Eastern Desert, Egypt: implication for supra-subduction zone ophiolite. In: Third international conference on the geology of Africa, Assiut University, Egypt, pp 371–388
El Bayoumi RM, Greiling RO (1984) Tectonic evolution of a Pan-African plate margin in southeastern Egypt—a suture zone overprinted by low angle thrusting? In: Klerkx J, Michot J (eds) Géologie Africaine-African
El Gaby S (2005.) Integrated evolution and rock classification of the Pan-African belt in Egypt. In: First symposium on the classification of the basement complex of Egypt, pp 1–9
El-Bialy MZ (2010) On the Pan-African transition of the Arabian-Nubian Shield from compression to extension: the post-collision Dokhan volcanic suite of KidMalhak region, Sinai, Egypt. Gondwana Res 17:26–43
El-Bialy MZ (2020) Precambrian basement complex of Egypt. In: Hamimi Z, El-Barkooky A, Martínez Frías J, Fritz H, Abd El-Rahman Y (eds) The geology of Egypt. Regional geology reviews. Springer Nature Switzerland, pp 81–129. https://doi.org/10.1007/978-3-030-15265-9_2
El-Bialy MZ, Hassen IS (2012) The late Ediacaran (580–590 Ma) onset of anorogenic alkaline magmatism in the Arabian-Nubian Shield: Katherina A-type rhyolites of Gabal Ma'ain, Sinai, Egypt. Precambrian Res 216–219:1–22

El-Gaby S, El Nady O, Khudeir A (1984) Tectonic evolution of the basement complex in the central Eastern Desert of Egypt. Geol Rundsch 73:1019–1036
El-Gaby S, List FK, Tehrani R (1988) Geology, evolution and metallogenesis of the Pan-African Belt in Egypt. In: El-Gaby S, Greiling RO (eds) The Pan-African belt of Northeast Africa and adjacent areas. Vieweg & Sohn, Weisbaden, pp 17–68
El-Gaby S, List FK, Tehrani R (1990) The basement complex of the Eastern Desert and Sinai. In: Said R (ed) The geology of Egypt. Balkema, Rotterdam, pp 175–184
El-Gaby, Khudier AA, Abdel Tawab M, Atalla RF (1991) The metamorphosed volcano-sedimentary succession of Wadi Kid, southeastern Sinai, Egypt. Ann Geol Surv Egypt XVII:19–35
Eliwa HA, Abu El-Enen MM, Khalaf IM, Itaya T, Murata M (2008) Metamorphic evolution of Neoproterozoic metapelites and gneisses in the Sinai, Egypt: insights from petrology, mineral chemistry and K-Ar age dating. J Afr Earth Sci 51:107–122
Eliwa HA, Breitkreuz C, Murata M, Khalaf IM, Bühler B, Itaya T, El Gameel K (2014a) SIMS zircon U-Pb and mica K–Ar geochronology, and Sr–Nd isotope geochemistry of Neoproterozoic granitoids and their bearing on the evolution of the north Eastern Desert, Egypt. Gondwana Res 25(4):1570–1598
Eliwa HA, El-Bialy MZ, Murata M (2014b) Ediacaran post-collisional volcanism in the Arabian-Nubian Shield: the high-K calc-alkaline Dokhan Volcanics of Gabal Samr El-Qaa (592 $\pm$ 5 Ma), North Eastern Desert, Egypt. Precambrian Res 246:180–207
El-Ramly MF (1972) A new geological map for the basement rocks in the Eastern and Southwestern Deserts of Egypt. Ann Geol Surv Egypt 2:1–18
El-Ramly MF, Akaad MK (1960) The basement complex in the CED of Egypt between lat. 24º 30' and 25º 40'. Geological Survey Egypt, Paper No 8, p 33
El Sharkawy MA, El Bayoumi RM (1979) The ophiolites of Wadi Ghadir area, Eastern Desert Egypt. Ann Geol Surv Egypt 9:125–135
El-Ramly MF, Greiling R, Kroner A, Rashwan AA (1984) On the tectonic evolution of the Wadi Hafafit area and environs, Eastern Desert of Egypt. King Abdulaziz Univ Jiddah Bull Fac Earth Sci 6:114–126
El-Ramly MF, Greiling RO, Rashwan AA, Ramsy AH (1993) Explanatory note to accompany the geological and structural maps of Wadi Hafafit area, Eastern Desert of Egypt. Ann Geol Surv Egypt 9:1–53
El-Sayed MM, Furnes H, Mohamed FH (1999) Geochemical constraints on the tectonomagmatic evolution of the late Precambrian Fawakhir ophiolite, Central eastern Desert, Egypt. J Afr Earth Sci 29:515–533
El-Shafei MK, Kusky TM (2003) Structural and tectonic evolution of the Neoproterozoic Feiran-Solaf metamorphic belt, Sinai Peninsula: implications for the closure of the Mozambique Ocean. Precambrian Res 123:269–293
Ernst RE, Pereira E, Hamilton MA, Pisarevsky SA, Rodriques J, Tassinari CC, Teixeira W, Van-Dunem V (2013) Mesoproterozoic intraplate magmatic 'barcode'record of the Angola portion of the Congo Craton: newly dated magmatic events at 1505 and 1110 Ma and implications for Nuna (Columbia) supercontinent reconstructions. Precambrian Res 230:103–118
Eyal M, Litvinovsky B, Jahn BM, Zanvilevich A, Katzir Y (2010) Origin and evolution of post-collisional magmatism: Coeval Neoproterozoic calc-alkaline and alkaline suites of the Sinai Peninsula. Chem Geol 269(3–4):153–179
Farahat ES, El-Mahalawi MM, Hoinkes G (2004) Continental back-arc basin origin of some ophiolites from the Eastern Desert of Egypt. Mineral Petrol 82:81–104
Farahat ES, Hoinkes G, Mogessie A (2011) Petrogenetic and geotectonic significance of Neoproterozoic suprasubduction mantle as revealed by the Wizer ophiolite complex, Central Eastern Desert, Egypt. Int J Earth Sci 100:1433–1450
Fowler A, El Kalioubi B (2002) The Migif-Hafafit gneissic complex of the Egyptian Eastern Desert: fold interference patterns involving multiply deformed sheath folds. Tectonophysics 346:247–275
Fowler A, Hamimi Z (2020) Structural and tectonic framework of neoproterozoic basement of Egypt: from gneiss domes to transpression belts. In: Hamimi Z, El-Barkooky A, Martínez Frías J, Fritz H, Abd El-Rahman Y (eds) The geology of Egypt. Regional geology reviews,. Springer Nature Switzerland, pp 81–129. https://doi.org/10.1007/978-3-030-15265-9_3
Fowler A, Hassan I (2008) Extensional tectonic origin of gneissosity and related structures of the Feiran-Solaf metamorphic belt, Sinai, Egypt. Precambrian Res 164:119–136
Fowler A, Osman AF (2009) The Sha'it-Nugrus shear zone separating Central and South Eastern Deserts, Egypt: a post-arc collision low-angle normal ductile shear zone. J Afr Earth Sci 53:16–32
Fowler AR, Khamees H, Dowidar H (2007) El Sibai gneissic complex, Central Eastern Desert, Egypt: folded nappes and syn-kinematic gneissic granitoid sheets—not a core complex. J Afr Earth Sci 49 (4):119–135
Frimmel HE (2009) Chapter 5.1 configuration of Pan-African orogenic belts in Southwestern Africa. Dev Precambrian Geol: 145–151
Frimmel HE (2010) Configuration of Pan-African orogenic belts in Southwestern Africa. In: Gaucher C, Sial A, Haverson G (eds) Neoproterozoic-cambrian tectonics, global change and evolution: a focus on south western Gondwana. Elsevier, pp 145–151
Frisch W, Pohl W (1986) Petrochemistry of some mafic and ultramafic rocks from the Mozambique Belt, SE-Kenya. Mitteilung Österreichischer Geologischer Gesellschaft 78:97–114
Fritz H, Messner M (1999) Intramontane basin formation during oblique convergence in the Eastern Desert of Egypt: magmatically versus tectonically induced subsidence. Tectonophysics 315:145–162
Fritz H, Wallbrecher E, Khudeir AA, Abu El Ela F, Dallmeyer DR (1996) Formation of Neoproterozoic core complexes during oblique convergence (Eastern Desert, Egypt). J Afr Earth Sci 23:311–329
Fritz H, Dallmeyer DR, Wallbrecher E, Loizenbauer J, Hoinkes G, Neumayr P, Khudeir AA (2002) Neoproterozoic tectonothermal evolution of the Central Eastern Desert, Egypt: a slow velocity tectonic process of core complex exhumation. J Afr Earth Sci 34:137–155
Fritz H, Tenczer VWallbrecher CA, Hauzenberger E, Hoinkes G, Muhongo S, Mogessie A (2005) Central Tanzanian tectonic map: a step forward to decipher Proterozoic structural events in the East AfricanOrogen. Tectonics 24, TC6013. http://dx.doi.org/10.1029/2005TC001796
Fritz H, Tenczer V, Hauzenberger C, Wallbrecher E, Muhongo S (2009) Hot granulite nappes—Tectonic styles and thermal evolution of the Proterozoic granulite belts in East Africa. Tectonophysics 477:160–173
Fritz H, Hauzenberger CA, Tenczer V (2012) East African and Kuunga Orogenies in Tanzania—South Kenya. EGU General Assembly 2012, held 22-27 April, 2012 in Vienna, Austria, (abstract) p 8754
Fritz H, Abdelsalam M, Ali KA, Bingen B, Collins AS, Fowler AR, Viola G (2013) Orogen styles in the East African Orogen: a review of the Neoproterozoic to Cambrian tectonic evolution. J Afr Earth Sci 86:65–106
Gahlan HA, Arai S (2009) Carbonate-orthopyroxenite lenses from the Neoproterozoic Gerf ophiolite, South Eastern Desert, Egypt: the first record in the Arabian Nubian Shield ophiolites. J Afr Earth Sci 53:70–82

Gahlan HA, Arai S, Abu El-Ela FF, Tamura A (2012) Origin of wehrlite cumulates in the Moho Transition Zone of the Neoproterozoic Ras Salatit Ophiolite, Central Eastern Desert, Egypt. Contrib Mineral Petrol 163:225–241

Gahlan HA, Azer MK, Khalil AES (2015) The neoproterozoic Abu Dahr ophiolite, South Eastern Desert, Egypt: petrological characteristics and tectonomagmatic evolution. Mineral Petrol 109:611–630

Genna A, Nehlig P, Le Goff E, Guerrot C, Shanti M (2002) Proterozoic tectonism of the Arabian Shield. Precambrian Res 117(1–2):21–40

Grantham GH, Maboko M, Eglington BM (2003) A review of the evolution of the Mozambique Belt and implications for the amalgamation and dispersal of Rodinia and Gondwana. In: Yoshida M, Windley BF, Dasgupta S (eds) Proterozoic East Gondwana: supercontinent assembly and breakup. Geological Society, London, Special Publications, 206, pp 411–425

Grantham GH, Macey PH, Horie K, Kawakami T, Ishikawa M, Satish-Kumar M, Tsuchiya N, Graser P, Azevedo S (2013) Comparison of the metamorphic history of the Monapo Complex, northern Mozambique and Balchenfjella and Austhameren areas, Sør Rondane, Antarctica: implications for the Kuunga Orogeny and the amalgamation of N and S. Gondwana. Precambrian Res 234:85–135

Gray DR, Foster DA, Meert JG, Goscombe BD, Armstrong R, Trouw RAJ, Passchier CW (2008) A Damara orogen perspective on the assembly of southwestern Gondwana. In: Pankhurst, R., Trouw, R., Brito Neves, B., De Wit, M. (Eds.), West Gondwana Pre-Cenozoic Correlations Across the South Atlantic Region, Geol Soc Lond Spec Publ 294(1):257–278

Greenwood WR, Hadley DG, Anderson RE, Fleck RJ, Schmidt DL (1976) Later Proterozoic cratonization in southwestern Saudi Arabia. Philos Trans R Soc Lond A 280:517–527

Greiling RO (1987) Directions of Pan-African thrusting in the Eastern Desert of Egypt derived from lineation and strain data. In: Matheis G, Schandelmeier H (eds) Current research in African Earth sciences. Balkema, Rotterdam, pp 83–86

Greiling RO (1997) Thrust tectonics in crystalline domains: the origin of a gneiss dome. Proc Ind Acad Sci (Earth Planet Sci) 106:209–220

Greiling RO, Kröner A, El-Ramley MF (1984) Structural interference patterns and their origin in the Pan-African basement of the southeastern Desert of Egypt. In: Kröner A, Greiling RO (eds) Precambrian Tectonics Illustrated. Schweitzerbart'sche Verlagsbuchhandlung, Stuttgart, Germany, pp 401–412

Greiling RO, Kröner A, El-Ramly MF, Rashwan AA (1988) Structural relationship between the southern and central parts of the Eastern desert of Egypt: details of a fold and thrust belt. In: El-Gaby S, Greiling RO (eds) The Pan-African belt of Northeast Africa and adjacent areas. Vieweg & Sohn, Weisbaden, Germany, pp 121–146

Greiling RO, Abdeen MM, Dardir AA, El Akhal H, El Ramly MF, Kamal El Din GM, Osman AF, Rashwan AA, Rice AH, Sadek MF (1994) A structural synthesis of the Proteorozoic Arabian-Nubian Shield in Egypt. Geol Rundsch 83:484–501

Grothaus BD, Eppler D, Ehrlich R (1979) Depositional environment and structural implications of the Hammamat Formation, Egypt. Ann Geol Surv Egypt 9:231–245

Hamdy MM, Abd El-Wahed MA, Gamal El Dien H, Morishita T (2017) Garnet hornblendite in the Meatiq core Complex, Central Eastern Desert of Egypt: Implications for crustal thickening preceding the ~600 Ma extensional regime in the Arabian-Nubian Shield. Precambrian Res 298:593–614

Hamimi Z, Abd El-Wahed MA (2020) Suture(s) and Major Shear Zones in the Neoproterozoic Basement of Egypt. In: Hamimi Z, El-Barkooky A, Martínez Frías J, Fritz H, Abd El-Rahman Y, The geology of Egypt. Regional geology reviews. Springer Nature Switzerland, pp 153–189. https://doi.org/10.1007/978-3-030-15265-9_5

Hamimi Z, El Amawy MA, Wetait M (1994) Geology and structural evolution of El-Shalul Dome and environs, Central Eastern Desert, Egypt. Egypt J GeolEgypt J Geol 38–2:575–959

Hamimi Z, Abd El-Wahed M, GahlanHA, Kamh SZ (2019) Tectonics of the Eastern Desert of Egypt: key to understanding the Neoproterozoic evolution of the Arabian-Nubian Shield (East African Orogen). In: Bendaoud A, Hamimi Z, Hamoudi M, Djemai S, Zoheir B (eds) Geology of the Arab World—an Overview, Springer Geology, 1–81. https://doi.org/10.1007/978-3-319-96794-3_1

Hanson RE (2003) Proterozoic geochronology and tectonic evolution of southern Africa. Lanka In: Yoshida M, Windley BF, Dasgupta S (eds) Proterozoic East Gondwana: supercontinent assembly and breakup. Geol Soc Lond Spec Publ 206:438–471

Hanson RE, Wilson TJ, Munyanyiwa H (1994) Geologic evolution of the Neoproterozoic Zambezi Orogenic belt in Zambia. J Afr Earth Sci 18(2):135–150

Hargrove US, Hanson RE, Martin MW, Blenkinsop TG, Bowring SA, Walker N, Munyanyiwa H (2003) Tectonic evolution of the Zambezi orogenic belt: geochronological, structural, and petrological constraints from northern Zimbabwe. Precambrian Res 123(2–4):159–186

Hargrove US, Stern RJ, Kimura J-I, Manton WI, Johnson PR (2006) How juvenile is the Arabian-Nubian Shield? Evidence from Nd isotopes and pre-Neoproterozoic inherited zircons in the Bir Umq suture zone, Saudi Arabia. Earth Planet Sci Lett 252:308–326

Harley SL, Fitzsimons ICW, Zhao Y (2013) Antarctica and supercontinent evolution: historical perspectives, recent advances and unresolved issues. Geol Soc lond Spec Publ 383(1):1–34. https://doi.org/10.1144/sp383.9

Harraz HZ, El-Sharkawy MF (2001) Origin of tourmaline in the metamorphosed Sikait pelitic belt, south Eastern Desert. Egypt. J. Afr. Earth Sci. 33(2):391–416

Hartnady C, Joubert P, Stowe C (1985) Proterozoic crustal evolution in southwestern Africa. Episodes 8:236–244

Hassan MA, Hashad AH (1990) Precambrian of Egypt. In: Said R (ed) The Geology of Egypt. Balkema, Rotterdam, pp 201–245

Hauzenberger CA, Bauernhofer AH, Hoinkes G, Wallbrecher E, Mathu EM (2004) Pan-African high pressure granulites from SE-Kenya: petrological and geothermobarometric evidence for a polycyclic evolution in the Mozambique belt. J Afr Earth Sci 40:245–268

Hauzenberger CA, Sommer S, Fritz H, Bauernhofer A, Kröner A, Hoinkes G, Wallbrecher E, Thöni M (2007) SHRIMP U-Pb zircon and Sm–Nd garnet ages from granulite facies basement of SE-Kenya: evidence for Neoproterozoicpolycyclic assembly of the Mozambique belt. J Geol Soc Lond 164:189–201

Helmy H, Kaindl R, Fritz H, Loizenbauer J (2004) The Sukari Gold Mine, Eastern Desert, Egypt: structural setting, mineralogy and fluid inclusion study. Miner Deposita 39:495–511

Hoffman R (1991) Did the breakup out of Laurentia turn Gondwana inside out? Science 252:1409–1412

Jacobs J, Thomas RJ (2004) Himalayan-type indenter-escape tectonics model for the southern part of the late Neoproterozoic-early Paleozoic East African-Antarctic orogen. Geology 32:721–724

Jacobs J, Bauer W, Thomas RT (2006) A Himalayantype indentor-escape tectonic model for the southern part of the Late Neoproterozoic/Early Paleozoic East African- Antarctic Orogen. Colloquium of African Geology (CAG21), 2006, Maputo, Mozambique. Abstract Volume, pp 71–72

Jarrar G, Wachendorf H, Zachmann D (1993) A Pan-African alkaline pluton intruding the Saramuj Conglomerate, South-West Jordan. Geological Rundschau 82:121–135

Johansson Å (2014) From Rodinia to Gondwana with the "SAMBA" model—a distant view from Baltica towards Amazonia and beyond. Precambrian Res 244:226–235
John T, Schenk V, Haase K, Scherer E, Tembo F (2003) Evidence for a Neo-proterozoic ocean in south-central Africa from mid-oceanic ridge-type geochemical signatures and pressure-temperature estimates of Zambian eclogites. Geology 31:243–246
Johnson PR (2006) Explanatory notes to the map of Proterozoic geology of western Saudi Arabia: Saudi Geological Survey Technical Report SGS-TR-2006-4, 62 p
Johnson PR (2014) An expanding Arabian-Nubian Shield geochronologic and isotopic dataset: defining limits and confirming the tectonic setting of a neoproterozoic accretionary orogen. Open Geol J 8(Suppl 1: M2):3–33
Johnson SP, Oliver GJH (2000) Mesoproterozoic oceanic subduction, island arc formation and the initiation of back-arc spreading in the Kibaran Belt of central southern Africa: evidence from the ophiolite terrane, Chewore Inliers, northern Zimbabwe. Precambrian Res 103:125–146
Johnson SP, Oliver GJH (2002) High fO2 Metasomatism during White schist Metamorphism, Zambezi Belt, Northern Zimbabwe. J PetrolJ Petrol 43(2):271–290
Johnson SP, Oliver GJH (2004) Tectonothermal history of the Kaourera Arc, northern Zimbabwe; implications for the tectonic evolution of the Irumide and Zambezi Belts of south central Africa. Precambrian Res 130:71–97
Johnson PR, Woldehaimanot B (2003) Development of the Arabian-Nubian Shield. Perspectives on accretion and deformation in the northern East African Orogen and the assembly of Gondwana. In. Yoshida M, Windley BF, Dasgupta S (eds) Proterozoic East Gondwana, Supercontinent Assembly and Breakup. Geological Society, London, Special Publication, vol 206, pp 290–325
Johnson SP, Rivers T, De Waele B (2005) A review of the Mesoproterozoic to early Palaeozoic magmatic and tectonothermal history of south-central Africa: implications for Rodinia and Gondwana. J Geol Soc Lond 162:433–450
Johnson PR, Andresen A, Collins AS, Fowler AR, Fritz H, Ghebreab W, Kusky T, Stern RJ (2011) Late Cryogenian-Ediacaran history of the Arabian-Nubian Shield: a review of depositional, plutonic, structural, and tectonic events in the closing stages of the northern East African Orogen. J Afr Earth Sci 61:167–232
Johnson P, Halverson G, Kusky T, Stern R, Pease V (2013) Volcanosedimentary Basins in the Arabian-Nubian Shield: markers of repeated exhumation and denudation in a neoproterozoic accretionary orogen. Geosciences 3(3):389–445
Jöns N, Schenk V (2011) The ultrahigh temperature granulites of southern Madagascar in a polymetamorphic context: implications for the amalgamation of the Gondwana supercontinent. Eur J Mineral 23:127–156
Jung S, Mezger K (2003) U-Pb garnet chronometry in high-grade rocks —case studies from the central Damara orogen (Namibia) and implications for the interpretation of Sm-Nd garnet ages and the role of high U-Th inclusions. Contrib Mineral Petrol 146(3):382–396
Kamal El Din GM, Khudeir AA, Greiling RO (1992) Tectonic evolution of a Pan-African gneiss culmination, Gabal El Sibai area, central Eastern Desert. Egypt 1991, vol 11. Zbl Geol Palaont Teil I, Stuttgart, pp 2637–2640
Kelsey DE, Wade BP, Collins AS, Hand M, Sealing CR, Netting A (2008) A Neoproterozoic basin precursor to UHT metamorphism in the Prydz Bay belt in east Antarctica. Precambrian Res 161:355–388
Kennedy WQ (1964) The structural differentiation of Africa in the Pan-African (± 500 m.y.) tectonic episode. Leeds Univ. Res Inst Afr Geol Annu Rep 8:48–49
Keppie JD, Nance RD, Murphy JB, Dostal J (2003) Tethyan, Mediterranean, and Pacific analogues for the Neoproterozoic-Paleozoic birth and development of the peri-Gondwanan terranes and their transfer to Laurentia andLaurussia. Tectonophysics 365:195–219
Kessel R, Stein M, Navon O (1998) Petrogenesis of late Neoproterozoic dikes in the northern Arabian-Nubian Shield, implications for the origin of A-type granites. Precambrian Res 92:195–213
Klitzch C, List F, Pöhlmann A (1987) Geological Map of Egypt (CONOCO), NG 36NE. Qusier scale 1:500000
Kröner A (1985) Ophiolites and evolution of tectonic boundaries in the Late Proterozoic Arabian-Nubian Shield of northeast Africa and Arabia. Precambrian Res 27:277–300
Kröner A (2006) The Mozambique Belt of East Africa and Madagascar: a Review. Colloquium of African Geology (CAG21), 2006, Maputo, Mozambique. Abstract Volume, 96
Kröner A, Stern RJ (2004) Pan-African Orogeny. In: Selley RC, Cocks R, Plimer I (eds) Encyclopedia of geology. 1. Elsevier, Amsterdam, p 1. ISBN 9780126363807
Kröner A, Todt W, Hussein IM, Mansour M, Rashwan AA (1992) Dating of late Proterozoic ophiolites in Egypt and the Sudan using the single grain zircon evaporation technique. Precambrian Res 59:15–32
Kröner A, Willner HP, Hegner E, Jaeckel P, Nemchin A (2001) Single zircon ages, PT evolution and Nd isotope systematics of high-grade gneisses in southern Malawi and their bearing on the evolution of the Mozambique Belt in southeastern Africa. Precambrian Res 109:257–291
Kuribara Y, Tsunogae T, Takamura Y, Tsutsumi Y (2018) Petrology, geochemistry, and zircon U-Pb geochronology of the Zambezi Belt in Zimbabwe: Implications for terrane assembly in southern Africa. Geosci Front. 10.1016/j.gsf.2018.05.019 (in press)
Laznicka Peter (2010) Giant Metallic deposits: future sources of industrial metals. Springer. ISBN 3642124046
Li ZX, Evans DAD (2011) Late Neoproterozoic 40○intraplate rotation withinAustralia allows for a tighter-fitting and longer-lasting Rodinia. Geology 39:39–42
Li ZX, Bogdanova SV, Collins AS, Davidson A, De Waele B, Ernst RE, Fitzsimons ICW, Fuck RA, Gladkochub DP, Jacobs J, Karlstrom KE, Lul S, Natapov LM, Pease V, Pisarevsky SA, Thrane K, Vernikovsky V (2008) Assembly, configuration, and break-up history of Rodinia: a synthesis. Precambrian Res 160:179–210
Liégeois J-P, Abdelsalam MG, Ennih N, Ouabadi A (2013) Metacraton: nature, genesis and behavior. Gondwana Res 23(1):220–237
Loizenbauer J, Wallbrecher E, Fntz H, Neumayr P, Khudeir AA, Kloetzil U (2001) Structural geology, single zircon ages and fluid inclusion studies of the Meatiq metamorphic core complex. Implications for Neoproterozoic tectonics in the Eastern Desert of Egypt. Precambrian Res 110:357–383
Lundmark AM, Andresen A, Hassan M, Augland LE, Boghdady GY (2012) Repeated magmatic pulses in the East African Orogen in the Eastern Desert, Egypt: an old idea supported by new evidence. Gondwana Res 22:227–237
Makroum FM (2001) Pan-African tectonic evolution of the Wadi El Mayit Area and its environs, Central Eastern Desert, Egypt. The second International Conference on the Geology of Africa, Assiut University, Egypt 2:219–233
Makroum FM (2017) Structural Interpretation of the Wadi Hafafit Culmination: a Pan African gneissic dome in the central Eastern Desert, Egypt. Lithosphere 9(5):759–773
Manhiça ADST, Grantham GH, Armstrong RA, Guise PG, Kruger FJ (2001) Polyphase deformation and metamorphism at the Kalahari Craton—Mozambique belt boundary. In: Miller JA, Holdsworth RE, Buick IS, Hand M (eds) Continental reactivation and reworking. Geological Society of London, Special Publication vol 184, pp 303–322

McMenamin MA, McMenamin DL (1990) The emergence of animals: the Cambrian breakthrough. Columbia University Press. ISBN 0-231-06647-3
McWilliams MO (1981) Palaeomagnetism and Precambrian tectonic evolution of Gondwana. Dev Precambrian Geol 4:649–687
Meert JG (2003) A synopsis of events related to the assembly of eastern Gondwana. Tectonophysics 362(1):1–40
Meert JG (2012) What's in a name? The Columbia (Paleopangaea/Nuna) supercontinent. Gondwana Res 21(4):987–993
Meert JG, Lieberman BS (2008) The Neoproterozoic assembly of Gondwana and its relationship to the Ediacaran-Cambrian radiation. Gondwana Res 14:5–21
Meert JG, Van Der Voo R (1997) The assembly of Gondwana 800-550 Ma. J Geodyn 23(3–4):223–235
Meert JG, Pandit MK, Pradhan VR, Kamenov G (2011) Preliminary report on the paleomagnetism of 1.88 Ga dykes from the Bastar and Dharwarcratons, peninsular India. Gondwana Res 20:335–343
Merdith AS, Williams SE, Müller RD, Collins AS (2017) Kinematic constraints on the Rodinia to Gondwana transition. Precambrian Res 299:132–150
Mohammad AT, El Kazzaz YA, Hassan SM, Taha MMN (2019) Neoproterozoic tectonic evolution and exhumation history of transpressional shear zones in the East African orogen: implications from kinematic analysis of Meatiq area, Central Eastern Desert of Egypt. Int J Earth Sci. https://doi.org/10.1007/s00531-019-01801-y
Moore JM (1979) Tectonics of the Najd transcurrent fault system, Saudi Arabia. J Geol Soc Lond 136:441–454
Mosley P (1993) Geological evolution of the late Proterozoic "Mozambique Belt" of Kenya. Tectonophysics 221:223–250
Moussa HE (2003) Geologic setting, petrography and geochemistry of the volcanosedimentary succession at Gebel Ferani area, southeastern Sinai, Egypt. Egypt J Geol 47:153–173
Müller MA, Jung S, Kröner A, Baumgartner LP, Poller U, Todt W (2001) Pan-African emplacement and granulite-facies metamorphism in the Mavuradonha Mountains, Zambezi Belt. Abstracts, EUG XI, Strasbourg, 564
Nettle D, Halverson GP, Cox GM, Collins AS, Schmitz M, Gehling J, Kadi K (2013) A middle-late Ediacaran volcano-sedimentary record from the eastern Arabian-Nubian shield. Terra Nova 26(2):120–129
Oliver GJH, Johnson SP, Williams IS, Herd DA (1998) Relict 1.4 Ga oceanic crust in the Zambezi Valley, northern Zimbabwe: evidence for Mesoproterozoic supercontinent fragmentation. Geology 26:571–573
Osman AF (1996) Structural, geological and geochemical studies of the Pan-African basement rocks, Wadi Zeidun Area, Central Eastern Desert, Egypt. Sci Ser Int Bur/Forschungszentrum Julich GmbH 39:262
Pin C, Poidevin JL (1987) U-Pb zircon evidence for a Pan-African granulite facies metamorphism in the Central African Republic. A new interpretation of the high-grade series of the northern border of the Congo Craton. Precambrian Res 36:303–312
Plavsa D, Collins AS, Foden JF, Kropinski L, Santosh M, Chetty TRK, Clark Ch (2012) Delineating crustal domains in Peninsular India: age and chemistry of orthopyroxene-bearing felsic gneisses in the Madurai Block. Precambrian Res 198–199:77–93
Powell CM (1993) Assembly of Gondwanaland—Open forum. In: Findlay RH et al (eds) Gondwana eight: Assembly, evolution and dispersal: Rotterdam. Balkema, Netherlands, pp 218–237
Quick JE (1990) Geology and origin of the Late Proterozoic Darb Zubaydah ophiolite, Kingdom of Saudi Arabia. Geol Soc Am Bull 102:1007–1020
Quick JE (1991) Late Proterozoic transpression of the Nabitah fault system-implications for the assembly of the Arabian shield. Precambrian Res 53:119–147
Ray J, Sen G, Ghosh B (2010) Topics in igneous petrology. Springer. ISBN 9048195993
Ries AC, Shackleton RM, Graham RH, Fitches WR (1983) Pan-African structures, ophiolites and mélanges in the Eastern Desert of Egypt: a traverse at 26_ N. J Geol Soc Lond 140:75–95
Robinson FA, Foden JD, Collins AS, Payne JL (2014) Arabian Shield magmatic cycles and their relationship with Gondwana assembly: insights from zircon U-Pb and Hf isotopes. Earth Planet Sci Lett 408:207–225
Rogers JW, Santosh M (2004) Continents and supercontinents. Oxford University Press Inc, 298p
Samuel MD, Moussa HE, Azer MK (2007) A-type volcanics in central Eastern Sinai, Egypt. J Afr Earth Sci 47:203–226
Samson SD, Patchett PJ (1991) The Canadian Cordillera as a modern analogue of Proterozoic crustal growth. Aus J Earth Sci 38:595–611
Schmidt DL, Hadley DG, Stoeser DB (1979) Late Proterozoic crustal history of the Arabian Shield, southern Najd province, Kingdom of Saudi Arabia. In: Al-Shanti AMS (ed) Evolution and mineralization of the Arabian–Nubian Shield. In: King Abdulaziz University, Institute of Applied Geology Bulletin 3, vol 2. Pergamon Press, pp 41–58
Schmitt RS, Trouw RAJ, Van Schmus WR, Pimentel MM (2004) Late amalgamation in the central part of West Gondwana: new geochronological data and the characterization of a Cambrian orogeny in the Ribeira Belt (SE Brazil). Precambrian Res 133:29–61
Shackleton RM (1986) Precambrian plate tectonics of eastern Gondwana: Società Geologia Italiana, Memorie 31:343–350
Shackleton RM (1994) The final collision zone between East and West Gondwana; where is it? J Afr Earth Sci 23:271–287
Shackleton RM (1996) The final collision between East and West Gondwana: where is it? J Afr Earth Sci 23:271–287
Shalaby A (2010) The northern dome of Wadi Hafafit culmination, Eastern Desert, Egypt: structural setting in tectonic framework of a scissor-like wrench corridor. J Afr Earth Sci 57:227–241
Shalaby A, Stüwe K, Makroum F, Fritz H, Kebede T, Klotzli U (2005) The Wadi Mubarak belt, Eastern Desert of Egypt: a Neoproterozoic conjugate shear system in the Arabian-Nubian Shield. Precambrian Res 136:27–50
Shalaby A, Stüwe K, Fritz H, Makroum F (2006) The El Mayah molasse basin in the Eastern Desert of Egypt. J Afr Earth Sci 45:1–
Shellnutt JG, Pham Y, Denyszyn P, Yeh M, Lee T (2017) Timing of collisional and post-collisional Pan-African Orogeny silicic magmatism in south-central Chad. Precambrian Res 301:113–123
Shellnutt JG, Yeh M, Lee T, Iizuka Y, Pham N, Yang C (2018) The origin of Late Ediacaran post-collisional granites near the Chad Lineament, Saharan Metacraton, South-Central Chad. Lithos 304–307:450–467
Shimron AE (1980) Proterozoic island arc volcanism and sedimentation in Sinai. Precambrian Res 12:437–458
Shimron AE (1984) Evolution of the Kid group, southeast Sinai Peninsula: thrusts, mélanges, and implication for accretionary tectonics during the Proterozoic of the Arabian-Nubian Shield. Geology 12:242–247
Stein M (2003) Tracing the plume material in the Arabian-Nubian Shield. Precambrian Res 2(123):223–34
Stein M, Goldstein SL (1996) From plume head to continental lithosphere in the Arabian Nubian shield. Nature 382:773–778
Stern RJ (1985) The Najd fault system, Saudi Arabia and Egypt: a Late Precambrian rift-related transform system. Tectonics 4:497–511
Stern RJ (1994a) Arc assembly and continental collision in the Neoproterozoic East African Orogen implications for the consolidation of Gondwanaland. Annu Rev Earth Planet Sci 22:319–351

Stern RJ (1994b) Neoproterozoic (900-550 Ma) arc assembly and continental collision in the east African orogeny. Annu Rev Earth Planet Sci 22:319–351

Stern RJ (2002) Crustal evolution in the East African Orogen: a neodymium isotopic perspective. J Afr Earth Sci 34:109–117

Stern RJ (2004) Subduction initiation: spontaneous and induced. Earth Planet Sci LettEarth Planet Sci Lett 226:275–292

Stern RJ (2018) Neoproterozoic formation and evolution of Eastern Desert continental crust—the importance of the infrastructure-superstructure transition. J Afr Earth Sci 146:15–27

Stern RJ, Hedge CE (1985) Geochronologic constraints on late Precambrian crustal evolution in the Eastern Desert of Egypt. Am J Sci 285:97–127

Stern RJ, Kröner A (1993) Geochronologic and isotopic constraints on the late Precambrian crustal evolution m northeast Sudan. J Geol 101:555–574

Stern RJ, Manton WI (1987) Age of Feiran basement rocks, Sinai: implications for late Precambrian crustal evolution in the northern Arabian-Nubian Shield. J Geol Soc Lond 144:569–575

Stern RJ, Nielasen KC, Best E, Sultan M, Arvidson RE, Kroner A (1990) Orientation of late Precambrian sutures in the Arabian-Nuhian Shield. Geology 18:1103–1106

Stern RJ, Johnson PR, Kröner A, Yibas B (2004) Neoproterozoic Ophiolites of the Arabian-Nubian Shield. Dev Precambrian Geol: 95–128

Stern RJ, Ali KA, Liégeois J-P, Johnson P, Wiescek F, Kattan F (2010) Distribution and significance of pre-Neoproterozoic zircons in juvenile Neoproterozoic igneous rocks of the Arabian-Nubian Shield. Am J Sci 310:791–811

Stoeser DB, Camp (1985) Pan-African microplate accretion of the Arabian Shield. Geol Soc Am Bull 96:817–826

Stoeser DB, Frost CD (2006) Nd, Pb, Sr, and O isotopic characterization of Saudi Arabian Shield terranes. Chem Geol 226(3–4):163–188

Sturchio NC, Sultan M, Batiza R (1983) Geology and origin of Meatiq Dome, Egypt: a Precambrian metamorphic core complex? Geology 11:72–76

Sultan M, Arvidson RE, Duncan IJ, Stern RJ, Kaliouby BE (1988) Extension of the Najd shear system from Saudi Arabia to the central Eastern Desert of Egypt based on integrated field and Landsat observations. Tectonics 7:1291–1306

Teixeira JBG, Misi A, da Glória da Silva M. (2007) Supercontinent evolution and the Proterozoic metallogeny of South America. Gondwana Res 11(3):346–361. https://doi.org/10.1016/j.gr.2006.05.009

Tohver E, Trindade RIF, Solum GF, Hall CM, Riccomini C, Nogueira AC (2010) Closing the Clymene Ocean and bending a Brasiliano belt: evidence for the Cambrian formation of Gondwana, southeast Amazon craton. Geology 38:267–270

Torsvik TH, Cocks LRM (2013) Gondwana from top to base in space and time. Gondwana Res 24(3):999–1030

Trindade RIF, D'Agrella-Filho MS, Epof I, Brito Neves BB (2006) Paleomagnetism of Early Cambrian Itabaiana mafic dikes (NE Brazil) and thefinal assembly of Gondwana. Earth Planet Sci Lett 244:361–377

Trompette R (1994) Geology of western Gondwana: Rotterdam. Balkema, Netherlands, p 350

Trompette R (2000) Gondwana evolution; its assembly at around 600 Ma. C R Acad Sci - Earth Planet Sci 330(5):305–315. https://doi.org/10.1016/s1251-8050(00)00125-7

Unrug R (1996) The assembly of Gondwanaland. Episodes 19:11–20

Unrug D (1997) Rodinia to Gondwana: the geodynamic map of Gondwana Supercontinent Assembly. A Publ Geol Soc Am 7(1):1–6

Valentine, Moores EM (1970) Plate-tectonic regulation of faunal diversity and sea level: a model. Nature 228: 657–659

van Hinsbergen DJ, Lippert PC, Dupont-Nivet G, McQuarrie N, Doubrovine PV, Spakman W, Torsvik TH (2012) Greater India Basin hypothesis and a two-stage Cenozoic collision between India and Asia. PNAS 109(20):7659–7664

Wegener A (1915) Die Entstehung der Kontinente und Ozeane. Vieweg, Braunschweig, p 94

Westerhof ABP, Lehtonen MI, Mäkitie H, Manninen T, Pekkala Y, Gustafsson B, Tahon A (2008) The Tete-Chipata Belt: a new multiple terrane element from western Mozambique and southern Zambia. Geological Survey of Finland, Special Paper 48, 145–166

Whitehouse MJ, Windley BF, Stoeser DB, Al-Khirbash S, Ba-Bttat MAO, Haider A (2001) Precambrian basement character of Yemen and correlations with Saudi Arabia and Somalia. PrecambrianRes 105:357–369

Wilde SA, Youssef K (2000) Significance of SHRIMP U-Pb dating of the imperial porphyry and associated Dokhan volcanics, Gebel Dokhan, north Eastern Desert, Egypt. J Afr Earth Sci 31:403–413

Windley BF, Witehouse MJ, Ba-Bttat MAO (1996) Early Precambrian gneiss terranes and Pan-African island arcs in Yemen: crustal accretion of the eastern Arabian Shield. Geology 24:313–134

Zhao G, Cawood PA, Wilde SA, Sun M (2002) Review of global 2.1–1.8 Ga orogens: implications for a pre-Rodinia supercontinent. Earth-Sci Rev 59(1):125–162

Zhao G, Sun M, Wilde SA, Li S (2004) A Paleo-Mesoproterozoic supercontinent: assembly, growth and breakup. Earth-Sci Rev 67 (1):91–123

Zimmer M, Kröner A, Jochum KP, Reischmann T, Todt W (1995) The Gabal Gerf complex: a Precambrian N-MORB ophiolite in the Nubian Shield, NE Africa. Chem Geol 123:29–51

Zoheir BA, Klemm DD (2007) The tectono-metamorphic evolution of the central part of the Neoproterozoic Allaqi-Heiani suture, south Eastern Desert of Egypt. Gondwana Res 12:289–304

Zoheir BA, Lehmann B (2011) Listvenite-lode association at the Barramiya gold mine, Eastern Desert, Egypt. Ore Geol Rev 39:101–115

Zoheir BA, Weihed P (2014) Greenstone-hosted lode-gold mineralization at Dungash mine, Eastern Desert, Egypt. J Afr Earth Sci 99 (1):165–187

Zoheir BA, Abd El-Wahed MA, Pour AB, Abdelnasser A (2019a) Orogenic Gold in Transpression and Transtension Zones: Field and Remote Sensing Studies of the Barramiya-Mueilha Sector, Egypt. Remote Sens 11(18):2122. https://doi.org/10.3390/rs11182122

Zoheir BA, Emam A, Abd El-Wahed MA, Soliman N (2019b) Gold endowment in the evolution of the Allaqi-Heiani suture, Egypt: a synthesis of geological, structural, and spaceborne imagery data. Ore Geol Rev 110:102938. https://doi.org/10.1016/j.oregeorev.2019.102938